VIBRATIONAL AND ROTATIONAL ANALYSES OF EMISSION SYSTEMS IN THE REGIONS (3460 − 3015Å) AND (4320 − 4000Å) AND Ar+ LASER EXCITED FLUORESCENCE STUDIES OF I_2

A Thesis Submitted
In Partial Fulfilment of the Requirements
for the Degree of
DOCTOR OF PHILOSOPHY

By

T. PRAMILA
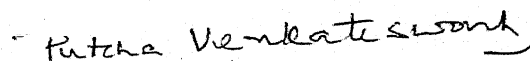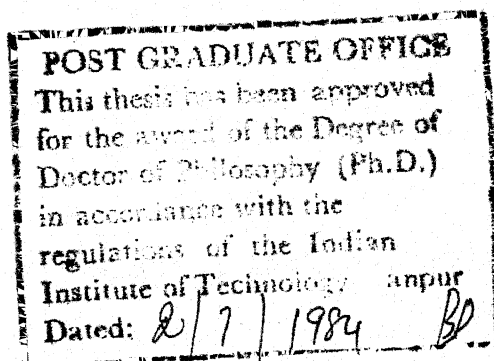
PHY- 1983-D- PRA -VIB

TO

MY MOTHER

CERTIFICATE

This is to certify that the work presented in this thesis titled 'Vibrational and Rotational Analyses of Emission Systems in the Regions (3460-3015 $\overset{o}{A}$) and (4320-4000 $\overset{o}{A}$) and Ar^+ Laser Excited Fluorescence Studies of I_2' is the original work of Mrs. T. Pramila, done under our supervision and it has not been submitted elsewhere for a degree.

(G.N. Rao)
Professor of Physics

(Putcha Venkateswarlu)
Professor of Physics

ACKNOELEDGEMENTS

But for them, I could not have achieved this ambition of
mine.

As words are highly inadequate to thank my husband,
Mr. Raghuram, for his forbearance and understanding during
the progress of this work, I do not attempt to do so.

T. Pramila

CONTENTS

LIST OF TABLES

LIST OF FIGURES

CHAPTER 1

INTRODUCTION

Study of molecular spectra is one of the best means
for understanding molecular structure. It enables one to
know about the motion of electrons in the molecule, and the
vibration and rotation of the nuclei and their position
inside the molecule. The theory of the molecular spectra
is treated in great detail in many text books on molecular
spectroscopy. The most extensive and authentic treatment of
the spectra of diatomic molecules is that of Herzberg. In
this chapter only those features which are most relevant to
the present work are discussed [1-3].

Formation of Molecular Quantum Numbers

In a diatomic molecule, there is a strong cylindrically symmetric electric field along the internuclear axis due to the electrostatic field of the nuclei whereas in an atom there is a spherically symmetric field of force. The result of this is the uncoupling of the orbital and spin angular momenta of the individual atoms and the formation of resultant total orbital and spin angular momenta for the molecule. The orbital angular momentum vector L precesses independent of the spin about the internuclear axis and has a constant component M_L along the internuclear axis. In an electric field if the direction of motion of all electrons is reversed the energy of the molecule remains unchanged although the sign of M_L is changed. It follows therefore that only states with different $|M_L|$ have different energies. Hence, these molecular energy states are characterized by a quantum number Λ, where $\Lambda = |M_L|$. Λ can take the values $0, 1, 2, \ldots, L$ and the diatomic electronic states are designated Σ, II, Δ, ... respectively. II, Δ, ... states are doubly degenerate since M_L can have two values for each Λ. Σ states are nondegenerate.

When the value of Λ is nonzero, there exists an internal magnetic field along the internuclear axis caused by the orbital motion of the electrons. The effect of this field is to make total electron spin vector S precess about this axis with a constant component M_S. For molecules M_S is denoted by Σ and

it can take the values S, S-1, ... , -S. That is, it can have (2S + 1) different values. This factor, which is called the multiplicity of the electronic state, is added as a left superscript to the electronic state symbol like $^3\Pi$ when S=1. Even though the value of Σ is not defined for a $\Lambda = 0$ state, the value of (2S + 1) is given as the multiplicity of a state irrespective of the value of Λ .

Now the component of total angular momentum along the internuclear axis which is called ω can be obtained by adding Λ and Σ, i.e.,

$$\Omega = |\Lambda + \Sigma| \qquad\qquad (1.1)$$

The value of $\Lambda + \Sigma$ is indicated as a right subscript to the main symbol of the state, i.e., for $\Lambda = 1$, S = 1 we get the states $^3\Pi_2$, $^3\Pi_1$ and $^3\Pi_0$.

The two-fold degeneracy of a state for $\Lambda \neq 0$ is not affected by the spin. It exists as long as $\Lambda \neq 0$. However, this degeneracy for the state with $\Omega = 0$ and $\Lambda \neq 0$ is lifted when the finer interactions of the electrons are considered and we get two sublevels with slightly different energies which are designated as 0^+ and 0^- states. Thus, for $^3\Pi_0$ state we get $^3\Pi_{0^+}$ and $^3\Pi_{0^-}$ states. For the states where $\Lambda = 0$, the wave function either changes sign or remains unchanged when reflected in any plane passing through both the nuclei. When the wave function changes sign, it is called

Σ^- and Σ^+ otherwise. The same is the case for $^3II_{0^-}$ and $^3II_{0^+}$ states and for states similar to them.

For homonuclear diatomic molecules there exists another kind of symmetry which is a centre of symmetry. The states are given the right subscripts g or u according as the wave function of the state does not or does change sign when all the electrons and the nuclei are reflected through a point which is the midpoint of the line joining the two nuclei. Here g stands for gerade and u for ungerade in German which means even and odd respectively. This property holds for both degenerate and non-degenerate states [4].

Electron Configuration in a Molecule

The stationary energy states of a molecule,obtained when each electron in a molecule is considered to be moving in an axially symmetric force field due to the two nuclei and the other electrons, can be charecterized by three quantum numbers. These can be obtained in two different ways. One way corresponds to very small internuclear distance and the other to very large internuclear distance. In both approaches λ, the component of orbital angular momentum (l) is a good quantum number. The possible values of λ are $0,1,2, \ldots l$ and an electron is called $\sigma, \pi, \delta, \varphi \ldots$ electron according as $\lambda = 0,1,2, \ldots$ respectively. As for the other two quantum numbers, in the united atom approach (r = 0),the states are

defined by the quantum numbers n and l which are still approximately defined. Thus, the energy levels are given by 2sσ, 3pπ, etc., where 2,3; s,p; and σ,π denote the values of n, l and λ respectively.

In the case where the internuclear distance is very large (r—>∞), the electrons may be considered to be with either of the nuclei and the quantum number λ is still defined. To designate an energy level, the values of n and l which an electron has while it is associated with one of the atoms are added after the symbol which gives the value of λ . For example, σls, π2p, etc. In the case of homonuclear molecules the electron states are even (g) or odd (u) according as the eigen function remains unchanged or changes sign when reflected at the origin. In the united atom approach, a state is odd or even depending on whether it has an odd or even l value, for example, $1s\sigma_g$, $2s\sigma_g$, $2p\pi_u$ etc., where as in the seperated atom approach there exists a u state for every g state. Thus, there are $\pi_u 2p$ and $\pi_g 2p$ states. These electronic energy states of a molecule , which correspond to the motion of electron apart from spin, are called orbitals [5]. The energy states corresponding to the internuclear distances which are intermediate to the above two limiting cases can be obtained by interpolating between the two limiting cases, keeping in mind that a σ or π state in the united atom approach can go over to a σ or π state only in the seperated atom approach. As for homonuclear molecules, a g

state would go to a g state and a u state to a u state only. Mulliken gives semi-quantitative energy curves for the intermediate internuclear distances on the basis of empirical data [6].

Just as in atoms, in molecules the number of electrons in an orbital is limited by the Pauli principle, according to which a σ orbital, for which $\lambda = 0$, is closed with two electrons and π or δ ... orbitals, for which $\lambda \neq 0$, are closed with four electrons. These are the maximum number of electrons for which all the four quantum numbers (n, l, m_l, m_s) are different. The electrons in a molecule which have the same n, l and m_l and also the same symmetry g or u are called equivalent electrons. While giving the electronic configuration the number of electrons in an orbital is given as an exponent. For example, for F_2 which is a homonuclear diatomic molecule with 18 electrons, the lowest electronic configuration is $(\sigma_g 1s)^2$ $(\sigma_u 1s)^2 (\sigma_g 2s)^2 (\sigma_u 2s)^2 (\sigma_g 2p)^2 (\pi_u 2p)^4 (\pi_g 2p)^4$. It is customary to denote the atomic orbitals which are unaffected by the formation of the molecule as K, L ... etc. So the above configuration can be written as KK $(\sigma_g 2s)^2 (\sigma_u 2s)^2 (\sigma_g 2p)^2$ $(\pi_u 2p)^4 (\pi_g 2p)^4$. The state corresponding to this configuration is the ground state of the molecule which is $^1\Sigma_g^+$ for F_2. All the halogen molecules have similar electronic configuration with the values of n varying from 2 to 5 in the outermost shell from F_2 to I_2. The excited states are obtained when one

or more of the outer electrons are transferred to higher orbitals. If a molecule under consideration is large, the seperated atom approach is more applicable to get the electronic configuration and corresponding electronic states, while the united atom approach is more applicable for small molecules.

Coupling of Angular Momenta

In a diatomic molecule in addition to the orbital and spin motions of the electrons, there can be a rotational motion of the two nuclei as a unit and the spin of one or both nuclei. Nuclear spin angular momentum is often neglected. Hund has considered five different possible ways of combining the motion of the electrons and the rotation of the nuclei in a molecule to get the total angular momentum of a molecule in a particular state. These are generally known as Hund's coupling cases. Four of these which have more practical importance are discussed below.

Case (a): In this case the internuclear distance is assumed to be small and the electric field of the two nuclei is strong enough to uncouple the orbital (L) and spin (S) angular momenta and to make them precess about the internuclear axis. In this case Λ, Σ and Ω described before are defined. Now, the nuclei in the rigid diatomic molecule may be regarded as rotating as a whole about an axis perpendicular to the internuclear axis and having angular momentum of rotation $Nh/2\pi$

along this direction. The quantum number associated with rotation is N. Ω and N are added vectorially to form a resultant angular momentum quantum number J, i.e., $J = N + \Omega$, where $J = \Omega$, $\Omega + 1$, ... For a given electronic state Ω is constant and levels with $J < \Omega$ do not occur.

Case (b) : This case differs from case (a) in that the magnetic field associated with the precession of L around internuclear axis is not strong enough to make S precess around this axis. In this case Λ combines directly with N to give resultant angular momentum apart from spin which is designated as K, which takes the values Λ , $\Lambda + 1$, ... This K combines with spin S to give total angular momentum J, where J takes the values $|K + S|$ ... , $|K - S|$. This implies that each rotational level with a particular K has $(2S + 1)$ components.

Case (c) : When the internuclear distance is large, the field due to the two nuclei will not be strong enough to uncouple L and S. Hence, L and S combine to give resultant angular momentum J_a which precesses around internuclear axis while L and S precess around J_a. The component of J_a along internuclear axis is Ω . Finally, Ω and N combine to give the total angular momentum J.

Case (d) :   In this case the interaction of L with nuclear
rotation is stronger than its interaction with the field due
to the two nuclei along the internuclear axis.   The nuclear
rotational angular momentum,which is denoted by R in this case,
combines with L to give K which finally combines with S to
give J, the total angular momentum.   Sometimes the coupling
between K and S is so small that it is disregarded and only
K is considered for all practical purposes.

Electronic Transitions in a Diatomic Molecule

The total energy of a molecule in a particular electro-
nic state is generally resolved into three components as

$$E = E_e + E_v + E_r \qquad (1.2)$$

where E_e is the minimum of the potential energy curve of the
electronic state and E_v is vibrational energy of the nuclei
and E_r is the energy corresponding to their rotation.   When
different parts are expressed in wave number units (cm^{-1})
we get

$$T = T_e + G + F \qquad (1.3)$$

where $G = \omega_e(v + \frac{1}{2}) - \omega_e x_e(v + \frac{1}{2})^2 + \ldots$ \qquad (1.4)

and $F = B_v[J(J + 1)] - D_v[J(J + 1)]^2 + \ldots$ \qquad (1.5)

Here ω_e, $\omega_e x_e$ ... are vibrational constants and B_v, D_v etc.,
are the rotational constants.   The suffix v for the rotational

constants denote that these constants are different for each vibrational level. The dependence of these constants on the vibrational quantum number v is given to first approximation by

$$B_v = B_e - \alpha_e(v + \tfrac{1}{2}) + \gamma_e(v + \tfrac{1}{2})^2 + \ldots \tag{1.6}$$

$$D_v = D_e + \beta_e(v + \tfrac{1}{2}) + \ldots \tag{1.7}$$

where B_e corresponds to the equilibrium internuclear separation (R_e). The following equation gives the relation between R_e and B_e.

$$B_e = h/8\pi^2 c\mu R_e^2 \tag{1.8}$$

where h is the Planck's constant, μ is the reduced mass of the molecule and c is the velocity of light. The wavenumbers of spectral lines, corresponding to a transition between two electronic states, are given by

$$\nu = T' - T'' = (T_e' - T_e'') + (G' - G'') + (F' - F'') \tag{1.9}$$

where single primed letters correspond to the upper state and double primed letters correspond to the lower state. Hereafter the same notation is followed. Equation (1.9) can be rewritten as

$$\nu = \nu_e + \nu_v + \nu_r \tag{1.10}$$

For a particular electronic transition ν_e is constant. When the vibrational structure of an electronic transition is considered, the $\nu_r = (F' - F'')$, the rotational contribution

to energy can in general be neglected as $\nu_r \ll \nu_v$. Now substituting Equation (1.4) for G' and G" in Equation (1.9) we get

$$\nu = \nu_e + [\omega_e'(v' + \tfrac{1}{2}) - \omega_e'x_e'(v' + \tfrac{1}{2})^2$$
$$+ \omega_e'y_e'(v' + \tfrac{1}{2})^3] - [\omega_e''(v'' + \tfrac{1}{2})$$
$$- \omega_e''x_e''(v'' + \tfrac{1}{2})^2 + \omega_e''y_e''(v'' + \tfrac{1}{2})^3] \quad (1.11)$$

Equation (1.11) represents all possible transitions between the different vibrational levels of the two particular states involved in an electronic transition . There is no selection rule for these vibrational transitions. Each vibrational level of the lower/upper electronic state can combine with each vibrational level of upper/lower electronic state. But the intensity of vibrational transitions is governed by Franck–Condon principle.

When the rotational structure of a particular vibrational transition between two electronic states is considered the quantity $\nu_o = \nu_e + \nu_v$ is constant, whereas ν_r, the rotational contribution, is a variable and depends on the rotational quantum numbers in the upper and lower states. For a particular ν_o, all the possible rotational transitions form a vibrational band whose line frequencies are given by

$$\nu = \nu_o + F'(J') - F''(J'') \quad (1.12)$$

where ν_0 corresponds to the zero line and is called band origin. Substituting for $F'(J')$ and $F''(J'')$, we get

$$\nu = \nu_0 + [B_v' J'(J' + 1) - D_v'(J'(J'+ 1))^2]$$

$$- [B_v''(J''(J'' + 1)) - D_v''(J''(J'' + 1))^2] \quad (1.13)$$

The selection rule for J is

$$\Delta J = 0, \pm 1 \text{ when } \Lambda \neq 0, \text{ and}$$

$$\Delta J = \pm 1 \quad \text{when } \Lambda = 0 \text{ for both the states involved}$$

When $\Delta J = 0$ we get a Q branch and when $\Delta J = \pm 1$ we get R and P branches respectively. The expressions for the wave numbers of these branches are as follows:

R branch : $\nu = \nu_0 + F_v'(J + 1) - F''(J) = R(J)$ (1.14)

P branch : $\nu = \nu_0 + F'(J - 1) - F''(J) = P(J)$ (1.15)

Q branch : $\nu = \nu_0 + F'(J) - F''(J) = Q(J)$ (1.16)

where J is the rotational quantum number of the lower state and F(J)s are given by Equation (1.5).

The following equations giving the combination diffe-rences are most useful in the rotational analysis of a band system. They give the separation between one particular rotational energy level in a vibrational state from the level which is next but one to it.

$$\Delta_2 F''(J) = R(J - 1) - P(J + 1) = F_v''(J + 1)$$
$$- F_v''(J - 1) \qquad (1.17)$$

$$\Delta_2 F'(J) = R(J) - P(J) = F_v'(J + 1) - F_v'(J - 1) \qquad (1.18)$$

Substituting for different $F(J)$, we get

$$\Delta_2 F''(J) = 4B_v'' \left(J + \tfrac{1}{2}\right) - 8D_v'' \left(J + \tfrac{1}{2}\right)^3 \qquad (1.19)$$

$$\Delta_2 F'(J) = 4B_v' \left(J + \tfrac{1}{2}\right) - 8D_v' \left(J + \tfrac{1}{2}\right)^3 \qquad (1.20)$$

It is evident that, if $\Delta_2 F$ vs J is plotted it will be straight line passing through* $J = -\tfrac{1}{2}$ with a slope $4B_v$, and also that the combination differences for different bands with common lower or upper vibrational state should agree within the experimental error. This fact is one of the best guidelines to decide the rotational numbering in a band while doing the rotational analysis.

* zero at

REFERENCES

1. G. Herzberg, Spectra of Diatomic Molecules, Van Nostrand, New York (1950).

2. B.P. Straughan and S. Walker, Spectroscopy, Vol.3, Chapman and Hall, London (1976).

3. L. Pauling and E.B. Wilson, Introduction to Quantum Mechanics, McGraw-Hill, New York (1935).

4. E. Wigner and E.E. Witmer, Z. Physik 51, 859 (1928).

5. R.S. Mulliken, Phys. Rev. 41, 49(1932).

6. R.S. Mulliken, Rev. Mod. Phys. 4, 1(1932).

CHAPTER 2

METHOD OF ROTATIONAL ANALYSIS

Introduction

A good part of the present work deals with the study of rotational structure of the electronic transitions of I_2. So, it was felt desirable to discuss the method of rotational analysis in this chapter.

Rotational analysis of molecular spectra consists of recognizing the band structure of the band system and grouping the measured line positions of the system into different bands. Once this is done, the band system can be analysed. Until recently, the approach to analysing a band system has been to treat each band separately while calculating the molecular constants. But, in many instances this approach leads to

multiple values for each of the molecular constants of the
common vibrational levels, as two or more bands in a band
system are likely to have a common upper or lower vibrational
level. This indicates that this approach is inadequate and
there must be a way to treat the system as a whole and get a
more precise 'single' value for each constant. It is possi-
ble to get a single value for these constants by simply taking
the average of multiple values but this would not indicate
anything about the precision of each value for the constant.
Even when the weighted averages are taken, the strong correla-
tions that exist between the errors of the many pairs of
molecular constants are ignored. To overcome this difficulty,
usually, some of the constants are held fixed at the values
which are obtained from high resolution data and the rest of
the constants together with the errors are then evaluated.
But even this method suffers from the disadvantage of assuming
that the error in the fixed value is negligible compared to
those in the other constants. To obviate such problems,
Albritton et al. [1,3] have suggested a general technique
in which the constants obtained from the band-by-band analysis
are merged to get the best single value for each molecular
constant. This method is generally being followed in analy-
sing the band systems. This method enables one to determine
the minimum variance value of a parameter giving proper stati-
stical weightage to different measurement precision and

correlation. This method is followed in analysing the rotational structure of the band systems of the iodine molecule in the regions (3460–3015 Å) and (4320–4000 Å) presented in Chapters 4 and 5. The details of the method are discussed in this chapter.

Rotational Analysis

The band systems, analysed in Chapters 4 and 5, are of the type $(^{3}\Pi_{2g} \longrightarrow {}^{3}\Pi_{2u})$ and $(\; 0_{g}^{+} \longrightarrow {}^{3}\Pi_{0^{+}u})$ respectively. According to the selection rules, the latter consists of only P and R branches in each band, while the former consists of strong P and R branches and a weak Q branch. The Q branch intensity falls off very rapidly with increasing J and is approximately proportional to

$$\frac{1}{J} \exp \left(\frac{-F_{v}(J)h\,c}{k\,T} \right)$$

where $F_{v}(J)$ is the term value corresponding to the upper state rotational level. Thus, the measurable structure in a vibrational band in both systems is only R and P branches. From Equation (1.13) the P and R branches can be expressed as

$$P(J) = \nu_{0} - B_{v}''[J(J + 1)] + B_{v}'[J(J - 1)]$$
$$+ D_{v}''[J(J + 1)]^{2} - D_{v}'[J(J - 1)]^{2} \quad (2.1)$$

and
$$R(J) = \nu_{0} - B_{v}'' [J(J + 1)] + B_{v}'[(J + 1)(J + 2)]$$
$$+ D_{v}''[J(J + 1)]^{2} - D_{v}'[(J + 1)(J + 2)]^{2}$$
$$(2.2)$$

where B_v'', D_v'' are the lower electronic state constants, B_v', D_v' are the upper electronic state constants and ν_o is the band origin or the $J' = 0 \longrightarrow J'' = 0$ transition of the vibrational band.

Equations (2.1) and (2.2) representing a vibrational band can be expressed by a single matrix equation [1] as

$$Y_k = X_k \, \beta_k + \delta_k \quad , \quad k = 1,2,3 \ldots \tag{2.3}$$

where Y_k is a column vector containing m elements which are the measured line positions of P and R branches of each band k. β_k is also a column vector with 5 elements which are the required molecular constants of upper and lower electronic states. X_k, the coefficient matrix, is of the order m x 5 and contains elements like 1, $J(J + 1)$, $J(J - 1)$, $[J(J + 1)]^2$, $[J(J - 1)]^2$ for representing P branch and elements like 1, $J(J + 1)$, $[(J + 1)(J + 2)]$, $[J(J + 1)]^2$, $[(J + 1)(J + 2)]^2$ for representing R branch for all the J values where J takes, on the whole, m values. δ_k gives the unknown measurement errors corresponding to each line.

The least-squares solution to Equation (2.3) giving the molecular constants β_k is

$$\beta_k = (X_k^T X_k)^{-1} \, X_k^T Y_k \tag{2.4}$$

and the corresponding variance-covariances are given by

$$V_k = \sigma_k^2 \, (X_k^T X_k)^{-1} \quad , \quad k = 1,2,3 \ldots \tag{2.5}$$

where the estimated variance is

$$\sigma_k^2 = (Y_k - X_k \beta_k)^T (Y_k - X_k \beta_k)/(m - 5) \qquad (2.6)$$

If a set of three bands, for example, (0-1), (0-2) and (0-3) in a band system is considered, the band-by-band reduction using Equations (2.3 - 2.6) would yield as many as 15 molecular constants, 5 per band and 3 accompanying 5 x 5 variance-covariance matrices V_k, k = 1,2,3. The differences in the precision of the molecular constants from different bands due to different measurement errors and also due to differences in the number of lines fitted is made evident in their variance-covariances. The multiple values for the constants for v' = 0 state will be very nearly equal but will almost never be identical. Out of the 15 constants in hand, only 11 are the required basic molecular constants. According to Albritton et al., the minimum variance, linear and unbiased values to the required constants, taking into account the different precision of values and the nonzero correlation between them can be obtained (as described below) by merging the output from the different band-by-band least-squares fits.

Merging of the Multiple Molecular Constants

The constants of (0-1), (0-2) and (0-3) bands considered above can be expressed in matrix form

$$Y = X\beta + \delta \qquad (2.7)$$

where Y, β are column vectors containing the rotational constants* which are obtained by separate band-by-band least-squares fits and the non-redundant single values for the constants respectively, and δ is also a column vector giving the errors in each constant. X is the coefficient matrix which relates the redundant constants in Y to the non-redundant ones in β through their individual errors. For example, if B'_o values from (0-1) and (0-2) bands are the second and seventh elements in the column vector Y, they can be seen to be related to their best single value as follows:

$$B'_{o(0-1)} = B'_o + \delta_2 \qquad (2.8a)$$

$$B'_{o(0-2)} = B'_o + \delta_7 \qquad (2.8b)$$

These equations indicate that apart from the unknown errors δ_2 and δ_7 the values obtained for B'_o from different bands are equal. The redundant values are almost never equal. The least-squares solution of the over-determined Equation (2.7), finds the values for the molecular constants β that minimize the sum of the squares of the unknown δ , subject to known interrelations among δ . These interrelations arise because the variance-covariance matrices V_k associated with each β_k, k = 1,2,3, generally, do not have equal diagonal elements and zero off-diagonal elements. To account for this unequal variance and nonzero covariance, Albritton et al. used the weighted, correlated least-squares formalism to find

* and band origins

the solution of the Equation (2.7). The molecular constants that minimize $\delta^T \delta$, subject to the interrelation contained in V_k, k= 1,2,3, are given by

$$\beta_M = (X^T V^{-1} X)^{-1} X^T V^{-1} Y \tag{2.9}$$

where V is the non-diagonal (15 x 15) matrix composed of the individual V_k as

$$V_k = \begin{bmatrix} V_1 & 0 & 0 \\ 0 & V_2 & 0 \\ 0 & 0 & V_3 \end{bmatrix}, \tag{2.10}$$

The precision of the estimates β_M, is indicated by their standard errors which are the square roots of the diagonal elements of the variance-covariances matrix associated with β_M given by

$$U = \sigma_M^2 V_M \tag{2.11}$$

where the merged dispersion matrix is given by

$$V_M = (X^T V^{-1} X)^{-1} \tag{2.12}$$

The estimated variance of the merged fit σ_M^2 is given by

$$\sigma_M^2 = (Y-X\beta_M)^T V^{-1} (Y-X\beta_M) / f_M \tag{2.13}$$

where the degrees of freedom of the merged fit are denoted by f_M which is equal to the difference between the redundant and non-redundant constants.

A computer programme which is run on a DEC-10 system is developed [4,5] to the above described formalism, in which provisions are made to change the rotational numbering of R

branch and P branch simultaneously, to change the absolute J numbering in the two branches or individually to change the relative J numbering. As both the band systems are red degraded, the head is formed in the R branch, and in the case of some bands the P and R branch lines are not resolved completely due to insufficient resolution of the spectrum. The R branch lines of particular rotational number J, are overlapping the P branch lines of rotational number (J-n) where n is varying from band to band. For this reason, the programme is so written that the 'n' value also can be varied at will. The programme was run for each band for different combinations of absolute and relative J numbering and the standard deviation and variances of the fit are calculated. The J numbering for a band is fixed depending upon the low variance of the constants and the goodness of the fit and the internal consistency of the rotational constants i.e., the expected smooth variation of B_v as a function of v for a particular electronic level. In addition, the agreement of the calculated band origins with those reported earlier is considered while assigning the J numbering.

In the case of bands sharing an upper or lower vibrational level the constants from the band-by-band least-squares fits are merged as described above to get the final constants.

REFERENCES

1. D.L. Albritton, A.L. Schmeltekopf and R.N. Zare, J. Mol. Spectrosc. 67, 132(1977).

2. D.L. Albritton, A.L. Schmeltekopf, W.J. Harrop, R.N. Zare and J. Czarny, J. Mol. Spectrosc. 67, 159 (1977).

3. D.L. Albritton, W.J. Harrop, A.L. Schmeltekopf, R.N. Zare and E.L. Crow, J. Mol. Spectrosc. 46, 67 (1973).

4. Samuel D. Conte and Carl de Boor, Elementary Numerical Analysis, McGraw-Hill Int. Book Co., Tokyo, Japan(1980).

5. F.B. Hilderbrand, Introduction to Numerical Analysis, Tata Mcgraw-Hill Co. Ltd., New Delhi (1982).

CHAPTER 3

VIBRATIONAL ANALYSIS OF
D' $\longrightarrow$ A' EMISSION SYSTEM OF I_2

Introduction

Diatomic molecules render themselves easy targets whenever attempts to study the molecular structure are made. Among them halogens are the most intensively studied class of molecules. There is an abundance of information about these molecules, theoretically as well as experimentally. Mulliken's classic review of I_2 [1] gives most of the information regarding iodine molecule. With the advent of lasers, there has been a renewed interest in halogen spectroscopy. Many of the high lying electronic states, which could not be studied through the conventional spectroscopic methods, can now be studied by laser spectroscopy, as these states have now become accessible through a variety of single and multiphoton

excitation processes [2-5]. In addition to this, a number of electronic transitions in halogens proved to be good laser sources in the ultraviolet and visible regions. Optically pumped molecular iodine and bromine lasers have been developed in the visible region [6,7]. Lasing has also been achieved in the ultraviolet transitions of iodine at 3400 Å [8,9], bromine at 2900 Å [10,11], chlorine at 2600 Å [12] and fluorine at 1600 Å [13].

In this chapter the vibrational analysis of the emission system of I_2 at 3400 Å is presented. The valence states of I_2 are described below in brief.

The molecular orbital electronic configuration of the type $\sigma_g^2 \; \sigma_u^2/\sigma_g^m \; \pi_u^n \; \pi_g^p \; \sigma_u^q$, with $m + n + p + q = 10$ and molecular orbitals σ_g, σ_u of the form $5s \pm 5s$ and $5p\sigma \pm 5p\sigma$ and π_u, π_g of the form $5p\pi \pm 5p\pi$ in the simplest LCAO approximation [1], gives the valence-shell electronic states of I_2 molecule. To denote different electronic configurations Mulliken used the notation mnpq. The ground state of I_2 corresponds to 2440 configuration. The lowest excited states belong to 2431 configuration, which is obtained by exciting one π_g electron to the vacant σ_u orbital. Similarly, other electronic states are obtained by exciting other electrons to the vacant orbitals. I_2 has 23 valence states which correlate with the ground term (^2P) atoms-10 arising from $^2P_{3/2} + ^2P_{3/2}$, 10 from $^2P_{3/2} + ^2P_{1/2}$ and 3 from $^2P_{1/2} + ^2P_{1/2}$. Above these,

the higher energy valence states have ion-pair structure and tend to dissociate into $I^-(^1S) + I^+(^3P_2$ or $^3P_1$ or $^3P_0$ or ^1D or $^1S)$. All these ion-pair states are expected to have at least one strong transition to the low lying valence states and a number of such transitions have actually been observed and studied.

When I_2 vapour at low pressures is excited by vacuum ultraviolet sources, its fluorescence displays a discrete resonance spectrum at short wavelengths, followed by numerous diffuse bands extending upto $\sim$4800 Å[1]. When inert buffer gas is added, the fluorescence spectrum undergoes a remarkable transformation, with most of the diffuse bands disappearing and several well-defined band systems appearing in their place [14]. The emission spectrum excited by a high frequency or Tesla discharge is very similar to the fluorescence spectrum in appearance and pressure dependence [15-19]. In the high pressure limit, all the band systems appear to originate from ion-pair states having near Boltzmann vibrational and rotational population distribution at temperatures near the ambient [19]. Of the band systems which appear in the high pressure emission spectrum, well developed vibrational structure appears in four: 2700-2500 Å, 2785-2730 Å, 3460-3015 Å and 4320-4000 Å. All these band systems except the one in the region (2785-2730 Å) were first recorded by Elliot [14]. The band system in this region was first reported by Venkateswarlu [16]. In addition to these four discrete band systems, Venkateswara Rao[20]

obtained a fifth band system in the region (2500–2400 Å)
by using a condensed transformer discharge. There is a
general consensus about the interpretation of the band
systems in the region (2700–2500 Å) and (4320–4000 Å) as
(F —> X) and (E —> B) respectively. The (2785–2730 Å)
system has recently been assigned $1g \longrightarrow A(^3II_{1u})$ [21].
However, the dominant band system around 3400 Å has remained
a subject of controversy and puzzlement. As this system is
of particular importance as a laser source [8,9], the vibra-
tional and rotational analysis of this system is taken up in
the present work. The vibrational analysis and the corres-
ponding discussion of this band system is presented in this
chapter, while the rotational analysis is presented in the
next chapter.

Vibrational Analysis

Earlier studies

Elliot has assigned this system to a transition termi-
nating on the X state [14]. Venkateswarlu [16], Weiland and
Waser [22] proposed different schemes with X state as the
lower state. Verma [17] suggested an entirely different ana-
lysis, according to which $B(^3II_{0}{}^+{}_u)$ is the lower state.

Venkateswarlu and Verma [23] reported a band system
of Bromine in the region (2950–2670 Å) which is analoguous to
3400 Å system of I_2. Similarly, Venkateswarlu and Khanna [24]

reported an analogous system of Cl_2 around 2500 Å. Later Briggs and Norrish [25] obtained the transient absorption spectra of Br_2 and Cl_2 in the region 2900 and 2500 Å, respectively, in flash photolysis in the presence of inert gas and suggested that these absorption band systems correspond to the emission band systems of these molecules in the corresponding regions. All of them suggested, the $B(^3II_{0^+u})$ state to be the lower state of these systems. However, the occurrence of the transient absorption of Br_2 and Cl_2 with life-time of about 50 μsec cast doubt on the assignment of $B(^3II_{0^+u})$ as the lower state. On this basis, Venkateswara Rao [26] during the period of his work in the University of Chicago (1963-65) reanalysed these band systems in transient absorption and suggested that $^3II_{2u}$, a metastable state of Br_2 as well as Cl_2 rather than $B(^3II_{0^+u})$ should be the lower state of these absorption band systems of Br_2 and Cl_2 obtained in flash photolysis.[++] This argument would hold good for the 3400 Å system of I_2, as this is analogous to the 2900 Å system of Br_2 and 2500 Å system of Cl_2.

Tellinghuisen reported briefly, his analysis of 3400 Å system of I_2 and 2900 Å system of Br_2 on the basis that the lower state is $^3II_{2u}$ [27]. The upper and lower states are designated as D' and A' respectively. While the work

---

presented in this chapterwas in progress,Tellinghuisen reported a detailed analysis of this system restricting himself to the region (3460-3300 $\mathring{A}$)[28]. He suggested that the bands below this region may probably belong to another system, D ---> X.

Present Vibrational Analysis

Attempts were made in the present work to fit all the bands reported [17] in the region (3460-3015 $\mathring{A}$)into a single vibrational scheme under two different assumptions: (i) B($^3II_{0+u}$) is the lower state and (ii) the $^3II_{2u}$ is the lower state. It is found that the analysis with the latter assumption explains most of the observed bands satisfactorily. While Tellighuisen's recent analysis of the bands covers the region(3460-3300 $\mathring{A}$)only, the present analysis covers the region 3460-3015 $\mathring{A}$. Most of the bands observed by Verma could be fitted into a single scheme with v' = 0 to 25 and v" = 0 to 39. All the bands which could be fitted into this scheme are least-squares fitted to the double-polynomial

$$\nu = \Delta T_e + \sum_{i=1}^{m} [\rho (v' + \tfrac{1}{2})]^i c_i' - \sum_{j=1}^{n} [\rho (v'' + \tfrac{1}{2})]^j c_j'' \tag{3.1}$$

with m = 4 and n = 4, where $\rho = 1.0$ for $^{127}I_2$ and $\rho = 0.99221$ for $^{129}I_2$.

The vibrational constants thus obtained are listed in Table 3.1. The constants of Tellinghuisen are also listed for comparison. In this present scheme, all the intense bands

are seen to be having low v' values. The difference between observed and calculated band head positions for Verma's data is at the most $\pm$ 3 cm^{-1}. The vibrational band heads along with their vibrational assignments are listed in Table 3.2. Though the ΔT_e value in the present work is the same as that of Tellighuisen, the other constants differ. This is because the present analysis includes more bands than those used by Tellighuisen.

Comments on High Temperature Absorption and Flash Discharge Absorption of the 3400 $\overset{o}{A}$ System of Iodine

Skorko [29] obtained under low dispersion the absorption spectrum of I_2 at high temperature. The bands reported by him are shown in Table 3.3. It is likely that these bands arise because of a transition between the same states as in emission . The emission bands which can be correlated with Skorko's bands are also listed in the Table 3.3. The agreement between them may be stated as satisfactory in view of the fact that Skorko recorded them under low dispersion.

As stated earlier, the 3400 $\overset{o}{A}$ system of I_2 is analogous to 2900 $\overset{o}{A}$ system of Br_2. Briggs and Norrish reported that while they could obtain in transient absorption through flash photolysis the 2900 $\overset{o}{A}$ system of Br_2 and 2500 $\overset{o}{A}$ system of Cl_2, they failed to observe the 3400 $\overset{o}{A}$ system of I_2. It may be noted that in the flash photolysis experiments high

pressures of foreign gas are used. Therefore, it is likely
that the lower state of the 3400 $\overset{\circ}{A}$ system gets quenched by
the presence of foreign gas where as it does not happen in
Br_2 and Cl_2.

Verma, Nagaraj and Venkateswarlu [30][++] carried out
flash discharge absorption experiments in iodine without using
foreign gas,so that the lower state of transient absorption
does not get quenched. The cell in which flash discharge
took place was a multiple reflection cell. With appropriate
time delay after the flash discharge,a separate Lymann conti-
nuous emissionwas flashed through the multiple reflection cell
for taking the transient absorption spectra. The band system
F —> X in the region (2700-2500 $\overset{\circ}{A}$) as well as 3400 $\overset{\circ}{A}$ system
of I_2 were recorded in this experiment. It was found on
comparison that the transient absorption data of Verma,
Nagaraj and Venkateswarlu agree closely with those of Skorko
in high temperature absorption and those in emission. This
suggests that the bands obtained in all these processes
correspond to one and the same electronic transition. It is
to be noted that while the lifetime of F —> X system was
observed to be of the order of 50 μsec, the lifetime of 3400 $\overset{\circ}{A}$
system was of the order of 6 μsec only. This observation

shows that the vibrational levels of lower state of 3400 $\overset{\circ}{A}$
system have a lifetime of about 6 μsec, while the vibrational
levels of the X state involved in F ⟶ X system have a life-
time of about 50 μsec. As the vibrational levels involved
in 2700 $\overset{\circ}{A}$ absorption are the higher vibrational levels
(v" > 42) of the X state, the above experiments indicate
that the lifetimes of the higher vibrational levels of X
state are of the order of 50 μsec while the lifetime of $^{3}II_{2u}$
state is 6 μsec. This probably sounds anamalous, as one
would expect the metastable $^{3}II_{2u}$ state to have longer life-
times than the higher vibrational levels of X state. Further
work will have to be done to explain this anamaly and to
confirm the assignment $^{3}II_{2g}$ ⟷ $^{3}II_{2u}$ of the system.

TABLE 3.1

Vibrational Constants of D' and A' States of I_2 valid for $v' = 0-25$ and $v'' = 0-39$

	Present work	Ref. (28)
ΔT_e	30341.15(40)	30340.82(92)
Upper state		
C'_1	103.705(158)	103.953(26)
C'_2	-0.182(25)	-0.2065(26)
C'_3	$-7.716(158) \times 10^{-4}$	-
C'_4	$8.647(32) \times 10^{-6}$	-
Lower state		
C''_1	105.90(10)	106.07(26)
C''_2	-0.810(12)	-0.813(27)
C''_3	0.03058(47)	0.03315(118)
C''_4	$5.337(62) \times 10^{-4}$	$6.203(179) \times 10^{-4}$

All the constants are in (cm^{-1}).

TABLE 3.2

The Wavenumbers and Vibrational Assignment of
D' $\longrightarrow$ A' System of $^{127}I_2$

v',v"	$\nu(cm^{-1})$	O–C	v',v"	$\nu(cm^{-1})$	O–C
2,21	28885.00	−1.77	8,32	29076.00	−1.37
3,23	.897.00	2.31	5,23	099.00	0.26
0,17	901.00	−0.64	0,14	099.00	1.63
4,25	913.00	1.20	7,28	105.00	0.91
7,34	.915.00	−3.77	8,31	105.00	−2.44
6,30	935.00	−1.82	2,17	105.00	−2.95
8,37	,935.00	0.69	5,25	114.00	−1.09
1,18	945.00	−0.51	6,25	118.00	2.91
7,33	945.00	−2.46	9,34	118.00	−1.71
4,24	956.00	2.78	1,15	135.00	2.45
7,32	975.00	−1.70	10,37	135.00	0.54
5,26	977.00	2.65	9,33	148.00	−0.39
2,19	994.00	2.16	3,18	151.00	−0.08
4,23	997.00	0.09	6,24	159.00	2.50
6,28	29003.00	−0.03	0,13	170.00	1.54
1,17	003.00	−1.98	8,29	170.00	−0.92
8,34	018.00	−1.44	8,29	173.00	2.08
0,15	029.00	−0.21	7,26	176.00	−0.86
7,30	036.00	−1.88	9,32	176.00	−1.64
9,37	036.00	1.42	5,21	193.00	−0.41
3,20	041.00	0.45	4,19	195.00	−1.65
4,22	041.00	−1.98	4,19	198.00	1.35
6,27	041.00	2.50	6,23	201.00	0.81
2,18	048.00	−0.48	8,28	206.00	1.25
8,33	048.00	−0.11	11,38	206.00	1.07
5,24	057.00	1.94	11,37	234.00	0.06
9,36	061.00	−2.08	11,37	235.00	1.06
1,16	067.00	−0.31	9,30	238.00	−0.82
7,29	070.00	−0.25	5,20	243.00	−1.61
6,26	076.00	0.20	0,12	243.00	0.52

TABLE 3.2 (Continued)

v',v''	$\nu(cm^{-1})$	O–C	v',v''	$\nu(cm^{-1})$	O–C
4,18	29252.00	−1.29	2,13	29376.00	−1.23
7,24	259.00	1.43	12,35	389.00	−0.79
9,29	270.00	−1.20	0,10	401.00	1.76
1,13	270.00	−1.80	6,19	401.00	1.06
3,16	270.00	−2.87	8,23	401.00	−0.02
1,13	273.00	1.20	3,14	407.00	0.73
8,26	280.00	2.47	11,31	407.00	−0.06
11,35	290.00	−0.72	10,28	407.00	2.60
6,21	297.00	2.14	5,17	413.00	−1.59
5,19	297.00	−1.49	1,11	420.00	−2.76
5,19	299.00	0.51	9,25	420.00	2.91
7,23	303.00	1.75	1,11	422.00	−0.76
9,28	303.00	−2.03	11,30	438.00	−0.18
2,14	303.00	−0.68	4,15	438.00	−2.33
10,31	306.00	−1.59	7,20	448.00	0.88
12,38	306.00	2.00	8,22	448.00	−0.01
4,17	311.00	−1.76	12,33	448.00	1.19
8,25	316.00	−0.82	9,24	461.00	2.49
0,11	320.00	0.58	0, 9	481.00	−0.89
0,11	322.00	2.58	8,21	499.00	2.41
12,37	335.00	1.99	9,23	503.00	0.80
9,27	340.00	−0.51	7,19	503.00	2.00
7,22	349.00	1.66	1,10	503.00	0.42
11,33	349.00	1.26	12,31	508.00	1.87
8,24	357.00	−1.23	4,14	508.00	−0.49
5,18	357.00	1.87	4,14	509.00	0.51
10,29	369.00	−2.07	10,25	520.00	3.03
9,26	376.00	−1.81	2,11	528.00	2.27
11,32	376.00	−0.99	8,20	545.00	−2.79
4,16	376.00	0.91	3,12	553.00	1.61

TABLE 3.2 (Continued)

v',v''	$\nu(cm^{-1})$	O–C	v',v''	$\nu(cm^{-1})$	O–C
10,24	29561.00	2.62	13,28	29702.00	-0.12
0,8	566.00	-1.33	3,10	706.00	-2.14
11,26	579.00	1.84	8,17	720.00	2.23
4,13	579.00	-0.58	4,11	731.00	0.46
8,16	579.00	0.62	0,6	746.00	-0.28
1,9	582.00	-3.23	7,15	746.00	1.33
1,9	584.00	-1.23	11,22	746.00	-1.63
9,21	595.00	-1.87	10,20	746.00	-1.93
9,21	596.00	-0.87	5,12	753.00	-2.44
8,19	599.00	-2.57	1,7	761.00	2.17
8,19	602.00	0.33	9,18	761.00	2.42
10,23	602.00	-0.07	2,8	774.00	0.36
12,28	604.00	0.55	8,16	779.00	-1.11
12,28	606.00	2.55	6,13	785.00	2.13
5,14	612.00	1.68	3,9	791.00	0.20
11,25	615.00	-1.44	11,21	796.00	-0.22
7,17	615.00	-2.10	12,23	799.00	-1.62
3,11	628.00	-0.32	10,19	800.00	-1.82
12,27	639.00	0.07	4,10	813.00	2.64
9,20	647.00	-1.06	7,14	813.00	0.16
10,22	647.00	-1.16	13,25	816.00	1.82
4,12	654.00	0.39	9,17	820.00	1.95
0,7	654.00	-1.49	5,11	832.00	-0.38
1,8	672.00	1.33	0,5	839.00	-0.62
5,13	684.00	2.58	8,15	846.00	0.66
2,9	686.00	-2.20	12,22	846.00	-0.70
2,9	688.00	-0.20	11,20	846.00	-1.41
10,21	696.00	-0.74	1,6	852.00	2.38
9,19	702.00	0.06	6,12	857.00	0.11
11,23	702.00	0.45	10,18	857.00	-1.46

TABLE 3.2 (Continued)

v',v''	ν (cm^{-1})	O–C	v',v''	ν (cm^{-1})	O–C
2,7	29861.00	−0.80	1,3	30135.00	−1.80
3,8	876.00	−0.24	0,2	135.00	1.27
9,16	882.00	1.62	11,15	146.00	1.03
7,13	882.00	−1.93	5,7	169.00	0.55
4,9	891.00	−2.01	10,13	186.00	1.25
11,19	899.00	−2.29	7,9	198.00	0.64
8,14	913.00	−0.50	11,14	214.00	0.87
5,10	913.00	0.81	8,10	214.00	−1.37
1,5	944.00	1.05	12,15	243.00	−1.04
12,20	947.00	0.52	3,4	243.00	−1.29
2,6	952.00	−0.59	10,12	259.00	0.23
11,18	960.00	2.07	5,6	259.00	−0.24
7,12	960.00	2.05	6,7	270.00	0.10
3,7	965.00	0.60	11,13	283.00	−1.22
10,16	979.00	−1.26	7,8	283.00	0.20
4,8	979.00	0.54	8,9	297.00	−1.03
8,13	982.00	−2.60	9,10	315.00	−0.65
5,9	995.00	0.15	10,11	334.00	−1.71
12,19	30003.00	2.64	3,3	341.00	−1.37
9,14	014.00	0.22	2,2	341.00	0.96
6,10	014.00	0.36	1,1	341.00	1.63
1,4	039.00	0.28	0,0	341.00	0.79
4,7	067.00	0.39	4,4	348.00	1.50
11,16	080.00	0.27	5,5	353.00	0.43
5,8	080.00	−0.29	6,6	363.00	2.31
9,13	087.00	2.13	7,7	370.00	−0.96
6,9	096.00	−0.30	12,13	385.00	1.70
10,14	113.00	−0.65	8,8	385.00	1.53
7,10	113.00	−1.70	9,9	399.00	0.70
8,11	135.00	−0.56	11,11	433.00	−2.18

TABLE 3.2 (Continued)

v',v''	$\nu(cm^{-1})$	O–C	v',v''	$\nu(cm^{-1})$	O–C
3,2	30440.00	−2.63	8,5	30655.00	−0.75
2,1	440.00	−2.14	17,16	667.00	−1.06
3,2	443.00	0.37	10,7	670.00	−1.78
2,1	443.00	0.66	11,8	682.00	−1.10
1,0	443.00	−0.55	13,10	714.00	1.26
12,12	458.00	0.68	14,11	729.00	−2.18
7,6	462.00	0.25	15,12	754.00	1.90
9,8	483.00	−0.74	4,0	754.00	2.66
10,9	499.00	0.82	8,4	754.00	2.48
15,15	540.00	1.18	9,5	754.00	−2.03
2,0	545.00	−1.52	11,7	771.00	−0.25
3,1	545.00	0.06	15,13	775.00	−0.52
4,2	545.00	0.16	17,14	799.00	−2.46
5,3	545.00	−1.42	16,12	849.00	−0.54
13,12	555.00	−0.99	7,2	849.00	−0.20
7,5	555.00	−0.08	6,1	849.00	−1.44
8,6	562.00	−0.42	8,3	849.00	−0.60
16,16	572.00	0.97	9,4	851.00	−0.79
9,7	572.00	0.10	6,1	851.00	0.56
10,8	583.00	−0.62	5,0	851.00	−2.17
11,9	599.00	1.34	10,5	857.00	1.10
12,10	615.00	0.93	17,13	870.00	−2.55
20,22	624.00	−0.58	12,7	870.00	−0.33
13,11	633.00	0.08	14,9	893.00	−0.66
3,0	649.00	−0.12	16,11	929.00	2.52
4,1	649.00	1.85	7,1	950.00	−1.50
5,2	649.00	2.31	8,2	950.00	0.13
6,3	649.00	1.13	9,3	950.00	0.12
7,4	649.00	−1.85	10,4	950.00	−1.67
14,12	655.00	0.75	20,16	956.00	−0.68

TABLE 3.2 (Continued)

v',v"	$\nu(cm^{-1})$	O–C	v',v"	$\nu(cm^{-1})$	O–C
6,0	30956.00	1.38	14,5	31250.00	–1.38
11,5	956.00	0.62	13,4	250.00	1.11
12,6	963.00	1.88	12,3	250.00	1.70
18,13	971.00	1.83	11,2	250.00	0.51
13,7	971.00	2.01	10,1	250.00	–2.32
21,17	986.00	–3.72	16,7	264.00	1.45
16,10	31006.00	–0.30	26,20	291.00	0.60
20,15	021.00	–0.91	23,15	306.00	–0.80
17,11	021.00	–2.51	20,11	312.00	–0.13
18,12	044.00	0.81	12,2	347.00	–1.56
12,5	055.00	0.55	13,3	347.00	0.03
7,0	055.00	–0.68	14,4	347.00	–0.15
8,1	055.00	2.83	15,5	347.00	–2.23
19,13	065.00	–0.38	22,13	353.00	1.49
14,7	065.00	–2.25	11,1	353.00	1.21
15,8	078.00	1.05	16,6	353.00	–0.34
17,10	102.00	–1.33	25,17	366.00	–1.08
21,15	115.00	–2.29	18,8	366.00	–2.04
19,12	136.00	–3.40	21,11	410.00	2.50
12,4	150.00	–0.22	25,16	426.00	–3.41
11,3	150.00	0.77	22,12	426.00	0.47
10,2	150.00	–0.02	23,13	447.00	0.05
9,1	150.00	–2.44	14,3	447.00	1.77
20,13	159.00	–2.17	15,4	447.00	2.00
14,6	159.00	0.95	16,5	447.00	0.33
16,8	172.00	–2.39	19,8	465.00	0.75
21,14	183.00	–2.45	21,10	487.00	–0.32
22,15	213.00	0.75	22,11	504.00	1.54
20,12	235.00	–0.19	23,12	521.00	0.02
23,16	242.00	0.44	24,13	541.00	0.81

TABLE 3.2 (Continued)

v',v"	$\nu(cm^{-1})$	O–C	v',v"	$\nu(cm^{-1})$	O–C
15,3	31541.00	−2.08	17,3	31739.00	1.44
16,4	541.00	−1.44	16,2	739.00	−1.79
13,1	548.00	−1.53	22,8	752.00	1.62
14,2	548.00	2.51	14,0	752.00	0.02
18,6	548.00	1.01	23,9	762.00	2.51
20,8	561.00	0.96	19,4	832.00	0.32
21,9	569.00	−0.98	19,3	932.00	1.72
15,2	644.00	0.65	19,2	32030.00	−0.64
19,6	644.00	0.80	21,3	121.00	−0.55
13,0	651.00	−2.72	21,1	325.00	−0.88
20,7	651.00	2.80	23,2	410.00	−1.20
24,11	692.00	0.86	24,2	506.00	0.04
20,6	739.00	0.01	25,2	600.00	1.14
19,5	739.00	2.47			
18,4	739.00	2.91			

O–C = Observed − Calculated

TABLE 3.3

Comparison of Absorption and Emission Bands of I_2 in the Region (3460–3015 Å)

Absorption Bands Skorko $\nu(cm^{-1})$	Emission Bands Ref.(17) $\nu(cm^{-1})$	Present Analysis v', v''
29239	29238	0, 12
29377	29376	2, 13
524	528	2, 11
673	672	1, 8
815	816	4, 10
940	944	1, 5
30048	30051	2, 5
211	214	8, 10
340	341	0, 0
452	458	6, 5
544	545	2, 0
637	633	5, 2
731	729	14, 11
807	805	14, 10
874	878	12, 7
970	971	13, 7
31056	31055	7, 0
133	136	19, 12
250	250	10, 1

TABLE 3.3 (cont.)

Absorption Bands Skorko $\nu(cm^{-1})$	Emission Bands Ref.(17) $\nu(cm^{-1})$	Present Analysis v', v"
358	353	10, 0
437	447	13, 2
526	525	16, 4
626	625	—
726	724	18, 4
827	831	22, 5
919	—	22, 6
32011	—	21, 4
32124	32121	20, 3
196	193	—
300	—	—
416	410	22, 11
500	506	24, 2
595	599	25, 2

REFERENCES

1. R.S. Mulliken, J. Chem. Phys. 55, 288 (1971).

2. M.D. Danyluk and G.W. King, Chem. Phys. 22, 59 (1977).

3. M. Kawasaki, K. Tsukiyama, M. Kuwana, K. Obi and I. Tanaka, Chem. Phys. Letters 67, 365 (1979).

4. H.P. Grienisen and R.E. Francke, Chem. Phys. Letters 88, 585 (1982).

5. U. Heemann, H. Knockel and Tiemann, Chem. Phys. Letters 90, 17 (1982).

6. J.B. Koffend and R.W. Field, J. Appl. Phys. 48, 4468 (1977).

7. F.J. Wodarczyk and H.R. Schlossberg, J. Chem. Phys. 67, 4476 (1977).

8. A.K. Hays, J.M. Hoffmann and G.C. Tisone, Chem. Phys. Letters, 39, 353 (1976).

9. J.J. Ewing, C.A. Brau, Appl. Phys. Letters, 27, 546 (1975).

10. J.R. Murray, J.C. Swingle and C.E. Turner, Jr., Appl. Phys. Letters, 28, 530 (1976).

11. J.J. Ewing, J.H. Jacob, J.A. Mangano, H.A. Brown, Appl. Phys. Letters, 28, 656 (1976).

12. A.K. Hays, Opt. Commun. 28, 209 (1979).

13. A.M. Diegelmann, and J.P. Reilly, Opt. Commun. 28, 104 (1979).

14. A. Elliot, Proc. Roy. Soc. London, A174, 273 (1940).

15. J. Waser and K. Wieland, Nature 160, 643 (1947).

16. P. Venkateswarlu, Phys. Rev. 81, 821 (1951).

17. R.D. Verma, Proc. Ind. Acad. Sci. 48A, 197 (1958).

18. K. Wieland, J.B. Tellinghuisen and A. Nobs, J. Mol. Spect. 41, 69 (1972).

19. A.L. Guy, K.S. Viswanathan, A. Sur and J. Tellinghuisen, Chem. Phys. Letters, 73, 582 (1980).

20. Y.V. Rao, Ph.D. Thesis (1961), Aligarh Muslim University, Aligarh.

21. K.S. Viswanathan, A. Sur and J.B. Tellinghuisen, J. Mol. Spect. 86, 38 (1981).

22. K. Wieland and J. Waser, Phys. Rev. 85, 385 (1952).

23. P. Venkateswarlu and R.D. Verma, Proc. Ind. Acad. Sci. 46A, 251 (1957).

24. P. Venkateswarlu and B.N. Khanna, Proc. Ind. Acad. Sci. 49A, 117 (1959).

25. A.G. Briggs and R.G.W. Norrish, Proc. Roy. Soc. 56, 276 (1963).

26. Y.V. Rao, Private Communication.

27. J. Tellinghuisen, Chem. Phys. Letters, 49, 485 (1977).

28. J. Tellinghuisen, J. Mol. Spect. 94, 231 (1982).

29. E. Skorko, Nature, 131, 366 (1933).

30. R.D. Verma, Nagaraj and P. Venkateswarlu, Private Communication.

CHAPTER 4

ROTATIONAL ANALYSIS OF
D' —> A' EMISSION SYSTEM OF I_2

Introduction

The vibrational analysis of emission system of I_2 in
the region (3460–3015 Å) is attempted by a number of resear-
chers as enumerated in Chapter 3, but the rotational analysis
has not been attempted so far. To make up for this deficiency,
the rotational analysis of this emission band system recorded
in high resolution is taken up in the present work and the
results are reported in this chapter.

Experimental

The emission spectra of I_2 in the presence of argon in
the regions (3460–3015 Å) and (4320–4000 Å) were excited by

an electrodeless discharge using the output from a 25 kV
transformer at 60 cycles/sec. The spectra were photographed
with a 7.3 m Ebert vacuum grating spectrograph. In the case
of the 2400 Å system, the spectra were taken in 17th and 18th
orders at dispersions ranging from 0.12 Å/mm to 0.14 Å/mm
and the pressure of argon was 400 torr. The (4320-4000 Å)
system was taken in 14th order with 80 torr of argon and at
a dispersion varying between 0.13 Å/mm to 0.16 Å/mm. Both
the systems were recorded on KODAK I-O plates. The spectra
were taken by Prof. P. Venkateswarlu at Herzberg Institute
of Astrophysics, N.R.C, Canada, as such high resolution faci-
lities are not available in this country. The spectral lines
were measured at this Institute on a Carl-Zeiss Abbe compara-
tor having a least count of one micron. The wavelengths and
wave numbers of the rotational lines were calculated using
a large number of iron standard lines which were fitted to
4th and 5th order polynomials by least-squares method. The
measurement of the rotational lines is repeated and the
avarages are taken. The measurement of the rotational lines
is accurate to $\pm$ 0.03 cm^{-1}.

The rotational analysis of the 3400 Å system is pre-
sented in this chapter while that of the system in the region
(4320-4000 Å) is presented in the following chapter.

Rotational Analysis

The rotational structure in $^3II_g \longleftrightarrow {}^3II_u$ type of
transitions has been discussed by Herzberg [1]. I_2 being
a heavy and large molecule belongs to Hunds' coupling case
'c'. In this type of transitions only the transitions with
$\Delta\Omega = 0$ can occur strongly [2]. Hence there will be four
sub-bands corresponding to $O_g^+ \longleftrightarrow O_u^+$, $O_g^- \longleftrightarrow O_u^-$, 1g $\longleftrightarrow$ 1u
and 2g $\longleftrightarrow$ 2u components. If the Ω doubling is not resolved,
each sub-band consists of a strong P and a strong R branch
and in the case of 1g $\longleftrightarrow$ 1u and 2g $\longleftrightarrow$ 2u a weak Q branch
also. As mentioned earlier, the intensity of Q branch falls
off very rapidly with increasing J.

As the 3460-3015 Å system is of the type $^3II_{2g} \longrightarrow {}^3II_{2u}$,
its rotational structure is expected to have strong P and R
branches and a weak Q branch. As there was no evidence of
any Q branch lines, only P and R branch lines were used in
calculating the rotational constants. The rotational lines
of P and R branches of a particular ($v' \longrightarrow v''$) band can be
expressed to a good approximation by equations 2.1 and 2.2.

In analysing the rotational structure of this system,
the results from the vibrational analysis (Chapter 3) and
also the information available from Ref. [3] have been uti-
lised. As all the bands analysed are red degraded, the head
is formed in the R branch. The P and R branch lines are
overlapped till a large J with R(J) lines coinciding with

P(J-n) lines where 'n' is an integer varying from 4 to 11.
The rotational lines could be picked out very clearly for
all these bands from a point slightly away from the head.
The P(J) and R(J) lines thus picked out are fitted to the
least-squares with an arbitrary value to J (as explained in
Chapter 2) and to 'n'. The least-squares results for diffe-
rent values of 'n' for a particular arbitrary J are obtained
and the value of 'n' for which the variance is minimum is
chosen. Then the least-squares programme is run with diffe-
rent values to J. The J numbering which gives the best fit
and minimum variance is chosen. The constants thus obtained
are used to calculate the frequencies of the rotational
lines which could not be picked out visually and by comparing
these frequencies with the measured frequencies, many other
rotational lines could be assigned. Finally all the lines
which could be assigned are incorporated in the fit to get
the rotational constants and variance-covariance matrices
for each band. In this manner seven bands viz. (0-11),
(0-10), (1-9), (4-6), (5-5), (2-13) and (7-12) bands are
rotationally analysed. After each band is separately fitted
the rotational constants of (0-10) and (0-11) bands are
merged as described in Chapter 2, to get a single set of
rotational constants for the $v' = 0$ level. The rotational
constants β_e, α_e, γ_e and D_e, β_e for the upper and lower ele-
ctronic states are obtained from different vibrational bands

by separate least-squares fits of B_v', B_v'', D_v', D_v'' to the
following equations

$$B_v = B_e - \alpha_e(v + \tfrac{1}{2}) + \gamma_e(v + \tfrac{1}{2})^2 \qquad (4.1)$$

$$D_v = D_e + \beta_e(v + \tfrac{1}{2}). \qquad (4.2)$$

The equilibrium internuclear distance R_e is calculated for
the upper and lower states from the equation

$$B_e = h/8\pi^2 c \, \mu \, R_e^2 \qquad (4.3)$$

The higher order terms like H_v in the rotational term value
expression are not taken into consideration as the rotational
terms calculated without considering H_v agree with those
observed well within the experimental errors. The rotational
constants for individual vibrational levels of the upper and
lower states are listed in Table 4.1. The rotational con-
stants of $v' = 0$ and $v'' = 10$ and 11 have been obtained by
merging the constants from separate least-squares fits of
bands involving those vibrational levels. The rotational
constants β_e, α_e, γ_e, and D_e, β_e and R_e for the upper and
lower states are listed in Table 4.2. The D_v' and D_v'' values
presented in Table 4.1 do not show a smooth variation with
v. Hence, they were smoothened by linear least-squares fits
and then B_v values are calculated by keeping D_v values fixed
at their smoothened values. Unfortunately, this has resulted
in a large fluctuation in B_v values which is not acceptable.

Then an attempt to calculate B_v values keeping B_vs fixed at the values obtained after smoothening them was made which yielded negative values to some D_vs. Finally, the possibility of obtaining D_v values showing a smooth variation with v by introducing higher order term like H_v was explored. But this has not only not resulted in any betterment in the variation of D_v values, but has also adversely affected the existing smooth variation of B_v values. Hence, the constants obtained from the analysis are presented as they are. The number of rotational lines observed in each band exceeds 100 in all the bands except one. The rotational assignments in individual bands along with the rotational line positions and the difference between the calculated and observed values are listed in Tables 4.3 to 4.9. The agreement between the observed rotational line positions and those calculated from the rotational constants is very good, the maximum deviation being $0.15 \, cm^{-1}$ in a very few cases as can be seen from the Tables. Part of the rotational structure of (0-10), (0-11), (1-9), (7-12), (4-6) and (5-5) bands is shown in Figs. 4.1 to 4.6.

Conclusions

The rotational constants of the upper $(^3II_{2g})D'$ and lower $(^3II_{2u})A'$ electronic states involved in the (3460-3015 Å) emission system of I_2 in the presence of argon have been calculated from the rotational analysis of this band system.

The rotational analysis is being reported for the first time. The value of internuclear distance R_e for the A' state (3.02 $\mathring{A}$) is very similar to the R_e for the B and A states [4,5] which is as it should be because they belong to the same electronic configuration (2431) and hence are expected to have similar internuclear distance R_e [2]. The D' state, being an ion-pair state is expected to have comparatively large internuclear distance [2] and the value obtained from the present analysis is very much in the expected range.

Even though rotational levels with J = 4 could be identified in some of the bands analysed, the absence of levels with J = 0 and 1 could not be confirmed. If this could be done, the assignment of the transition as $^3II_{2g} \longrightarrow {}^3II_{2u}$ would have been confirmed. Moreover, it is surprising that no Q branch could be identified in the present analysis even at the low J values. This might be partly because of the overlapping of P, Q and R branches. However, further work with still higher dispersion and greater resolution is needed to find out the lowest value of J in the rotational structure as well as to check the presence of the Q branch and thus confirm the assignment.
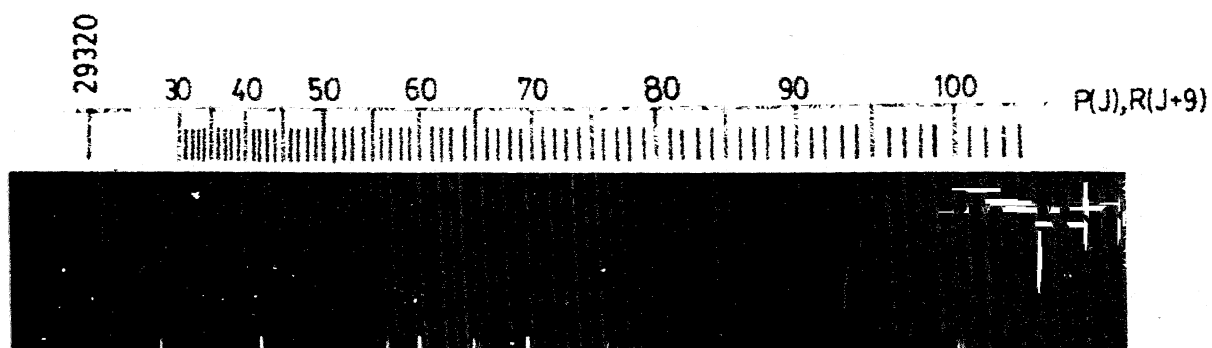
FIG. 4·1 ROTATIONAL STRUCTURE OF (0-11) BAND
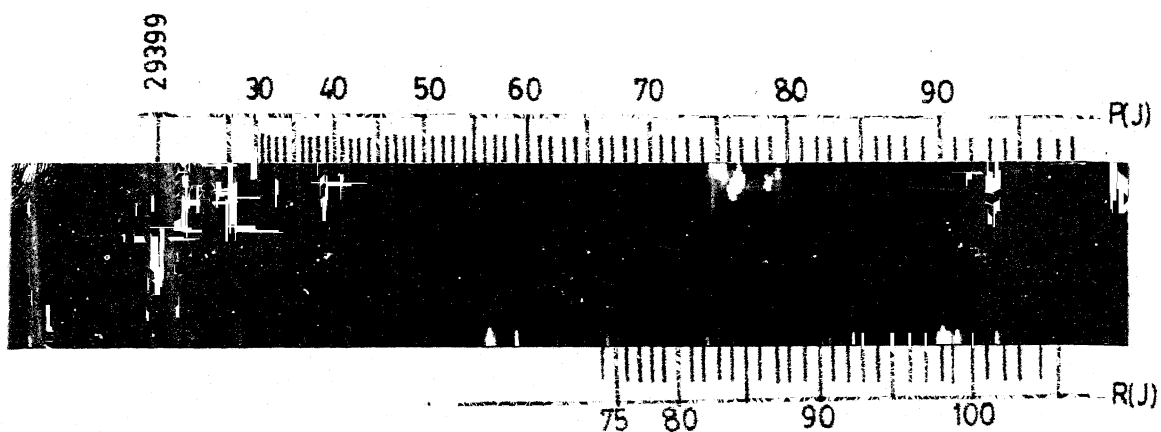
FIG. 4·2 ROTATIONAL STRUCTURE OF (0-10) BAND
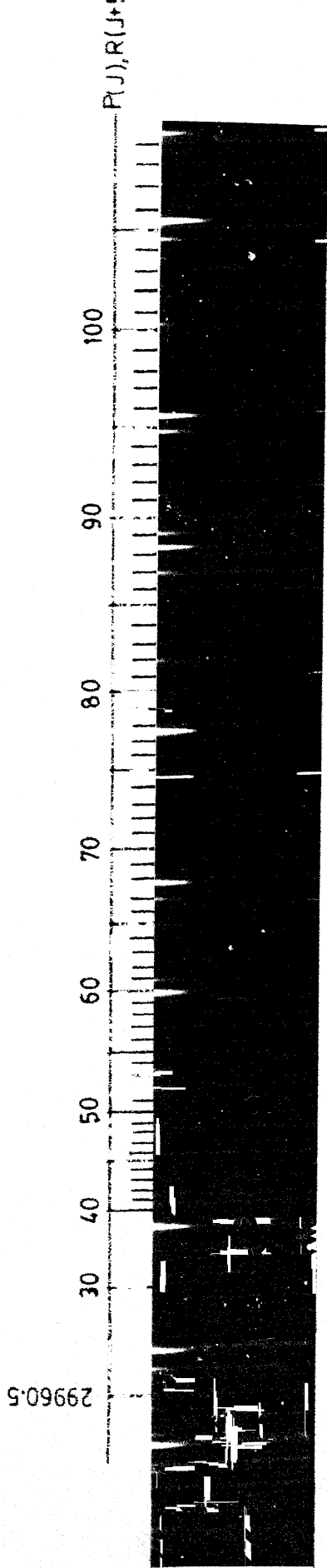
FIG. 4.3 ROTATIONAL STRUCTURE OF (7–12) BAND
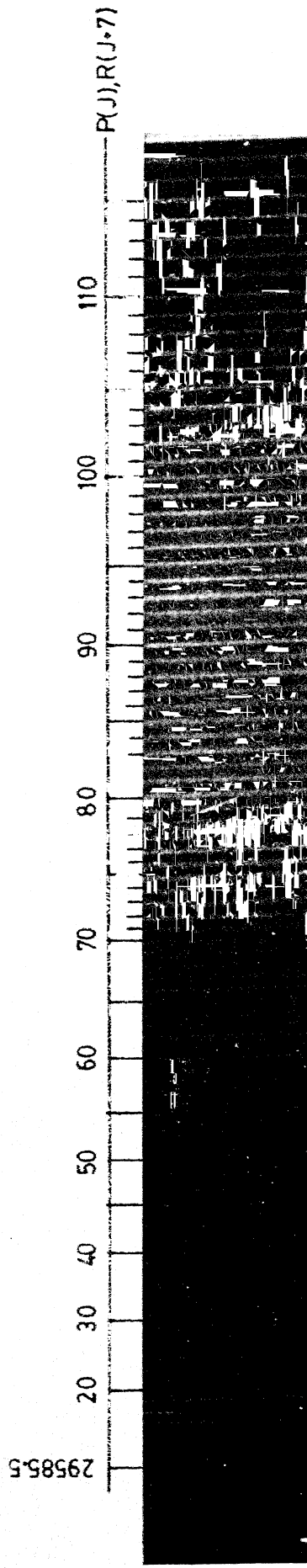
FIG. 4.4 ROTATIONAL STRUCTURE OF (1–9) BAND
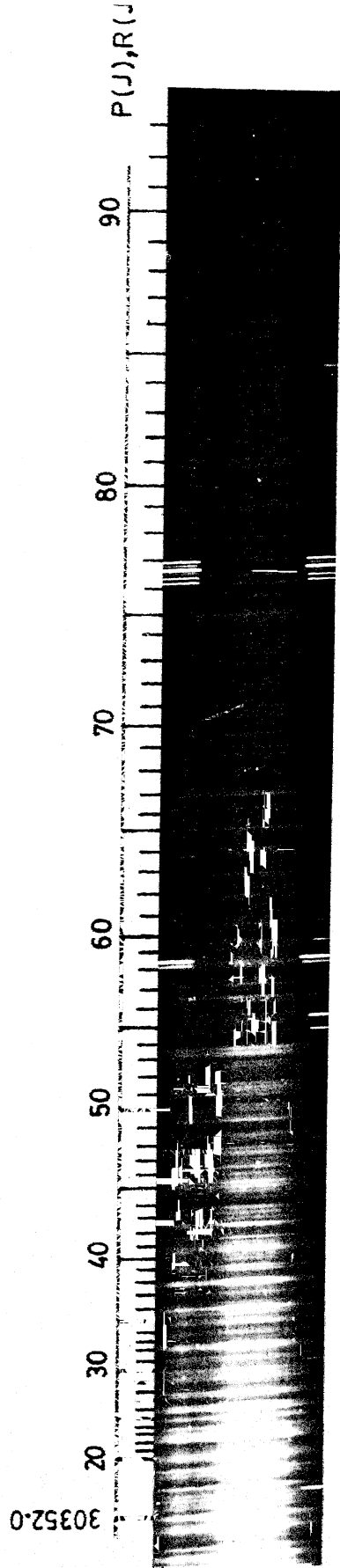
FIG. 4·5 ROTATIONAL STRUCTURE OF (5-5) BAND
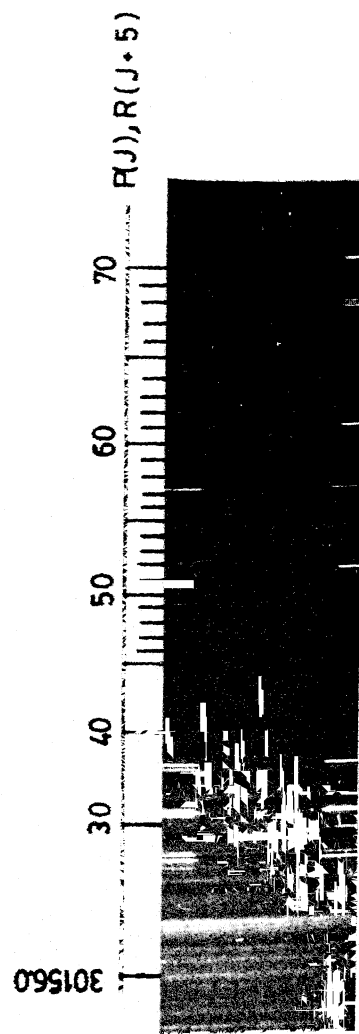
FIG. 4·6 ROTATIONAL STRUCTURE OF (4-6) BAND

TABLE 4.1

Rotational Constants (cm^{-1}) for Different
Vibrational Levels of D' and A' States

v	B_v x10^2	D_v x10^7
D' state		
0	2.110(14)	0.3344(129)
1	2.060(23)	0.8186(106)
2	2.003(10)	0.3435(115)
4	1.984(15)	0.2284(132)
5	1.854(14)	0.5737(124)
7	1.812(30)	0.9772(156)
A' state		
5	2.782(14)	0.8609(127)
6	2.778(16)	0.3263(136)
9	2.651(23)	1.0610(102)
10	2.639(18)	0.5480(186)
11	2.580(10)	0.4324(133)
12	2.535(30)	1.3601(158)
13	2.504(12)	0.4267(118)

TABLE 4.2

Rotational Constants (cm^{-1}) for D' $\longrightarrow$ A'
System

	D' state	A' state
B_e	$2.126(18) \times 10^{-2}$	$2.908(67) \times 10^{-2}$
α_e	4.1633×10^{-4}	1.4749×10^{-4}
γ_e	-1.1867×10^{-6}	-1.1580×10^{-5}
D_e	1.4560×10^{-8}	1.1103×10^{-8}
β_e	8.437×10^{-9}	3.251×10^{-9}
$R_e(\overset{\circ}{A})$	3.535	3.023

TABLE 4.3

WAVENUMBERS (cm-1) OF THE ROTATIONAL LINES IN THE
(0-11) BAND OF D'-A' SYSTEM.

$\nu_o = 29319.96$

J	R(J)	O-C	P(J)	O-C
13.0			29318.56	0.00
16.0			29318.06	0.05
17.0			29317.77	-0.04
19.0			29317.39	0.01
20.0			29317.15	0.00
21.0			29316.90	-0.01
22.0	29318.56	0.00		
24.0			29316.15	0.02
25.0	29318.06	0.05	29315.84	-0.02
26.0	29317.77	-0.04	29315.57	0.00
27.0			29315.26	-0.01
28.0	29317.39	0.01	29314.99	0.02
29.0	29317.15	-0.00	29314.62	-0.04
30.0	29316.90	-0.01	29314.34	0.01
31.0			29314.01	0.01
32.0			29313.69	0.03
33.0	29316.15	0.02	29313.30	-0.01
34.0	29315.84	-0.02	29312.94	-0.01
35.0	29315.57	0.00	29312.56	-0.02
36.0	29315.26	0.01	29312.22	0.02
37.0	29314.99	0.02	29311.82	0.01
38.0	29314.62	-0.04	29311.42	0.00
39.0	29314.34	0.01	29311.03	0.02
40.0	29314.01	0.01	29310.58	-0.02
41.0	29313.69	0.03	29310.18	0.01
42.0	29313.30	-0.01	29309.73	-0.01
43.0	29312.94	-0.01	29309.30	0.00
44.0	29312.56	-0.02	29308.86	0.01
45.0	29312.22	0.02	29308.39	-0.03
46.0	29311.82	0.01	29307.89	0.03
47.0	29311.42	0.00	29307.47	-0.03
48.0	29311.03	0.02	29306.92	0.00

TABLE 4.3 Contd.

J	R(J)	O-C	P(J)	O-C
49.0	29310.58	-0.02	29306.45	-0.01
50.0	29310.18	0.01	29305.94	0.01
51.0	29309.73	-0.01	29305.44	0.01
52.0	29309.30	0.00	29304.92	0.01
53.0	29308.86	0.01	29304.37	0.00
54.0	29308.39	-0.03	29303.81	-0.02
55.0	29307.89	0.03	29303.30	0.02
56.0	29307.47	-0.03	29302.70	-0.02
57.0	29306.92	0.00	29302.12	-0.03
58.0	29306.45	-0.01	29301.57	0.00
59.0	29305.94	0.00	29301.01	0.02
60.0	29305.44	0.01	29300.41	0.02
61.0	29304.92	0.01	29299.82	0.03
62.0	29304.37	0.00	29299.18	0.01
63.0	29303.81	-0.02	29298.55	0.00
64.0	29303.30	0.02	29297.93	0.01
65.0	29302.70	-0.02	29297.26	-0.02
66.0	29302.12	-0.03	29296.62	-0.01
67.0	29301.57	0.00	29295.93	-0.04
68.0	29301.01	0.02	29295.30	-0.01
69.0	29300.41	0.02	29294.64	0.01
70.0	29299.82	0.03	29293.94	-0.01
71.0	29299.18	0.01	29293.23	-0.03
72.0	29298.55	0.00	29292.54	-0.02
73.0	29297.93	0.01	29291.84	-0.01
74.0	29297.26	-0.02	29291.13	0.00
75.0	29296.62	-0.01	29290.43	0.03
76.0	29295.93	-0.04	29289.67	0.01
77.0	29295.30	-0.01	29288.94	0.02
78.0	29294.64	0.01	29288.19	0.02
79.0	29293.94	-0.01	29287.40	-0.01
80.0	29293.23	-0.03	29286.65	0.01
81.0	29292.54	-0.02	29285.87	0.01
82.0	29291.84	-0.01	29285.09	0.02
83.0	29291.13	0.00	29284.27	-0.01
84.0	29290.43	0.03	29283.47	0.00

TABLE 4.3 Contd.

J	R(J)	O-C	P(J)	O-C
85.0	29289.67	0.01	29282.65	-0.01
86.0	29288.94	0.02	29281.80	-0.04
87.0	29288.19	0.02	29281.00	-0.01
88.0	29287.40	-0.01	29280.17	0.00
89.0	29286.65	0.01	29279.30	-0.03
90.0	29285.87	0.01	29278.47	0.00
91.0	29285.09	0.02	29277.63	0.02
92.0	29284.27	-0.01	29276.72	-0.02
93.0	29283.47	0.00	29275.88	0.02
94.0	29282.65	-0.01	29274.97	0.01
95.0	29281.80	-0.04	29274.12	0.04
96.0	29281.00	-0.01	29273.21	0.03
97.0	29280.17	0.00	29272.28	0.01
98.0	29279.30	-0.03	29271.36	0.01
99.0	29278.47	0.00	29270.43	0.01
100.0	29277.63	0.00	29269.56	0.07
101.0	29276.72	-0.02	29268.54	0.04
102.0	29275.88	0.02	29267.59	0.09
103.0	29274.97	-0.01		
104.0	29274.12	0.04		
105.0	29273.21	0.03		
106.0	29272.28	0.01		
107.0	29271.36	0.01		
108.0	29270.43	0.01		
109.0	29269.56	0.07		
110.0	29268.54	0.04		
111.0	29267.59	0.09		

TABLE 4.4

WAVENUMBERS (cm-1) OF THE ROTATIONAL LINES IN THE
(0-10) BAND OF D'-A' SYSTEM.

$v_0 = 29399.05$

J	R(J)	O-C	P(J)	O-C
10.0			29398.07	0.03
12.0			29397.71	-0.01
15.0			29397.22	0.07
18.0	29398.07	0.04	29396.44	-0.05
20.0	29397.71	0.00	29396.07	0.08
21.0			29395.75	0.02
22.0			29395.49	0.03
23.0	29397.22	0.08	29395.24	0.07
24.0			29394.84	-0.04
25.0			29394.59	0.02
26.0	29396.44	-0.04	29394.30	0.04
27.0			29393.97	0.04
28.0	29396.07	0.09	29393.61	0.01
29.0	29395.75	0.03	29393.26	0.01
30.0	29395.49	0.04	29392.86	-0.04
31.0	29395.24	0.08	29392.59	0.06
32.0	29394.84	-0.03	29392.17	0.02
33.0	29394.59	0.02	29391.73	-0.03
34.0	29394.30	0.05	29391.39	0.02
35.0	29393.97	0.04	29390.95	-0.01
36.0	29393.61	0.02	29390.51	-0.03
37.0	29393.26	0.01	29390.13	0.02
38.0	29392.86	-0.03	29389.67	0.00
39.0	29392.59	0.06	29389.18	-0.05
40.0	29392.17	0.02	29388.74	-0.03
41.0	29391.73	-0.04	29388.29	-0.01
42.0	29391.39	0.02	29387.82	0.00
43.0	29390.95	-0.02	29387.32	-0.01
44.0	29390.51	-0.04	29386.79	-0.04
45.0	29390.13	0.00	29386.32	0.00
46.0	29389.67	-0.02	29385.78	-0.02
47.0	29389.18	-0.06	29385.26	-0.01

TABLE 4.4 Contd

J	R(J)	O-C	P(J)	O-C
48.0	29388.74	-0.05	29384.70	-0.03
49.0	29388.29	-0.03	29384.17	-0.01
50.0	29387.82	-0.02	29383.64	0.02
51.0	29387.32	-0.04	29383.05	0.00
52.0	29386.79	-0.07	29382.45	-0.02
53.0	29386.32	-0.04	29381.90	0.02
54.0	29385.78	-0.06	29381.30	0.02
55.0	29385.26	-0.06	29380.64	-0.04
56.0	29384.70	-0.08		
57.0	29384.17	-0.06	29379.44	0.01
58.0	29383.64	-0.04		
59.0	29383.05	-0.06	29378.15	0.01
60.0	29382.45	-0.09	29377.44	-0.04
61.0	29381.90	-0.06	29376.76	-0.06
62.0	29381.30	-0.06	29376.08	-0.06
63.0			29375.45	0.00
64.0			29374.70	-0.06
65.0	29379.44	-0.08	29374.04	-0.01
66.0	29378.87	-0.02		
67.0	29378.15	-0.10	29372.54	-0.07
68.0			29371.87	0.00
69.0			29371.12	-0.01
70.0	29376.24	-0.03	29370.30	-0.08
71.0	29375.65	0.06	29369.55	-0.06
72.0	29374.94	0.04	29368.83	-0.01
73.0	29374.26	0.06	29368.11	0.05
74.0	29373.52	0.03	29367.31	0.04
75.0	29372.78	0.00	29366.47	0.00
76.0	29372.10	0.05	29365.73	0.07
77.0	29371.36	0.04	29364.86	0.02
78.0	29370.64	0.07	29364.02	0.00
79.0	29369.84	0.02	29363.24	0.06
80.0	29369.14	0.08	29362.35	0.01
81.0	29368.31	0.02	29361.50	0.02
82.0	29367.58	0.07	29360.64	0.02

TABLE 4.4 Contd.

J	R(J)	O-C	P(J)	O-C
83.0	29366.73	0.01	29359.73	-0.02
84.0	29365.94	0.02	29358.90	0.03
85.0	29365.16	0.05	29357.99	0.01
86.0	29364.38	0.08	29357.08	0.00
87.0	29363.51	0.04	29356.19	0.02
88.0	29362.67	0.03	29355.29	0.04
89.0	29361.84	0.04	29354.33	0.00
90.0	29360.98	0.03		
91.0	29360.12	0.03	29352.49	0.04
92.0	29359.27	0.05	29351.53	0.03
93.0	29358.40	0.05	29350.63	0.09
94.0	29357.49	0.03	29349.54	-0.04
95.0	29356.59	0.02	29348.60	0.00
96.0	29355.73	0.06	29347.58	-0.04
97.0	29354.74	-0.02	29346.58	-0.04
98.0	29353.83	-0.01	29345.58	-0.04
99.0	29352.94	0.03	29344.61	0.00
100.0	29351.97	-0.01		
101.0	29351.03	-0.01		
102.0	29350.02	-0.07		
103.0	29349.13	0.00		
104.0	29348.11	-0.05		
105.0	29347.11	-0.07		
106.0	29346.11	-0.09		
107.0	29345.13	-0.08		

TABLE 4. 5

WAVENUMBERS (cm-1) OF THE ROTATIONAL LINES IN THE
(1-9) BAND OF D'-A' SYSTEM.

v_o = 29585.44

J	R(J)	O-C	P(J)	O-C
5. 0			29585. 03	-0. 03
6. 0	29585. 47	-0. 01	29584. 90	-0. 04
7. 0	29585. 47	0. 03		
8. 0	29585. 41	0. 03		
10. 0			29584. 22	0. 04
12. 0	29585. 03	-0. 02		
13. 0	29584. 99	-0. 04	29583. 75	-0. 08
16. 0			29583. 10	-0. 08
17. 0	29584. 42	0. 05		
18. 0			29582. 76	0. 08
19. 0			29582. 47	0. 05
20. 0	29583. 75	-0. 07		
23. 0	29583. 10	-0. 07	29581. 17	-0. 07
24. 0			29580. 91	-0. 01
25. 0	29582. 76	0. 08		
26. 0	29582. 47	0. 06	29580. 28	0. 04
29. 0			29579. 06	-0. 07
30. 0	29581. 17	-0. 06	29578. 77	0. 03
31. 0	29580. 91	0. 00	29578. 29	-0. 05
33. 0	29580. 28	0. 05	29577. 47	-0. 02
34. 0			29576. 97	-0. 09
35. 0			29576. 65	0. 04
36. 0	29579. 06	-0. 06	29576. 21	0. 06
37. 0	29578. 77	-0. 04	29575. 69	0. 02
38. 0	29578. 29	-0. 04		
39. 0			29574. 77	0. 07
40. 0	29577. 47	-0. 01	29574. 25	0. 06
41. 0	29576. 97	0. 08		
42. 0	29576. 65	0. 05		
43. 0	29576. 21	0. 07		
44. 0	29575. 69	0. 03		
46. 0	29574. 77	0. 08		
47. 0	29574. 25	0. 07		

TABLE 4.5 Contd.

J	R(J)	O−C	P(J)	O−C
55. 0	29569. 63	−0. 10	29565. 27	0. 00
56. 0			29564. 56	−0. 02
58. 0			29563. 23	0. 04
59. 0			29562. 54	0. 07
60. 0			29561. 79	0. 05
61. 0			29561. 02	0. 01
62. 0	29565. 27	0. 02	29560. 33	0. 07
63. 0	29564. 56	0. 01	29559. 54	0. 04
64. 0			29558. 74	0. 00
65. 0	29563. 23	0. 06		
66. 0	29562. 54	0. 08	29557. 15	−0. 02
67. 0	29561. 79	0. 06	29556. 31	−0. 06
68. 0	29561. 02	0. 02		
69. 0	29560. 33	0. 08	29554. 74	0. 00
70. 0	29559. 54	0. 05	29553. 96	0. 05
71. 0	29558. 74	0. 02	29553. 02	−0. 05
73. 0	29557. 15	−0. 01	29551. 31	−0. 05
74. 0	29556. 31	−0. 05	29550. 47	−0. 02
76. 0	29554. 74	0. 01	29548. 69	−0. 03
77. 0	29553. 96	0. 06		
78. 0	29553. 02	−0. 04		
80. 0	29551. 31	−0. 04	29545. 00	−0. 05
81. 0	29550. 47	−0. 01	29544. 04	−0. 07
82. 0			29543. 11	0. 05
83. 0	29548. 69	−0. 01	29542. 16	−0. 05
84. 0			29541. 20	−0. 04
85. 0			29540. 26	0. 00
86. 0			29539. 24	−0. 03
87. 0	29545. 00	−0. 04	29538. 28	0. 01
88. 0	29544. 04	−0. 06	29537. 17	−0. 09
89. 0	29543. 11	−0. 04	29536. 20	−0. 05
90. 0	29542. 16	−0. 03	29535. 16	−0. 06
91. 0	29541. 20	−0. 03	29534. 21	−0. 02
92. 0	29540. 26	0. 01	29533. 10	−0. 04
93. 0	29539. 24	−0. 02	29532. 04	−0. 04
94. 0	29538. 28	0. 02	29530. 97	−0. 06
95. 0	29537. 17	−0. 08	29529. 89	−0. 07
96. 0	29536. 20	−0. 04	29528. 85	−0. 02

TABLE 4.5 Contd.

J	R(J)	O-C	P(J)	O-C
97.0	29535.16	-0.05	29527.75	-0.04
98.0	29534.21	0.03	29526.69	0.00
99.0	29533.10	-0.03	29525.60	0.02
100.0	29532.04	-0.04	29524.43	-0.03
101.0	29530.97	-0.05	29523.37	0.03
102.0	29529.89	-0.06	29522.22	0.01
103.0	29528.85	-0.02	29521.06	0.00
104.0	29527.75	-0.03	29519.93	0.02
105.0	29526.69	0.01	29518.78	0.02
106.0	29525.60	-0.03	29517.64	0.05
107.0	29524.43	-0.03	29516.48	0.07
108.0	29523.37	0.03	29515.26	0.03
109.0	29522.22	0.02	29514.08	0.04
110.0	29521.06	0.00	29512.91	0.07
111.0	29519.93	0.02	29511.65	0.02
112.0	29518.78	0.03	29510.51	0.09
113.0	29517.64	0.05	29509.23	0.04
114.0	29516.48	0.07	29508.04	0.08
115.0	29515.26	0.03	29506.77	0.05
116.0	29514.08	0.04	29505.53	0.06
117.0	29512.91	0.07	29504.21	-0.01
118.0	29511.65	0.02	29502.99	0.03
119.0	29510.51	0.09	29501.74	0.05
120.0	29509.23	0.04	29500.44	0.03
121.0	29508.04	0.08	29499.09	-0.04
122.0	29506.77	0.05	29497.78	-0.05
123.0	29505.53	0.05	29496.53	0.00
124.0	29504.21	-0.01	29495.15	-0.08
125.0	29502.99	0.03	29493.88	-0.04
126.0	29501.74	0.05	29492.59	-0.01
127.0	29500.44	0.02	29491.19	-0.08
128.0	29499.09	-0.04		
129.0	29497.78	-0.06		
130.0	29496.53	-0.01		
131.0	29495.15	-0.09		
132.0	29493.88	-0.05		
133.0	29492.59	-0.02		
134.0	29491.19	-0.09		

TABLE 4.6

WAVENUMBERS (cm-1) OF THE ROTATIONAL LINES IN THE
(2-13) BAND OF D'-A' SYSTEM.

$v_0 = 29376.44$

J	R(J)	O-C	P(J)	O-C
6. 0			29376. 08	0. 09
9. 0			29375. 66	0. 03
11. 0			29375. 36	0. 02
13. 0			29374. 95	-0. 06
14. 0	29376. 08	0. 09		
15. 0			29374. 71	0. 07
17. 0	29375. 66	0. 03	29374. 29	0. 06
18. 0			29374. 04	0. 03
19. 0	29375. 36	0. 02		
20. 0			29373. 54	0. 00
21. 0	29374. 95	-0. 06	29373. 24	-0. 05
23. 0	29374. 71	0. 07	29372. 79	0. 03
25. 0	29374. 29	0. 06	29372. 07	-0. 12
26. 0	29374. 04	0. 03	29371. 78	-0. 11
28. 0	29373. 54	0. 00		
29. 0	29373. 24	-0. 05		
30. 0			29370. 62	0. 03
31. 0	29372. 79	0. 03		
32. 0			29369. 85	-0. 03
33. 0	29372. 07	-0. 12	29369. 55	0. 04
34. 0	29371. 78	-0. 11	29369. 13	-0. 01
36. 0			29368. 32	-0. 03
38. 0	29370. 62	0. 03	29367. 58	0. 06
40. 0	29369. 85	-0. 03		
41. 0	29369. 55	0. 03		
42. 0	29369. 13	-0. 01	29365. 72	-0. 03
43. 0			29365. 18	-0. 11
44. 0	29368. 31	-0. 03	29364. 83	0. 02
46. 0	29367. 58	0. 06		
47. 0			29363. 21	-0. 11
49. 0			29362. 30	0. 02
50. 0	29365. 72	-0. 03	29361. 75	0. 01

TABLE 4.6 Contd.

J	R(J)	O-C	P(J)	O-C
51.0	29365.18	-0.11		
52.0	29364.83	0.02	29360.57	-0.07
53.0			29360.11	0.03
55.0	29363.21	-0.11	29358.86	-0.06
56.0			29358.40	0.07
57.0	29362.30	0.02		
58.0	29361.75	0.01	29357.10	-0.01
59.0			29356.55	0.06
60.0	29360.57	-0.07		
61.0	29360.11	0.03	29355.25	0.03
63.0	29358.86	-0.06	29353.84	-0.06
64.0	29358.40	0.07		
65.0			29352.47	-0.08
66.0	29357.10	-0.01	29351.93	0.06
67.0	29356.55	0.06		
68.0			29350.54	0.08
69.0	29355.25	0.03		
70.0			29349.11	0.10
71.0	29353.84	-0.07		
72.0			29347.58	0.05
73.0	29352.47	-0.09		
74.0	29351.93	0.06	29346.06	0.05
76.0	29350.54	0.08		
77.0			29343.59	-0.07
78.0	29349.11	0.10		
79.0			29342.08	0.04
80.0	29347.58	0.05		
82.0	29346.06	0.05		
84.0			29337.87	0.02
85.0	29343.59	-0.07		
86.0			29336.11	0.01
87.0	29342.08	0.04	29335.11	-0.11
92.0	29337.87	0.03	29330.64	0.11
94.0	29336.11	0.01		
95.0	29335.11	-0.10		
100.0	29330.64	-0.01		

TABLE 4.7

WAVENUMBERS (cm-1) OF THE ROTATIONAL LINES IN THE
(4-6) BAND OF D'-A' SYSTEM.

$\upsilon_o = 30156.61$

J	R(J)	O-C	P(J)	O-C
9.0			30155.56	0.02
12.0			30154.86	-0.03
13.0			30154.67	0.02
14.0	30155.56	0.02	30154.37	-0.02
17.0	30154.86	-0.03		
18.0	30154.67	0.02	30153.13	-0.05
19.0	30154.38	-0.01	30152.82	-0.02
20.0			30152.53	0.05
23.0	30153.13	-0.05	30151.23	-0.09
24.0	30152.82	-0.02		
25.0	30152.53	0.05		
26.0			30149.93	-0.08
27.0			30149.57	0.03
28.0	30151.23	-0.09	30148.98	-0.08
29.0			30148.62	0.06
30.0			30148.20	0.16
31.0	30149.93	-0.08	30147.46	-0.05
32.0	30149.57	0.03	30146.95	-0.02
33.0	30148.98	-0.08	30146.39	-0.01
34.0	30148.62	0.06		
35.0	30148.20	0.15	30145.36	0.13
36.0	30147.46	-0.05		
37.0	30146.95	-0.02	30144.13	0.13
38.0	30146.39	-0.01		
39.0			30142.61	-0.09
40.0	30145.36	0.12	30142.06	0.03
42.0	30144.13	0.13		
43.0			30139.87	-0.05
44.0	30142.61	-0.09	30139.17	-0.02
45.0	30142.06	0.03	30138.45	0.01
46.0			30137.70	0.03
48.0	30139.87	-0.05	30136.19	0.10

TABLE 4.7 Contd.

J	R(J)	O-C	P(J)	O-C
49.0	30139.17	-0.01		
50.0	30138.45	0.02	30134.33	-0.12
51.0	30137.70	0.03	30133.58	-0.06
52.0			30132.76	0.01
53.0	30136.19	0.10		
54.0			30130.88	-0.10
55.0	30134.33	-0.11		
56.0	30133.58	-0.03	30129.10	-0.05
57.0	30132.76	0.01	30128.25	0.13
59.0	30130.88	-0.10		
60.0			30125.31	0.00
61.0	30129.10	-0.05	30124.34	0.02
62.0	30128.25	0.13		
63.0			30122.11	-0.16
64.0			30121.25	0.02
65.0	30125.31	0.00	30120.16	-0.01
66.0	30124.34	0.02	30119.11	0.02
67.0			30118.05	0.05
68.0	30122.11	-0.16	30116.91	0.01
69.0	30121.25	0.02	30115.80	0.03
70.0	30120.16	-0.01		
71.0	30119.11	0.02		
72.0	30118.05	0.05		
73.0	30116.91	0.01		
74.0	30115.80	0.02		

TABLE 4.8

WAVENUMBERS (cm-1) OF THE ROTATIONAL LINES IN THE (5-5) BAND OF D'-A' SYSTEM.

$V_o = 30351.94$

J	R(J)	O-C	P(J)	O-C
14.0	30350.71	0.16		
15.0			30349.08	-0.08
16.0			30348.90	0.07
17.0			30348.50	0.03
18.0			30348.09	-0.01
19.0	30349.08	-0.08	30347.79	0.07
20.0	30348.90	0.07		
21.0	30348.50	0.03	30346.93	0.05
22.0	30348.09	-0.01	30346.46	0.02
23.0	30347.79	0.07		
24.0			30345.51	0.01
25.0	30346.93	0.05		
26.0	30346.46	0.02	30344.28	-0.20
27.0			30343.78	-0.17
28.0	30345.51	0.01		
29.0			30342.61	-0.21
30.0	30344.28	-0.20		
31.0	30343.78	-0.17		
32.0			30340.96	0.04
33.0	30342.61	-0.21	30340.32	-0.04
34.0			30339.59	-0.10
35.0			30338.88	-0.13
36.0	30340.96	-0.04	30338.27	-0.05
37.0	30340.32	-0.04		
38.0	30339.59	-0.10		
39.0	30338.88	-0.13	30336.08	-0.03
40.0	30338.27	-0.05		
41.0			30334.37	-0.18
42.0			30333.61	-0.14
43.0	30336.08	-0.03	30332.86	-0.06
45.0	30334.37	-0.18	30331.08	-0.14
46.0	30333.61	-0.14	30330.19	-0.15
47.0	30332.86	-0.06	30329.34	0.11
48.0			30328.36	-0.18
49.0	30331.08	-0.14	30327.53	-0.08
50.0	30330.19	-0.15		
51.0	30329.34	-0.11	30325.73	0.04
52.0	30328.36	-0.18	30324.70	-0.01
53.0	30327.53	-0.08	30323.58	-0.13
55.0	30325.73	0.04		

TABLE 4. 8 Contd.

J	R(J)	O-C	P(J)	O-C
56. 0	30324. 70	−0. 01	30320. 58	−0. 02
57. 0	30323. 58	−0. 13	30319. 52	−0. 01
58. 0			30318. 45	0. 01
60. 0	30320. 58	−0. 02	30316. 20	−0. 01
61. 0	30319. 52	−0. 01	30315. 08	0. 01
62. 0	30318. 45	0. 01	30313. 85	−0. 07
63. 0			30312. 84	0. 10
64. 0	30316. 20	−0. 01		
65. 0	30315. 08	0. 01	30310. 31	−0. 03
66. 0	30313. 85	−0. 07	30309. 11	−0. 01
67. 0	30312. 84	0. 10	30308. 01	0. 13
68. 0			30306. 64	0. 02
69. 0	30310. 39	−0. 03	30305. 46	0. 12
70. 0	30309. 11	−0. 01	30304. 09	0. 04
71. 0	30308. 01	0. 13		
72. 0	30306. 64	0. 02	30301. 53	0. 11
73. 0	30305. 46	0. 12	30300. 07	0. 00
74. 0	30304. 09	0. 04	30298. 81	0. 10
75. 0			30297. 44	0. 10
76. 0	30301. 53	0. 11	30296. 03	0. 08
77. 0	30300. 07	0. 00	30294. 57	0. 03
78. 0	30298. 81	0. 09	30293. 21	0. 10
79. 0	30297. 44	0. 10	30291. 69	0. 02
80. 0	30296. 03	0. 08	30290. 25	0. 03
81. 0	30294. 57	0. 03	30288. 85	0. 11
82. 0	30293. 21	0. 10	30287. 39	0. 14
83. 0	30291. 69	0. 02	30285. 78	0. 03
84. 0	30290. 25	0. 03	30284. 23	0. 10
85. 0	30288. 85	0. 11	30282. 76	0. 07
86. 0	30287. 39	0. 14	30281. 06	−0. 07
87. 0	30285. 78	0. 03	30279. 58	0. 02
88. 0	30284. 23	0. 00		
89. 0	30282. 76	0. 07	30276. 43	0. 05
90. 0	30281. 06	−0. 07	30274. 73	−0. 03
91. 0	30279. 58	0. 02	30273. 17	0. 04
93. 0	30276. 43	0. 05	30269. 77	−0. 05
94. 0	30274. 73	−0. 03		
95. 0	30273. 17	0. 04	30266. 37	−0. 07
97. 0	30269. 77	−0. 05		
99. 0	30266. 37	−0. 08		

TABLE 4.9

WAVENUMBERS (cm-1)OF THE ROTATIONAL LINES IN THE
(7-12) BAND OF D′-A′ SYSTEM.

$v_o = 29960.60$

J	R(J)	O-C	P(J)	O-C
3.0			29960.37	-0.04
8.0	29960.37	-0.04		
9.0			29959.70	0.07
11.0			29959.35	0.10
12.0			29959.04	0.00
14.0	29959.70	0.07	29958.67	0.09
15.0			29958.33	0.00
16.0	29959.35	0.10		
17.0	29959.04	0.00	29957.88	0.10
18.0			29957.55	0.07
19.0	29958.67	0.09	29957.23	0.05
20.0	29958.33	0.00	29957.00	0.15
21.0			29956.57	0.06
22.0	29957.88	0.10	29956.26	0.10
23.0	29957.55	0.06	29955.79	-0.00
24.0	29957.23	0.05	29955.40	-0.01
25.0	29957.00	0.15		
26.0	29956.57	0.05	29954.69	0.08
27.0	29956.26	0.10	29954.15	-0.04
28.0	29955.79	-0.01	29953.83	0.08
29.0	29955.40	-0.02	29953.36	0.06
30.0			29952.81	-0.03
31.0	29954.69	0.07	29952.33	-0.03
32.0	29954.15	-0.04	29951.86	0.00
33.0	29953.83	-0.07		
34.0	29953.36	0.06		
35.0	29952.81	-0.03	29950.34	0.04
36.0	29952.33	-0.03		
37.0	29951.86	-0.01	29949.23	0.04
39.0			29948.10	0.07
40.0	29950.34	0.03	29947.47	0.00
41.0			29946.84	0.03
42.0	29949.23	0.03		
43.0			29945.55	0.02
44.0	29948.10	0.07	29944.84	-0.04
45.0	29947.42	-0.01	29944.15	-0.06
46.0	29946.84	0.03	29943.55	0.03
48.0	29945.55	0.01	29942.04	-0.07
49.0	29944.84	-0.04	29941.30	-0.09
50.0	29944.15	-0.06	29940.56	-0.09

TABLE 4.9 Contd.

J	R(J)	O-C	P(J)	O-C
51. 0	29943. 55	0. 02	29939. 83	-0. 07
52. 0			29939. 05	-0. 09
53. 0	29942. 04	-0. 08		
54. 0	29941. 30	-0. 01	29937. 54	-0. 03
55. 0	29940. 56	-0. 10	29936. 69	-0. 08
56. 0	29939. 83	-0. 08	29935. 79	-0. 16
57. 0	29939. 05	0. 09	29935. 06	-0. 07
58. 0			29934. 22	-0. 06
59. 0	29937. 54	-0. 04	29933. 37	-0. 06
60. 0	29936. 69	-0. 09	29932. 53	-0. 03
61. 0	29935. 79	-0. 17	29931. 61	-0. 07
62. 0	29935. 06	-0. 07	29930. 66	-0. 13
63. 0	29934. 22	-0. 07	29929. 89	0. 00
64. 0	29933. 37	-0. 07	29928. 98	0. 01
65. 0	29932. 53	-0. 04	29927. 93	-0. 11
66. 0	29931. 61	-0. 08	29926. 94	-0. 16
67. 0	29930. 66	-0. 14		
68. 0	29929. 89	0. 00	29925. 08	-0. 10
69. 0	29928. 98	0. 00	29924. 16	-0. 04
70. 0	29927. 93	-0. 12	29923. 16	-0. 05
71. 0	29926. 94	-0. 17	29922. 09	-0. 12
72. 0			29921. 13	-0. 07
73. 0	29925. 08	-0. 11	29920. 12	-0. 05
74. 0	29924. 16	-0. 05	29919. 05	-0. 08
75. 0	29923. 16	-0. 06	29917. 99	-0. 09
76. 0	29922. 09	-0. 13		
77. 0	29921. 19	-0. 07		
78. 0	29920. 12	-0. 06	29914. 83	-0. 03
79. 0	29919. 05	-0. 08	29913. 78	0. 01
80. 0	29917. 99	-0. 10	29912. 68	0. 02
81. 0			29911. 51	-0. 03
82. 0			29910. 39	-0. 02
83. 0	29914. 83	-0. 04	29909. 32	0. 05
84. 0	29913. 78	0. 01	29908. 20	0. 08
85. 0	29912. 68	0. 01	29907. 00	0. 04
86. 0	29911. 51	-0. 04	29905. 81	0. 03
87. 0	29910. 39	-0. 03	29904. 61	0. 01
88. 0	29909. 32	0. 04	29903. 46	0. 06
89. 0	29908. 20	0. 08	29902. 23	0. 03
90. 0	29907. 00	0. 04	29901. 08	0. 10
91. 0	29905. 81	0. 02	29899. 79	0. 04
92. 0	29904. 61	0. 01	29898. 60	0. 08
93. 0	29903. 46	0. 05	29897. 36	0. 09

TABLE 4.9 Contd.

J	R(J)	O-C	P(J)	O-C
94.0	29902.23	0.03	29896.10	0.09
95.0	29901.08	0.10	29894.89	0.15
96.0	29899.79	0.03	29893.53	0.12
97.0	29898.60	0.08	29892.24	0.07
98.0	29897.36	0.09	29890.99	0.11
99.0	29896.10	0.09	29889.66	0.09
100.0	29894.89	0.15	29888.34	0.09
101.0	29893.53	0.12	29887.03	0.11
102.0	29892.24	0.06	29885.67	0.08
103.0	29890.99	0.11	29884.33	0.09
104.0	29889.66	0.05	29882.98	0.09
105.0	29888.34	0.09	29881.63	0.11
106.0	29887.03	0.11	29880.22	0.07
107.0	29885.67	0.08	29878.80	0.03
108.0	29884.33	0.09	29877.43	0.06
109.0	29882.98	0.10	29876.01	0.04
110.0	29881.63	0.11	29874.62	0.05
111.0	29880.22	0.07	29873.15	0.00
112.0	29878.80	0.04	29871.63	-0.09
113.0	29877.43	0.06	29870.20	-0.09
114.0	29876.01	0.04		
115.0	29874.62	0.06	29867.25	-0.14
116.0	29873.15	0.01	29865.80	-0.13
117.0	29871.63	-0.09	29864.29	-0.18
118.0	29870.20	-0.08		
120.0	29867.25	-0.14		
121.0	29865.80	-0.13		
122.0	29864.29	-0.17		

REFERENCES

1. G. Herzberg, Spectra of Diatomic Molecules, Van Nostrand, New York (1950).

2. R.S. Mulliken, J. Chem. Phys. 55, 288 (1971).

3. J. Tellinghuisen, J. Mol. Spectrosc. 94, 231 (1982).

4. P. Luc, J. Mol. Spectrosc. 80, 41 (1980).

5. K.S. Viswanathan, A. Sur and J.B. Tellinghuisen, J. Mol. Spectrosc. 86, 38 (1981).

CHAPTER 5

VIBRATIONAL AND ROTATIONAL ANALYSES OF

$E \longrightarrow B(^3II_{0_u}+)$ SYSTEM OF I_2
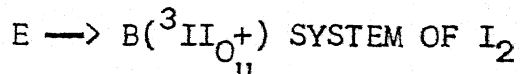
Introduction

The emission system of iodine in the region($4320-4000$Å)

was first observed by Elliot [1] in a predominant atmosphere of

N_2 alongwith the other band systems mentioned in the Chapter 3.

Later, it was obtained by Waser and Wieland [2],Venkateswarlu

and Verma [3,4]. The former excited iodine by high frequency

discharge in a predominant atmosphere of argon,while the latter

used transformer discharge to excite iodine in the presence of

argon. They obtained bands over a more extended region than

that of Elliot. From their analyses of this system, all of

them agreed that the lower state involved in this transition

is the well-known $B(^3II_{0^+u})$ state. There are different opinions about the upper state of this band system. The upper state is called the E state [5]. Venkateswarlu [3] suggested that the upper state of this system is very probably a O_g^+ state corresponding to $\overline{2242}\ ^1\Sigma_g^+$, whereas Waser and Wieland [2] are of the opinion that it is $1432\ ^3II_{0^+g}$ state.

Using normal and slightly radioactive isotopes of iodine, Wieland et al. [6] have re-recorded and repeated the vibrational analysis of this band system to bring the band head formula of Ref.(2) in accordance with the latest B state constants of that time. The isotopic effect studied by them supports the assignment of B state as the lower state of this band system and the upper state (E) is an ion-pair state with $T_e = 41411.8\ cm^{-1}$. Rousseau and Williams [7] excited the E state through two-photon excitation via B state and could observe only doublet structure in the resulting E —> B fluorescence spectrum. Later Rousseau [8] determined the lifetime of E —> B emission to be 27 nsec., and hence suggested the electronic assignment of the E state to be $^3II_{0g}^+$, for E —> B emission to be strongly allowed and to have a short fluorescence lifetime. Danyluk and King [9] using sequential two-photon absorption (E <— B <— X) reported five even parity (g) states which they labeled as $\alpha, \beta, \gamma, \delta$ and ϵ states in the region 40000-44000 cm^{-1}. They claimed that the emission bands in the region (4320-4000 Å) can be interpreted to be due

to transitions from three of these states to the well-known B state. Williamson [10] repeated the experiment choosing low vibrational levels of B state, whereas King et al. used the vibrational levels of B state near the dissociation limit. Unlike King et al., he could observe only one even parity state and his observations are in good agreement with those of Wieland et al. [6]. Moreover, he found that the ε state observed by King et al. could be the same as the E state with a change of +12 in the vibrational numbering. This observation was later confirmed by King et al. [11]. Cunha et al. [12] using the same technique as that of King and Williamson, studied the E —> B fluorescence system with the lower vibrational levels of B state as the intermediate step, and reported the molecular constants. But they do not find any agreement between their constants and those of the five states reported by King et al. The rotational structure of the E state is studied by polarization spectroscopy also by Brand et al. [13,14], who, from their observations, ascertain the absence of Q branch and thus support the designation of O_g^+ to the E state. The rotational constants reported by them are comparable to those reported in Ref. [11]. Chevaleyre et al. [15] excited the states in the E state region choosing intermediate vibrational levels of B state $(40 \leq v_B \leq 70)$ as the first step of excitation. In the fluorescence spectrum, they could observe two different vibrational progressions, one with doublet structure and the other

with triplet structure. From their observations, they conclude that transitions from B state are taking place to two different higher electronic states (O_g^+ (E) and 1g). They attribute three of the five ion-pair states observed by King et al. to perturbation effects. This possibility, of some of the band systems observed by King et al. being due to perturbation effects, was earlier pointed out by Guy et al. [16]. As all the rotational constants reported earlier were derived from the results of laser excited fluorescence experiments, they are not expected to be very accurate as the available data is not extensive. Hence, it was thought worthwhile to study the high resolution spectra of this emission system excited by conventional techniques, where all the possible rotational transitions could be observed and to calculate the rotational constants. In the present chapter, the rotational analysis of this system is presented. In addition to this, the results of the vibrational analysis of this band system are also reported. In this vibrational analysis, an attempt is made to account for all the bands reported by Venkateswarlu [3] and Wieland et al. [6]. The vibrational constants for the E state are obtained in accordance with the high precision constants of the B state from Ref. (17).

Vibrational Analysis

The band head positions of all the bands observed by Wieland et al. [6] both for $^{127}I_2$ and $^{129}I_2$ alongwith all

the extra bands reported by Venkateswarlu are fitted to a
polynomial in v', after subtracting the $G''(v'' + \frac{1}{2})$ calculated
from the B state constants from the band head values. The
values of $G''(v'' + \frac{1}{2})$ are calculated from the expression given
below:

$$G''(v'' + \frac{1}{2}) = \sum_{i=1}^{m} C_i''[\rho(v'' + \frac{1}{2})]^i \ , \ m = 11 \qquad (5.1)$$

and the vibrational constants of the E state are obtained
from a least-squares solution of the polynomial given below:

$$\nu_i = \Delta T_e + \sum_{j=1}^{n} C_j'[\rho(v' + \frac{1}{2})]^j, \ n = 4 \qquad (5.2)$$

In the above two equations

$$\rho = 1.0000 \quad \text{for} \ ^{127}I_2 \ \text{and}$$

$$\rho = 0.99221 \quad \text{for} \ ^{129}I_2.$$

The solution to Equation (5.2) is obtained in a manner
similar to that followed in rotational analysis as explained
in Chapter 2, in which all the band heads are expressed in a
matrix form. The constants obtained for the upper state are
reported in Table 5.1, along with those given by Wieland
et al. for comparison. These constants do not differ much
from those of Ref. [6] and they explain all the bands fitted
to the least-squares within $\pm$ 3 cm^{-1}. The vibrational assign-
ments, the band head positions and the differences between the
observed and the calculated band heads are listed in Table 5.2.

TABLE 5.1

Vibrational Constants (cm^{-1}) for the E State of I_2

	Present work	Ref.(6)
ΔT_e	41410.71(25)	41411.8
$C_1^!$ (ω_e)	102.473(23)	101.59
$C_2^!$ ($-\omega_e\, x_e$)	-0.4813	-0.2380
$C_3^!$ ($\times 10^2$)	1.920 (110)	-
$C_4^!$ ($\times 10^4$)	-4.491 (124)	-

TABLE 5.2

VIBRATIONAL BANDS IN (4320-4000A) SYSTEM

$^{127}I_2$			$^{129}I_2$		
v',v"	FOBS (cm-1)	O-C (cm-1)	v',v"	FOBS (cm-1)	O-C (cm-1)
0,29	22731.0	2.72(P)			
7,37	22911.0	-3.08(P)			
8,28	22955.0	-1.53			
8,37	23014.0	2.28(P)			
			2,28	23018.0	-0.57
3,29	23032.0	1.32(P)			
1,28	23058.5	0.40	1,28	23070.0	-1.17
2,27	23079.0	-0.38			
3,28	23104.5	0.48	3,28	23117.5	-0.37
8,37	23109.0	0.29(P)			
0,24	23115.5	-2.12	0,24	23131.5	0.48
4,29	23132.0	1.89	4,29	23142.5	-0.80
1,25	23137.0	1.37	1,25	23149.5	-0.99
7,33	23153.0	0.13(P)			
2,26	23157.0	0.13	2,26	23170.5	-0.60
3,27	23179.5	0.06	3,27	23192.5	-0.65
6,31	23184.0	-2.95(P)			
8,34	23199.0	1.45			
4,28	23201.0	-2.46			
0,23	23200.5	1.30	0,23	23215.0	0.60
1,24	23217.0	-0.19	1,24	23230.0	-1.81
5,29	23230.0	1.01	5,29	23241.5	0.07
2,25	23235.5	-0.90	2,25	23249.5	-0.98
8,33	23248.0	-2.41(P)			
8,20	23254.0	-2.42			
3,26	23257.0	0.07	3,26	23270.5	0.04
4,27	23279.5	0.62	4,27	23294.0	2.17
7,31	23282.0	-2.89(P)			
0,22	23286.0	1.22	0,22	23300.0	0.42
5,26	23301.0	-1.33			
1,23	23301.0	0.23	1,23	23315.5	0.39

Table 5.2(Continued)

VIBRATIONAL BANDS IN(4320-4000A) SYSTEM

127_{I_2}			129_{I_2}		
v',v''	FREQ (cm-1)	O-C (cm-1)	v',v''	FREQ (cm-1)	O-C (cm-1)
9,32	23315.0	-0.37(P)			
2,24	23318.0	0.04	2,24	23331.0	-0.80
6,29	23325.0	0.03			
3,25	23330.0	-0.46	3,25	23347.5	-2.28
9,33	23347.0	-0.57(P)			
4,26	23357.5	1.14			
0,21	23373.0	0.67	2,21	23387.5	0.71
1,22	23380.0	-0.35	1,22	23401.0	0.63
2,23	23401.5	-0.04	9,32	23424.0	1.87
2,24	23422.0	3.32	3,24	23433.0	1.90
4,25	23437.0	1.11	4,25	23444.0	-4.45
0,20	23462.5	0.66	0,20	23470.5	0.58
1,21	23473.5	-0.40	7,28	23487.0	-0.57
2,22	23489.0	1.89	2,22	23500.0	-0.36
3,23	23501.0	-0.60	3,23	23512.0	2.48
4,24	23518.0	0.55	4,24	23527.0	-2.77
5,25	23534.0	-0.77	9,30	23560.5	2.17
0,19	23554.0	0.71	0,19	23568.0	1.05
2,21	23573.5	-1.17	2,21	23586.0	-1.57
3,22	23587.0	-0.17	3,22	23600.0	0.34
5,24	23615.0	-1.33(P)			
0,18	23647.5	0.84	0,18	23660.5	0.03
1,19	23654.5	-0.36	1,19	23668.0	0.26
2,20	23664.0	-0.18	2,20	23676.5	-0.20
			4,22	23697.0	-1.33
5,23	23699.0	-0.91			
6,24	23716.0	1.28	6,24	23755.5	0.85
0,17	23742.5	0.58			
1,18	23748.0	-0.23	1,18	23760.5	-0.16
2,19	23755.0	-0.63			
3,20	23763.0	-1.24			

Table 5.2(Continued)

VIBRATIONAL BANDS In(4320-4000A) SYSTEM

$^{127}I_2$			$^{129}I_2$		
v',v"	FREQ (cm-1)	0-C (cm-1)	v',v"	FREQ (cm-1)	0-C (cm-1)
4,21	23773.0	-1.16			
5,22	23783.0	3.52			
6,23	23799.0	1.21			
7,24	23814.0	1.34			
8,25	23830.5	1.86			
0,16	23840.0	0.95			
1,17	23843.5	0.01	1,17	23856.0	0.55
3,19	23855.5	-0.19	3,19	23866.5	-0.53
4,20	23866.5	2.83			
6,22	23885.0	1.13(P)			
8,24	23914.0	3.80			
9,25	23924.0	-1.80(P)			
0,15	23939.0	0.96			
1,16	23940.5	-0.13	1,16	23952.0	-0.06
2,17	23945.0	0.74			
3,18	23950.0	0.95			
4,19	23957.0	1.88			
5,20	23963.0	0.45			
8,23	23994.0	0.22(P)			
10,25	24022.0	-0.62(P)			
0,14	24040.0	1.14	0,14	24050.5	0.54
1,15	24040.0	0.39			
2,16	24041.0	-0.39			
4,18	24047.0	-1.19			
7,21	24068.0	-1.37(P)			
9,33	24087.0	-3.94(P)			
10,24	24104.0	-0.18(P)			
0,13	24140.0	-1.48			
1,14	24140.5	0.07			
2,15	24140.5	0.12			
			3,16	24152.0	0.65

TABLE 5.2(Continued)

VIBRATIONAL BANDS IN(B320-4000A) SYSTEM

$^{127}I_2$

v',v''	FREQ (cm-1)	O-C (cm-1)
7,20	24153.5	0.62
15,29	24195.5	0.55
2,14	24239.0	-2.20
3,15	24240.5	-0.44
10,22	24270.0	2.67(P)
14,26	24327.5	-0.73
4,15	24340.5	0.63
10,21	24342.0	0.75
3,13	24442.0	-1.83
4,14	24442.0	1.31
0,10	24462.0	2.03(P)
5,14	24540.0	0.43(P)
4,13	24544.0	0.69
0,9	24560.0	-3.06(P)
18,27	24626.0	2.06(P)
5,13	24642.0	-0.19
3,11	24658.0	3.54(P)
1,9	24668.0	-3.17
6,13	24739.0	-1.57(P)
5,12	24746.5	-0.10
1,8	24784.0	1.50(P)
11,17	24827.5	0.56
7,13	24840.5	1.98

$^{129}I_2$

v',v''	FREQ (cm-1)	O-C (cm-1)
9,22	24188.0	3.46
11,24	24210.0	2.19
3,15	24250.5	0.70
4,16	24250.5	0.47
4,15	24349.5	1.03
10,21	24370.0	2.16
4,14	24448.5	-0.21
4,13	24552.0	1.27
5,12	24753.0	0.33
9,15	24836.0	1.32

TABLE 5.2(Continued)

VIBRATIONAL BANDS IN(4320-4000A) SYSTEM

$^{127}I_2$			$^{129}I_2$		
v',v''	FREQ (cm-1)	O-C (cm-1)	v',v''	FREQ (cm-1)	O-C (cm-1)
			0,6	24913.0	-1.04
			12,17	24920.5	1.06
9,15	24935.0	-1.06(P)	9,13	24945.0	4.49
18,25	24947.0	-1.10(P)			
5,10	24958.5	-2.18	5,10	24963.5	-1.86
3,8	24985.0	1.07			
5,9	25072.0	1.09			
12,25	25110.0	-1.17			

The extra bands observed by Prof. Venkateswarlu which are
fitted to least-squares to get the constants are denoted by(P).

Rotational Analysis

The rotational structure of each vibrational band consists of P and R branches only and thus supports the assignment of the transition as $O_g^+ \longrightarrow O_u^+$ given by the earlier workers. The individual bands, which are all red degraded, are observed to be having well-defined rotational structure and the rotational lines in each band could be picked out very easily almost upto the band head. Moreover, the P and R branches are seen to get separated after an initial over-lapping at lower J values for most of the bands analysed. As the lower state of this emission system is the well-chara-cterised B state [17], the assignment of rotational numbering is rather simplified. After picking out the P and R branches the combination differences for each band for the lower and upper states given by

$$\Delta_2 F''(J) = R(J-1) - P(J+1) \qquad (5.3)$$

$$\Delta_2 F'(J) = R(J) - P(J) \qquad (5.4)$$

respectively are calculated with an arbitrary J numbering in both the branches, then the J numbering in one of the bran-ches (P) is adjusted by trial and error so that the $\Delta_2 F$ values for all the bands with a common upper or lower vibra-tional levels agree within the experimental error. Now the relative J is determined and the absolute J is decided upto an additive constant. An additional check on this relative

J numbering is made by comparing the $\Delta_2 F''$ values for all the bands with the $\Delta_2 F''$ values calculated from the B state constants [17]. The agreement between these values is very satisfactory adding credence to the relative J numbering decided upon. Now the observed $\Delta_2 F$ values are plotted against J and the absolute J numbering is fixed at the value for which a straightline passing through $J = -\frac{1}{2}$ is obtained. After the assignment of J values to the rotational lines in P and R branches is thus made, the rotational constants for each band are calculated. Whenever more than one band shared an upper or lower vibrational level, the constants from the least-squares fits of the individual bands are merged to get a single set of rotational constants for each level. To get constants for individual bands and then to merge them, the procedure described in Chapter 2 is followed.

Results and Discussion

The rotational structure of nine bands, i.e., (0-20), (0-19), (0-18), (0-17), (1-24), (1-14), (3-13), (3-15) and (2-21), is analysed for the first time in the present work and the results are reported. In most of the bands, the P and R branches are clearly seen at high J values. The single values for the constants for v= 0 level of the E state are evaluated by merging the constants obtained from the individual fits of (0-17), (0-18), (0-19) and (0-20) bands, and

those for $v = 1$ level of the E state by merging the constants from the fits of the bands (1-14) and (1-24). Similarly, the constants obtained from (3-13) and (3-15) bands are merged to get single values for the constants for $v = 3$ of the E state. Finally the B_v and D_v values for the upper and lower states are least-squares fitted to the Equations (1.6) and (1.7) to get B_e, α_e, γ_e, D_e and β_e. The internuclear distance R_e is calculated from the B_e values for the upper and lower states using Equation (1.8). The rotational constants B_v and D_v for the E and B states are tabulated in Tables 5.3 and 5.4 along with the values obtained by the previous workers. In Table 5.5, the values of B_e, α_e, γ_e, D_e, β_e and R_e for the E and B states are listed. The rotational assignments along-with the observed wave numbers and the differences between the observed and calculated wave numbers in each band are presented in Tables 5.6 - 5.14. A reproduction of the rotational structure of (0-20), (0-18), (0-17), (1-14), (3-13) and (3-15) bands is given in Figs. 5.1 - 5.6.

Conclusions

In the present work, the rotational constants of the E state are calculated from the rigorous rotational analysis of nine bands belonging to E $\longrightarrow$ B emission system. These constants are considered more meaningful than the previously reported ones as they are derived from a very extensive data with more than 220 rotational lines in each of six of the

bands while the others are having more than 150 lines per band. Only one band (1-24) has 106 rotational lines. All the bands analysed have only P and R branches. In the region which is covered by these bands, no other prominent band which has well-developed structure showing P, R and Q branches was observed. This is contrary to what one would expect on the basis of the work of Chevaleyre et al. [15]. According to them the $(^3\Pi_{1g})$ state lies very close to the E state with almost equal internuclear distance. With this as the initial state, there should be another transition giving raise to bands with P, Q and R branches, for which there is no evidence in the present experiments.

The results obtained in this work as well as those of the earlier workers clearly shows that the transition involved in this system is $O_g^+ \longrightarrow O_u^+$. The lower state is $B(^3\Pi_{O_u}+)$. From the electronic scheme given by Mulliken, there are four O_g^+ states which lie above $B(^3\Pi_{O_u}+)$ state, one arising from 0442 configuration, two from 2242 configuration and one from 1432 configuration. As the first of these states lies far above the region of interest, it can not be the upper state of this band system. The other three O_g^+ states correspond to $^3\Pi_{O_g}+$, $^1\Sigma_g^+$ and $^3\Sigma_{O_g}^-+$ in case 'a'. Though $^3\Pi_{O_g}+$ and $^1\Sigma_g^+$ states are considered as the possible upper states of this band system, the $^3\Sigma_{O_g}^-+$ state is not considered as the upper state so far. There does not seem to be

enough reason for not considering the $^3\Sigma^-_{0^+g}$ state as the
possible upper state of this band system. In fact, considering
that ti is band system is much weaker than the band system at
3400 $\overset{\circ}{A}$, it is more probable that the upper state is $^3\Sigma^-_{0^+g}$, in
which case the transition will be a less allowed one and there
by a less intense one. Further work will be needed to unambi-
guously identify the origin of the 0^+_g state corresponding to
the upper state of the band system discussed in this chapter.
A step by step excitation to various levels in the region
40000-55000 cm^{-1} through two or three proton processes might
reveal the various electronic states that lie in this region
and their nature.
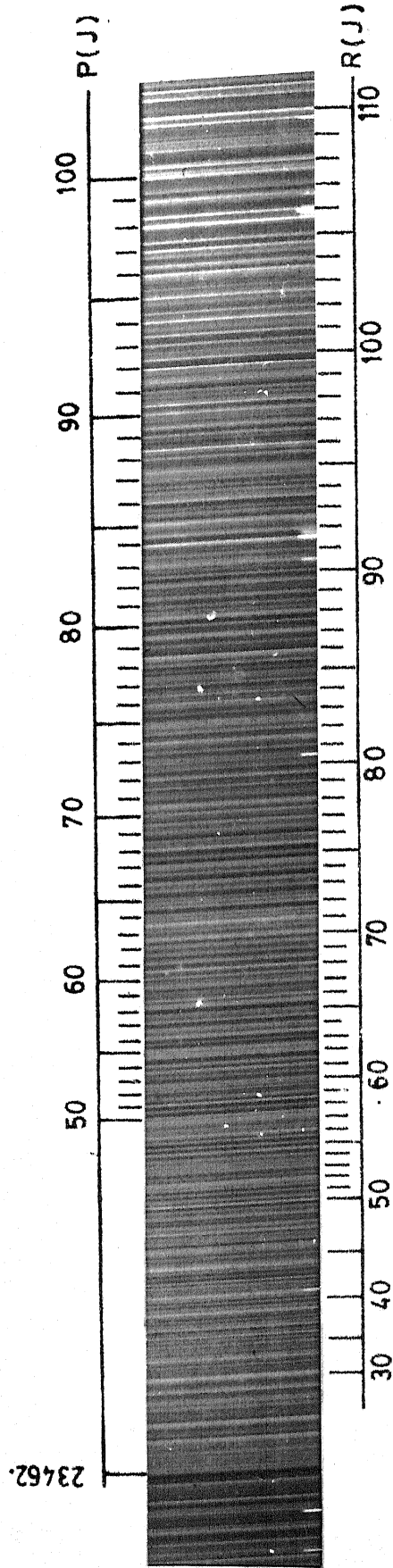
FIG. 5·1   ROTATIONAL STRUCTURE OF (0–20) BAND
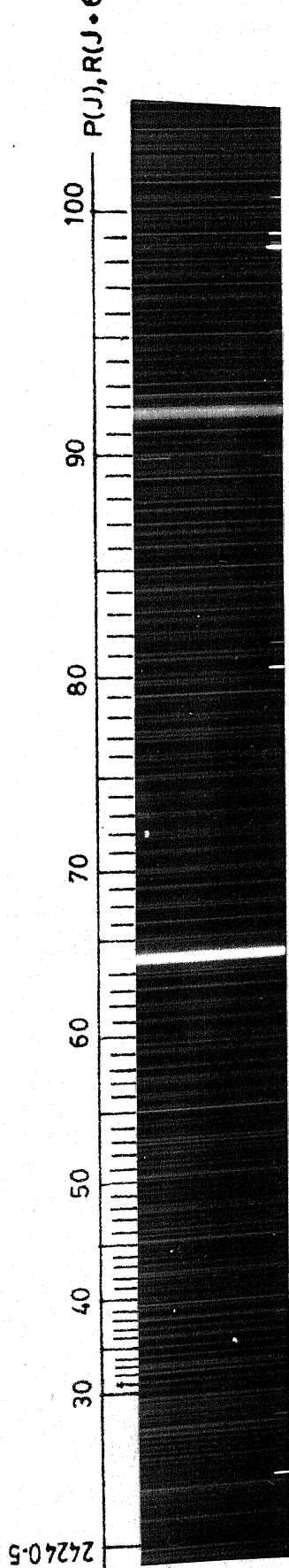
FIG. 5·2   ROTATIONAL STRUCTURE OF (3–15) BAND
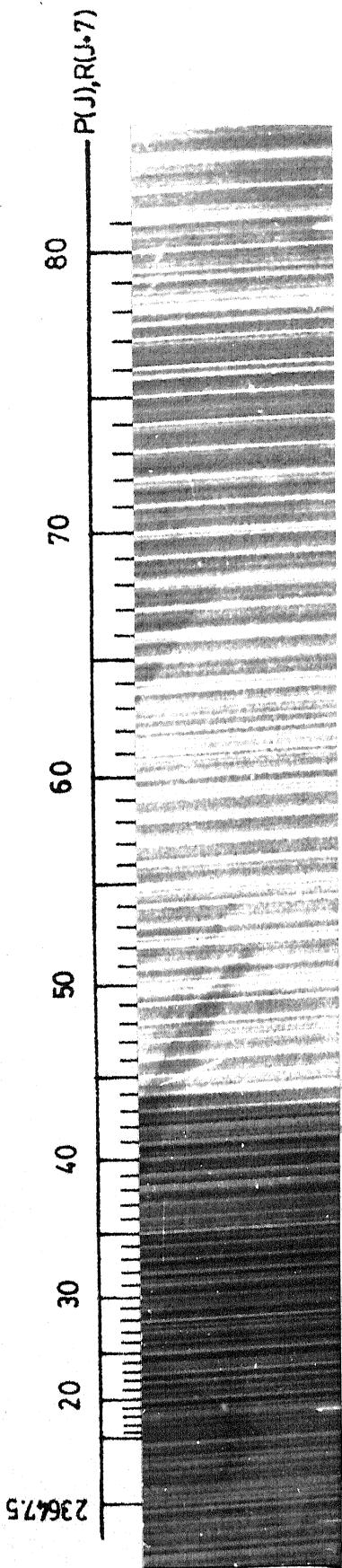
FIG. 5.3 ROTATIONAL STRUCTURE OF (0-18) BAND
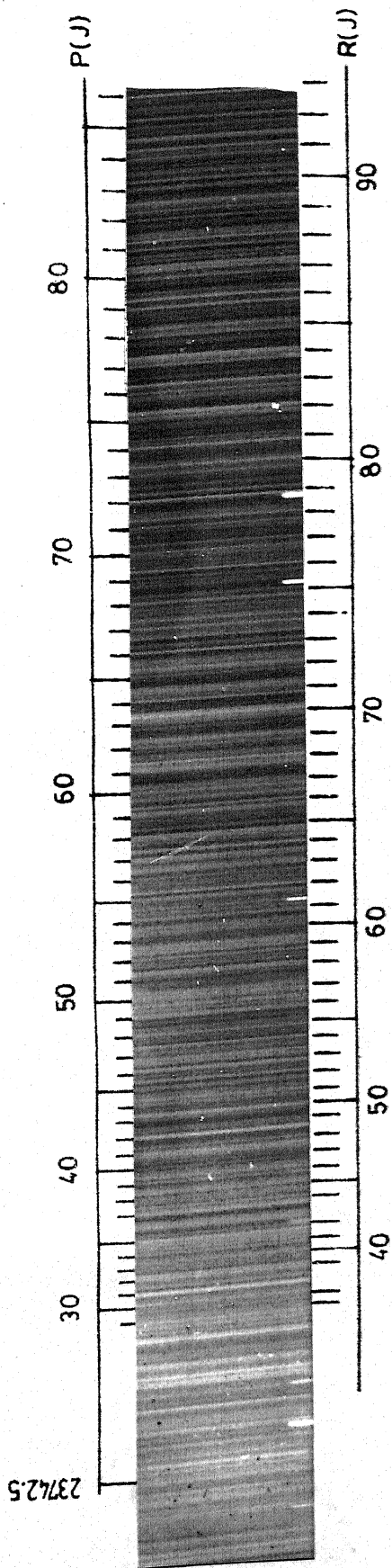
FIG. 5.4 ROTATIONAL STRUCTURE OF (0-17) BAND
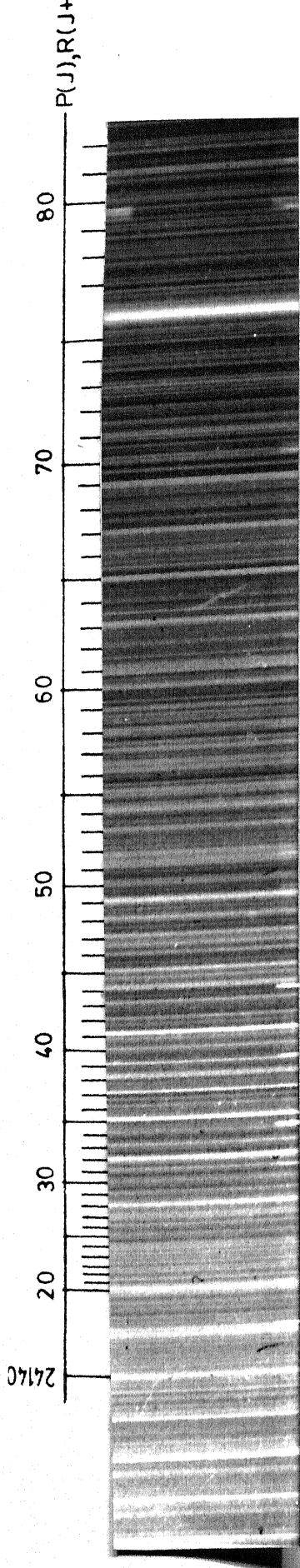
FIG. 5.5 ROTATIONAL STRUCTURE OF (1-14) BAND
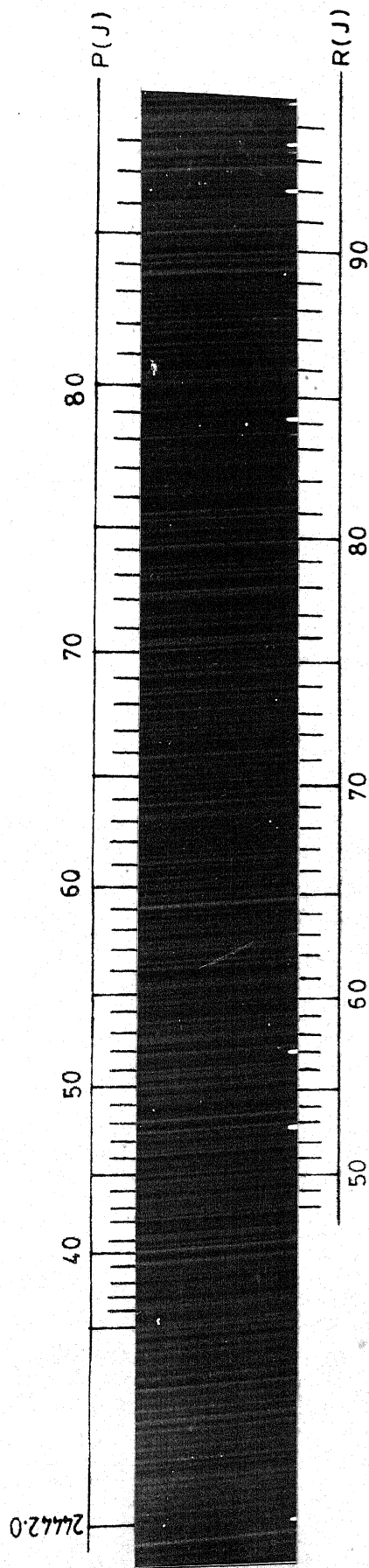
FIG. 5.6 ROTATIONAL STRUCTURE OF (3-13) BAND

TABLE 5.3

Rotational Constants (cm^{-1}) for the E State of I_2

| v | Present work | | Ref.(10) | Ref.(11) |
	$10^2 B_v$	$10^8 D_v$	$10^2 B_v$	$10^2 B_v$
0	1.9981(12)	0.424(43)	2.0150(21)	1.9929(56)
1	1.9930(21)	0.313(112)	2.0320(31)	1.9919(74)
2	1.9816(39)	0.488(135)	2.0255(44)	1.9863(28)
3	1.9710(42)	0.290(194)	1.9780(13)	1.9831(25)

TABLE 5.4

Rotational Constants (cm^{-1}) for the B State of I_2

v	Present work		Ref.(17)	
	$10 B_v$	$10^7 D_v$	$10^2 B_v$	$10^7 D_v$
13	2.6659(42)	0.0790(194)	2.6733	0.08386
14	2.6588(20)	0.1071(116)	2.6541	0.08564
15	2.6277(42)	0.0443(197)	2.6345	0.08822
17	2.5979(13)	0.1057(45)	2.5941	0.09340
18	2.5776(12)	0.1114(45)	2.5732	0.09624
19	2.5561(13)	0.1140(45)	2.5519	0.09941
20	2.5349(13)	0.1205(45)	2.5302	0.10299
21	2.5083(39)	0.1216(136)	2.5079	0.10638
24	2.4368(21)	0.0258(139)	2.4381	0.18034

TABLE 5.5

Molecular Constants (cm^{-1}) for E $\longrightarrow$ B System of I_2

	Present work		Values from the literature for E state				
	B state	E state	Ref.(10)	Ref.(11)	Ref.(12)	Ref.(14)	Ref.(15)
$10^2 B_e$	2.798(40)	2.0044(22)	2.0255(68)	2.0116(20)	2.052(2)	1.997	2.0043(11)
$10^5 \alpha_e$	3.285	9.240(95)	8.340(98)	8.76(44)	16.0(6)	5.449	5.42(3)
$10^6 \gamma_e$	−4.684	—	—	1.86(23)	—	0.024	—
$10^9 D_e$	3.365	3.653	—	—	—	3.246	16.00(30)
$10^{10} \beta_e$	4.177	3.207	—	—	—	0.116	—
R_e(Å)	3.082	3.6409	—	3.6342	3.6	—	—

TABLE 5. 6

WAVENUMBERS (cm-1) OF THE ROTATIONAL LINES IN THE
(0-20) BAND OF E-B SYSTEM.

$v_0 = 23462.54$

J	R(J)	O-C	P(J)	O-C
4. 0			23462. 35	0. 05
6. 0			23462. 09	0. 02
7. 0			23461. 96	0. 00
8. 0			29461. 80	-0. 03
9. 0			23461. 64	-0. 06
13. 0			23460. 81	-0. 04
15. 0	23461. 96	0. 07		
16. 0	23461. 80	0. 04	23460. 42	-0. 02
17. 0	23461. 64	0. 02	23460. 19	-0. 03
18. 0	23461. 48	0. 02	23459. 97	-0. 01
19. 0	23461. 26	-0. 04	23459. 72	-0. 02
20. 0	23461. 12	-0. 01	23459. 47	-0. 02
21. 0	23460. 94	0. 00	23459. 20	0. 02
22. 0	23460. 72	-0. 02	23458. 95	0. 00
23. 0	23460. 53	0. 01	23458. 68	0. 02
24. 0	23460. 27	-0. 05	23458. 36	0. 00
25. 0	23460. 09	0. 00	23458. 05	0. 00
26. 0	23459. 85	0. 00	23457. 73	0. 00
27. 0	23459. 60	0. 00	23457. 43	0. 02
28. 0	23459. 33	-0. 01	23457. 05	-0. 02
29. 0	23459. 05	-0. 02	23456. 70	0. 02
30. 0	23458. 81	0. 02	23456. 33	-0. 02
31. 0	23458. 49	-0. 01	23455. 99	0. 00
32. 0	23458. 19	-0. 01	23455. 60	0. 00
33. 0	23457. 89	0. 01	23455. 21	0. 00
34. 0	23457. 57	0. 01	23454. 79	-0. 01
35. 0	23457. 25	0. 02	23454. 40	-0. 01
36. 0	23456. 87	-0. 01	23453. 95	-0. 03
37. 0	23456. 50	-0. 02	23453. 51	-0. 02
38. 0	23456. 15	-0. 01	23453. 08	0. 00
39. 0	23455. 81	0. 03	23452. 62	0. 00
40. 0	23455. 37	-0. 02	23452. 17	0. 01
41. 0	23455. 07	0. 08	23451. 67	0. 00
42. 0	23454. 58	-0. 01	23451. 17	-0. 02
43. 0	23454. 17	0. 00	23450. 69	0. 00
44. 0	23453. 75	0. 01	23450. 19	0. 00

TABLE 5.6 Contd.

J	R(J)	O-C	P(J)	O-C
45.0	23453.29	-0.01	23449.69	0.02
46.0	23452.83	-0.02	23449.14	0.00
47.0	23452.38	0.00	23448.57	-0.02
48.0	23451.89	-0.02	23448.08	0.04
49.0	23451.47	0.04	23447.48	0.00
50.0	23450.92	-0.02	23446.90	0.00
51.0	23450.42	-0.01	23446.31	0.00
52.0	23449.91	-0.01	23445.72	0.00
53.0	23449.41	0.02	23445.11	-0.01
54.0	23448.86	-0.01	23444.53	0.02
55.0	23448.30	-0.01	23443.87	0.01
56.0	23447.76	0.00	23443.28	0.04
57.0	23447.19	-0.01	23442.58	-0.02
58.0	23446.60	0.01	23441.95	0.00
59.0	23446.04	-0.03	23441.28	0.00
60.0	23445.40	-0.01	23440.60	0.00
61.0	23444.81	-0.01	23439.92	0.01
62.0	23444.20	0.00	23439.18	-0.03
63.0	23443.57	0.00	23438.51	0.01
64.0	23442.91	-0.02	23437.79	0.00
65.0	23442.26	-0.02	23437.06	0.00
66.0	23441.62	0.00	23436.32	0.00
67.0	23440.93	-0.02	23435.55	-0.02
68.0	23440.27	0.00	23434.82	0.01
69.0	23439.54	-0.04	23434.04	0.00
70.0	23438.90	0.02	23433.28	0.02
71.0	23438.19	0.02	23432.48	0.02
72.0	23437.44	-0.01	23431.69	0.02
73.0	23436.72	0.00	23430.86	0.01
74.0	23435.97	0.00	23430.06	0.03
75.0	23435.24	0.01	23429.19	-0.01
76.0	23434.46	0.00	23428.36	0.00
77.0	23433.71	0.02	23427.52	0.02
78.0	23432.89	-0.01	23426.66	0.02
79.0	23432.11	0.00	23425.79	0.02
80.0	23431.31	0.00	23424.90	0.01
81.0	23430.52	0.03	23424.01	0.02
82.0	23429.65	-0.02	23423.12	0.03
83.0	23428.83	0.00	23422.19	0.01

TABLE 5. 6 Contd.

J	R(J)	O-C	P(J)	O-C
84. 0	23427. 99	0. 00	23421. 27	0. 02
85. 0	23427. 13	-0. 01	23420. 35	0. 03
86. 0	23426. 27	0. 00	23419. 40	0. 02
87. 0	23425. 42	0. 02	23418. 46	0. 03
88. 0	23424. 61	0. 03	23417. 48	0. 02
89. 0	23423. 65	0. 03	23416. 49	0. 00
90. 0	23422. 71	-0. 01	23415. 51	0. 00
91. 0	23421. 80	0. 00	23414. 54	0. 03
92. 0	23420. 89	0. 01	23413. 53	0. 02
93. 0	23419. 97	0. 03	23412. 50	0. 00
94. 0	23419. 01	0. 01	23411. 48	0. 01
95. 0	23418. 08	0. 03	23410. 44	0. 00
96. 0	23417. 10	0. 02	23409. 41	0. 01
97. 0	23416. 12	0. 01	23408. 37	0. 02
98. 0	23415. 14	0. 01	23407. 30	0. 02
99. 0	23414. 15	0. 02	23406. 18	-0. 03
100. 0	23413. 13	0. 03	23405. 14	0. 01
101. 0	23412. 09	-0. 03	23404. 04	0. 00
102. 0	23411. 10	0. 01	23402. 94	0. 00
103. 0	23410. 07	0. 01	23401. 81	-0. 01
104. 0	23409. 03	0. 01	23400. 69	-0. 01
105. 0	23408. 01	0. 04	23399. 59	0. 02
106. 0	23406. 91	0. 00	23398. 44	0. 01
107. 0	23405. 83	0. 00	23397. 28	0. 00
108. 0	23404. 75	0. 00	23396. 12	0. 00
109. 0	23403. 66	0. 00	23394. 96	0. 01
110. 0	23402. 59	0. 03	23393. 77	0. 00
111. 0	23401. 45	0. 00	23392. 58	-0. 01
112. 0	23400. 29	-0. 04	23391. 38	-0. 01
113. 0	23399. 21	0. 01	23390. 16	-0. 02
114. 0	23398. 05	-0. 02	23388. 96	0. 00
115. 0	23396. 92	0. 00	23387. 73	-0. 01
116. 0	23395. 74	-0. 02	23386. 50	0. 00
117. 0	23394. 58	-0. 01	23385. 25	-0. 01
118. 0	23393. 40	-0. 02	23383. 95	-0. 05
119. 0	23392. 21	-0. 02	23382. 69	-0. 05
120. 0	23391. 03	0. 00	23381. 44	-0. 02
121. 0	23389. 83	0. 00	23380. 21	0. 03
122. 0	23388. 60	-0. 02	23378. 89	0. 00
123. 0	23387. 38	-0. 01	23377. 55	-0. 03

TABLE 5. 6 Contd.

J	R(J)	O-C	P(J)	O-C
124. 0	23386. 15	-0. 01	23376. 25	-0. 02
125. 0	23384. 94	0. 02	23374. 93	-0. 01
126. 0	23383. 67	0. 00	23373. 61	0. 03
127. 0	23382. 39	-0. 02	23372. 31	-0. 02
128. 0	23381. 09	-0. 05	23370. 92	-0. 02
129. 0	23379. 88	0. 02	23369. 54	-0. 04
130. 0	23378. 54	-0. 03	23368. 20	-0. 01
131. 0	23377. 24	-0. 03	23366. 82	-0. 02
132. 0	23375. 96	0. 00	23365. 46	0. 01
133. 0	23374. 63	-0. 02	23364. 03	-0. 03
134. 0	23373. 31	-0. 01	23362. 63	-0. 03
135. 0	23371. 98	-0. 01	23361. 24	-0. 01
136. 0	23370. 69	0. 04	23359. 82	0. 00
137. 0	23369. 26	-0. 04	23358. 38	-0. 01
138. 0	23367. 93	0. 00	23356. 94	-0. 02
139. 0	23366. 58	0. 01	23355. 52	0. 01
140. 0	23365. 17	-0. 02	23354. 03	-0. 03
141. 0	23363. 82	0. 02	23352. 58	-0. 01
142. 0	23362. 42	0. 01	23351. 13	0. 02
143. 0	23361. 08	0. 08	23349. 70	0. 07
144. 0	23359. 58	0. 00	23348. 14	0. 00
145. 0	23358. 15	-0. 01	23346. 72	0. 08
146. 0	23356. 71	-0. 02		
147. 0	23355. 27	-0. 02		
148. 0	23353. 79	-0. 05		
149. 0	23352. 34	-0. 04		
150. 0	23350. 88	-0. 04		
151. 0	23349. 44	0. 00		
152. 0	23347. 97	0. 01		

TABLE 5.7

WAVENUMBERS (cm-1) OF THE ROTATIONAL LINES IN THE
(0-19) BAND OF E-B SYSTEM.

v_0 = 23553.96

J	R(J)	O-C	P(J)	O-C
5.0			23553.64	0.03
6.0	23554.04	0.02		
7.0	23554.04	0.06	23553.37	-0.01
8.0	23554.04	0.10	23553.25	0.00
9.0			23553.11	0.00
10.0	23553.79	-0.01	23552.97	0.01
11.0			23552.79	-0.01
12.0	23553.64	0.02	23552.61	-0.01
13.0			23552.44	0.00
14.0	23553.37	-0.03	23552.24	0.00
15.0	23553.25	-0.02	23552.03	-0.01
16.0	23553.11	-0.02	23551.81	-0.01
17.0	23552.97	-0.01	23551.57	-0.02
18.0	23552.79	-0.03	23551.35	0.00
19.0	23552.61	-0.04	23551.09	-0.01
20.0	23552.44	-0.03	23550.83	0.00
21.0	23552.24	-0.03	23550.54	-0.02
22.0	23552.03	-0.04	23550.28	0.01
23.0	23551.81	-0.04	23549.90	-0.08
24.0	23551.57	-0.05	23549.65	-0.02
25.0	23551.35	-0.03	23549.32	-0.03
26.0	23551.09	-0.04	23549.01	-0.01
27.0			23548.70	0.02
28.0	23550.54	0.06	23548.32	-0.01
29.0	23550.28	-0.04		
30.0	23549.90	-0.07	23547.60	0.01
31.0	23549.65	-0.06	23547.19	-0.02
32.0			23546.79	-0.02
33.0	23549.01	-0.06	23546.45	0.05
34.0	23548.70	-0.03	23545.99	0.00
35.0	23548.32	-0.02	23545.53	-0.03
36.0	23547.97	-0.05	23545.14	0.02
37.0	23547.60	-0.05	23544.68	0.02
38.0	23547.19	-0.08	23544.21	0.01
39.0			23543.76	0.03
40.0	23546.45	-0.02	23543.23	-0.01

TABLE 5.7 Cont'd

J	R(J)	O-C	P(J)	O-C
41. 0	23545. 99	-0. 06	23542. 71	-0. 04
42. 0	23545. 53	-0. 09	23542. 22	-0. 02
43. 0	23545. 14	-0. 05	23541. 71	-0. 01
44. 0	23544. 68	-0. 06	23541. 20	0. 01
45. 0			23540. 62	-0. 03
46. 0			23540. 09	-0. 01
47. 0	23543. 33	0. 00	23539. 47	-0. 07
48. 0	23542. 82	-0. 01	23538. 96	-0. 01
49. 0	23542. 34	0. 01	23538. 37	-0. 02
50. 0	23541. 81	0. 00		
51. 0			23537. 18	0. 01
52. 0	23540. 75	0. 00		
53. 0	23540. 20	0. 00	23535. 94	0. 00
54. 0	23539. 65	0. 00	23535. 30	0. 00
55. 0	23539. 07	-0. 01	23534. 68	0. 02
56. 0	23538. 49	0. 00	23534. 01	0. 01
57. 0	23537. 91	0. 01	23533. 33	0. 01
58. 0	23537. 31	0. 01	23532. 65	0. 01
59. 0	23536. 70	0. 01		
60. 0	23536. 06	0. 00	23531. 25	0. 00
61. 0	23535. 43	0. 00	23530. 54	0. 01
62. 0	23534. 79	0. 01	23529. 81	0. 00
63. 0	23534. 13	0. 00	23529. 07	0. 00
64. 0	23533. 47	0. 01	23528. 33	0. 00
65. 0	23532. 78	0. 00	23527. 58	0. 01
66. 0	23532. 10	0. 01	23526. 82	0. 02
67. 0	23531. 40	0. 01	23526. 04	0. 02
68. 0	23530. 68	0. 00	23525. 25	0. 02
69. 0	23529. 97	0. 01	23524. 45	0. 02
70. 0	23529. 24	0. 04	23523. 63	0. 01
71. 0	23528. 49	0. 00	23522. 81	0. 01
72. 0	23527. 75	0. 02	23521. 98	0. 02
73. 0	23526. 99	0. 02	23521. 13	0. 01
74. 0	23526. 21	0. 02	23520. 27	0. 01
75. 0	23525. 42	0. 01	23519. 39	-0. 01
76. 0	23524. 63	0. 02	23518. 54	0. 02
77. 0	23523. 81	0. 00	23517. 64	0. 00
78. 0	23523. 01	0. 02	23516. 75	0. 01
79. 0	23522. 19	0. 03	23515. 76	-0. 07

TABLE 5.7 Contd.

J	R(J)	O-C	P(J)	O-C
80. 0	23521. 35	0. 03	23514. 91	-0. 01
81. 0	23520. 50	0. 03	23513. 96	-0. 03
82. 0	23519. 61	0. 00	23513. 04	-0. 01
83. 0	23518. 73	-0. 01	23512. 07	-0. 03
84. 0	23517. 91	0. 05	23511. 11	-0. 02
85. 0	23517. 00	0. 03	23510. 17	0. 00
86. 0	23516. 07	0. 00	23509. 21	0. 02
87. 0	23515. 14	-0. 01	23508. 20	0. 01
88. 0	23514. 22	-0. 01	23507. 19	0. 00
89. 0	23513. 28	-0. 02	23506. 18	0. 00
90. 0	23512. 35	0. 00	23505. 14	-0. 01
91. 0	23511. 36	-0. 04	23504. 12	0. 00
92. 0	23510. 40	-0. 03	23503. 08	0. 00
93. 0	23509. 47	0. 01	23502. 04	0. 02
94. 0	23508. 47	0. 00	23500. 97	0. 01
95. 0			23499. 87	-0. 01
96. 0	23506. 47	0. 00	23498. 80	0. 01
97. 0	23505. 46	0. 01	23497. 70	0. 00
98. 0	23504. 43	0. 01	23496. 59	0. 00
99. 0	23503. 38	-0. 01	23495. 47	-0. 01
100. 0	23502. 34	0. 00	23494. 34	-0. 01
101. 0	23501. 28	0. 00	23493. 24	0. 03
102. 0	23500. 22	0. 01	23492. 06	0. 00
103. 0	23499. 14	0. 01	23490. 91	0. 00
104. 0	23498. 06	0. 01	23489. 72	-0. 02
105. 0	23496. 93	-0. 01	23488. 55	-0. 01
106. 0	23495. 83	0. 00	23487. 36	-0. 01
107. 0	23494. 71	0. 00	23486. 17	0. 00
108. 0	23493. 58	0. 00	23484. 96	0. 00
109. 0	23492. 45	0. 01	23483. 74	0. 00
110. 0	23491. 30	0. 01	23482. 50	-0. 01
111. 0	23490. 13	0. 00	23481. 27	-0. 01
112. 0	23488. 92	-0. 04	23480. 03	0. 00
113. 0	23487. 76	-0. 02	23478. 76	-0. 02
114. 0	23486. 59	0. 00	23477. 51	0. 01
115. 0	23485. 41	0. 02	23476. 21	-0. 01
116. 0	23484. 20	0. 02	23474. 93	0. 00
117. 0	23482. 95	-0. 01	23473. 63	0. 00
118. 0	23481. 73	0. 00	23472. 33	0. 02
119. 0	23480. 49	0. 00	23471. 00	0. 00

TABLE 5.7 Contd.

J	R(J)	O-C	P(J)	O-C
120. 0	23479. 24	0. 00	23469. 66	−0. 01
121. 0	23478. 00	0. 02	23468. 33	0. 00
122. 0	23476. 71	0. 00	23466. 98	0. 00
123. 0	23475. 45	0. 02	23465. 64	0. 02
124. 0	23474. 13	−0. 01	23464. 25	−0. 01
125. 0	23472. 85	0. 01	23462. 91	0. 03
126. 0	23471. 52	−0. 01	23461. 48	−0. 01
127. 0	23470. 21	0. 00	23460. 09	0. 00
128. 0	23468. 88	0. 00	23458. 68	0. 00
129. 0	23467. 55	0. 01	23457. 25	−0. 02
130. 0	23466. 19	−0. 01	23455. 81	−0. 03
131. 0	23464. 85	0. 01	23454. 40	0. 00
132. 0	23463. 47	0. 00	23452. 96	0. 00
133. 0	23462. 09	0. 00	23451. 47	−0. 03
134. 0	23460. 72	0. 01	23450. 04	0. 01
135. 0	23459. 33	0. 02	23448. 57	0. 01
136. 0	23457. 89	−0. 01		
137. 0	23456. 50	0. 01		
138. 0	23455. 07	0. 01		
140. 0	23452. 17	−0. 01		
141. 0	23450. 69	−0. 04		
142. 0	23449. 27	0. 00		
143. 0	23447. 77	−0. 02		
144. 0	23446. 31	0. 00		
145. 0	23444. 81	−0. 01		
146. 0	23443. 28	−0. 04		
147. 0	23441. 81	0. 01		
148. 0	23440. 27	−0. 02		
149. 0	23438. 79	0. 02		
150. 0	23437. 24	0. 01		

TABLE 5.8

WAVENUMBERS (cm-1) OF THE ROTATIONAL LINES IN THE
(0-18) BAND OF E-B SYSTEM.

$v_0 = 23647.35$

J	R(J)	O-C	P(J)	O-C
11.0	23647.09	0.02		
12.0	23646.94	-0.03		
13.0			23645.76	-0.02
14.0	23646.73	-0.01	23645.55	-0.02
15.0	23646.58	-0.02	23645.36	0.00
16.0	23646.47	0.01	23645.12	-0.01
17.0	23646.31	0.01	23644.88	-0.02
18.0	23646.18	0.05	23644.63	-0.02
19.0	23645.98	0.03	23644.38	-0.01
20.0	23645.76	0.00	23644.11	-0.01
21.0	23645.55	-0.01	23643.79	-0.04
22.0	23645.36	0.02	23643.51	-0.03
23.0	23645.12	0.00	23643.22	-0.01
24.0	23644.88	0.00	23642.92	0.00
25.0	23644.63	0.00	23642.58	-0.01
26.0	23644.38	0.01	23642.22	-0.03
27.0	23644.11	0.01	23641.87	-0.02
28.0	23643.79	-0.02	23641.52	-0.01
29.0	23643.51	-0.01	23641.14	-0.01
30.0	23643.22	0.01	23640.76	-0.01
31.0	23642.92	0.03	23640.35	-0.02
32.0	23642.58	0.02	23639.96	0.00
33.0	23642.22	0.00	23639.53	-0.01
34.0	23641.87	0.00	23639.08	-0.02
35.0	23641.52	0.02	23638.64	-0.02
36.0	23641.14	0.01	23638.18	-0.02
37.0	23640.76	0.02	23637.71	-0.03
38.0	23640.35	0.01	23637.25	-0.01
39.0	23639.96	0.03	23636.76	-0.01
40.0	23639.53	0.02	23636.24	-0.02
41.0	23639.08	0.01	23635.76	0.01
42.0	23638.64	0.01	23635.22	-0.01
43.0	23638.18	0.01	23634.67	-0.02
44.0	23637.71	0.00	23634.13	-0.01
45.0	23637.25	0.02	23633.56	-0.02
46.0	23636.76	0.02	23633.01	0.00
47.0	23636.24	0.01	23632.40	-0.03

TABLE 5. 8 Contd.

J	R(J)	O-C	P(J)	O-C

---

48. 0	23635. 76	0. 02	23631. 82	-0. 02
49. 0	23635. 22	0. 02	23631. 22	-0. 01
50. 0	23634. 67	0. 01	23630. 62	0. 00
51. 0	23634. 13	0. 02	23629. 97	-0. 02
52. 0	23633. 56	0. 01	23629. 33	-0. 02
53. 0	23633. 02	0. 03	23628. 68	-0. 00
54. 0	23632. 40	0. 00	23628. 03	-0. 01
55. 0	23631. 82	0. 01	23627. 35	-0. 02
56. 0	23631. 22	0. 02	23626. 67	-0. 01
57. 0	23630. 62	0. 03	23625. 99	0. 00
58. 0	23629. 97	0. 01	23625. 25	-0. 03
59. 0	23629. 33	0. 01	23624. 54	-0. 02
60. 0	23628. 68	0. 02	23623. 78	-0. 05
61. 0	23628. 03	0. 01	23623. 07	-0. 02
62. 0	23627. 35	0. 01	23622. 33	-0. 01
63. 0	23626. 67	0. 03	23621. 56	-0. 02
64. 0	23625. 99	-0. 01	23620. 79	-0. 01
65. 0	23625. 25	0. 00	23620. 01	-0. 01
66. 0	23624. 54	-0. 03	23619. 21	-0. 01
67. 0	23623. 78	0. 00	23618. 40	-0. 01
68. 0	23623. 07	0. 01	23617. 60	0. 01
69. 0	23622. 33	0. 00	23616. 76	0. 00
70. 0	23621. 56	0. 01	23615. 94	0. 02
71. 0	23620. 79	0. 01	23615. 07	0. 00
72. 0	23620. 01	0. 01	23614. 21	0. 01
73. 0	23619. 21	0. 00	23613. 32	-0. 01
74. 0	23618. 40	0. 02	23612. 45	0. 01
75. 0	23617. 60	0. 01	23611. 55	0. 00
76. 0	23616. 76	0. 03	23610. 64	0. 00
77. 0	23615. 94	0. 01	23609. 73	0. 01
78. 0	23615. 07	0. 02	23608. 80	0. 01
79. 0	23614. 21	0. 00	23607. 85	0. 00
80. 0	23613. 32	0. 01	23606. 90	0. 01
81. 0	23612. 45	0. 01	23605. 94	0. 01
82. 0	23611. 55	0. 01	23604. 96	0. 01
83. 0	23610. 64	0. 01	23603. 99	0. 02
84. 0	23609. 73	0. 01	23602. 99	0. 02
85. 0	23608. 80	0. 01	23601. 98	0. 02
86. 0	23607. 85	0. 00	23600. 97	0. 02

TABLE 5.8 Contd

J	R(J)	O-C	P(J)	O-C
87.0	23606.90	0.00	23599.93	0.01
88.0	23605.94	0.00	23598.89	0.02
89.0	23604.96	0.00	23597.85	0.03
90.0	23603.99	0.01	23596.78	0.02
91.0	23602.99	0.00	23595.72	0.03
92.0	23601.98	0.00	23594.63	0.03
93.0	23600.97	0.01	23593.53	0.02
94.0	23599.93	-0.01	23592.43	0.03
95.0	23598.89	-0.01	23591.32	0.04
96.0	23597.85	0.00	23590.19	0.03
97.0	23596.78	-0.01	23589.05	0.03
98.0	23595.72	0.00	23587.88	0.01
99.0	23594.63	-0.01	23586.76	0.05
100.0	23593.53	-0.02	23585.58	0.04
101.0	23592.43	-0.01	23584.39	0.03
102.0	23591.32	-0.01	23583.19	0.03
103.0	23590.19	-0.02		
104.0	23589.05	-0.02		
105.0	23587.88	-0.04		
106.0	23586.76	-0.01		
107.0	23585.58	-0.02		
108.0	23584.39	-0.03		
109.0	23583.19	-0.04		
110.0	23582.01	-0.03		
111.0	23580.78	-0.05		
112.0	23579.58	-0.05	23570.66	0.00
113.0	23578.33	-0.05	23569.34	-0.01
114.0	23577.11	-0.02	23568.04	0.01
115.0	23575.82	-0.06	23566.71	0.01
116.0	23574.57	-0.05	23565.36	0.00
117.0	23573.28	-0.07	23564.01	0.00
118.0	23572.02	-0.02	23562.65	0.00
119.0	23570.77	-0.00	23561.26	-0.01
120.0	23569.47	0.00	23559.89	0.00
121.0	23568.11	-0.04	23558.50	0.00
122.0	23566.82	-0.02	23557.10	0.00
123.0	23565.49	0.00	23555.69	0.01
124.0	23564.14	-0.01	23554.26	0.00
125.0	23562.80	-0.01	23552.83	0.00
126.0	23561.42	0.00	23551.38	0.00

TABLE 5. 8 Contd

J	R(J)	O-C	P(J)	O-C
127. 0	23560. 05	0. 00	23549. 93	0. 00
128. 0	23558. 66	0. 00	23548. 42	-0. 04
129. 0	23557. 26	0. 00	23547. 00	0. 01
130. 0	23555. 85	0. 01	23545. 52	0. 02
131. 0	23554. 45	-0. 01	23544. 01	0. 00
132. 0	23553. 01	0. 00	23542. 51	0. 01
133. 0	23551. 61	0. 03	23540. 99	0. 00
134. 0	23550. 12	-0. 01	23539. 45	-0. 01
135. 0	23548. 74	0. 07	23537. 92	-0. 01
136. 0	23547. 21	0. 01	23536. 38	0. 00
137. 0	23545. 68	-0. 04	23534. 81	-0. 02
138. 0	23544. 25	0. 02	23533. 24	-0. 02
139. 0	23542. 74	0. 00	23531. 67	-0. 01
140. 0	23541. 21	-0. 02	23530. 09	-0. 01
141. 0	23539. 68	-0. 03	23528. 51	0. 01
142. 0	23538. 19	0. 01	23526. 83	-0. 06
143. 0	23536. 60	-0. 04	23525. 26	-0. 02
144. 0	23535. 11	0. 02	23523. 64	-0. 02
145. 0	23533. 50	-0. 04	23522. 00	-0. 02
146. 0	23531. 97	0. 00	23520. 39	0. 01
147. 0	23530. 36	-0. 03	23518. 75	0. 03
148. 0	23528. 81	0. 01	23517. 03	-0. 03
149. 0	23527. 23	0. 02	23515. 38	-0. 01
150. 0	23525. 61	0. 01	23513. 72	0. 02
151. 0	23523. 98	0. 00	23512. 02	0. 01
152. 0			23510. 28	-0. 03
153. 0	23520. 74	0. 02		
154. 0	23519. 12	0. 04		
155. 0	23517. 46	0. 04		
156. 0	23515. 81	0. 05		
157. 0	23514. 13	0. 05		
158. 0	23512. 40	0. 00		
159. 0	23510. 66	-0. 04		

TABLE 5.9

WAVENUMBERS (cm-1) OF THE ROTATIONAL LINES IN THE
(0-17) BAND OF E-B SYSTEM.

v_0 : 23742.59

J	R(J)	O-C	P(J)	O-C
23. 0	23740. 26	0. 02		
24. 0	23740. 04	0. 05	23737. 94	-0. 10
25. 0	.		23737. 57	-0. 09
26. 0	23739. 49	0. 03	23737. 26	-0. 09
27. 0			23737. 01	0. 02
28. 0	23738. 86	-0. 02		
29. 0	23738. 57	0. 00	23736. 23	0. 01
30. 0			23735. 83	0. 01
31. 0	23737. 94	0. 02	23735. 47	0. 06
32. 0	23737. 57	-0. 01	23734. 99	0. 00
33. 0	23737. 26	0. 04	23734. 55	-0. 01
34. 0	23736. 86	0. 00	23734. 11	0. 00
35. 0	23736. 48	0. 00	23733. 65	0. 00
36. 0	23736. 09	0. 00	23733. 13	-0. 05
37. 0	23735. 70	0. 02	23732. 74	0. 04
38. 0	23735. 27	0. 00	23732. 24	0. 04
39. 0	23734. 85	0. 01	23731. 69	-0. 01
40. 0	23734. 40	-0. 01	23731. 17	0. 01
41. 0	23733. 96	0. 01	23730. 65	0. 00
42. 0	23733. 49	0. 00	23730. 10	-0. 01
43. 0			23729. 54	-0. 01
44. 0	23732. 53	0. 00	23729. 00	0. 01
45. 0	23732. 04	0. 00	23728. 43	0. 02
46. 0	23731. 50	-0. 03	23727. 83	0. 01
47. 0	23731. 02	0. 02	23727. 24	0. 02
48. 0	23730. 47	0. 00	23726. 62	0. 01
49. 0	23729. 93	0. 00	23725. 99	0. 01
50. 0	23729. 36	-0. 01	23725. 39	0. 04
51. 0	23728. 83	0. 03	23724. 72	0. 02
52. 0	23728. 20	-0. 02	23724. 02	-0. 02
53. 0	23727. 62	-0. 01	23723. 37	0. 00
54. 0	23727. 04	0. 02	23722. 67	-0. 01
55. 0	23726. 41	0. 00	23721. 96	-0. 03
56. 0	23725. 81	0. 03	23721. 27	-0. 01
57. 0	23725. 17	0. 03	23720. 58	0. 02
58. 0	23724. 49	0. 00	23719. 82	-0. 01
59. 0	23723. 84	0. 01	23719. 05	-0. 04

TABLE 5. 9 Contd.

J	R(J)	O-C	P(J)	O-C
60. 0	23723. 16	0. 01	23718. 33	-0. 01
61. 0	23722. 48	0. 01	23717. 57	0. 00
62. 0	23721. 77	0. 00	23716. 78	-0. 01
63. 0	23721. 06	0. 00	23716. 01	0. 01
64. 0	23720. 33	-0. 01	23715. 20	0. 00
65. 0	23719. 60	0. 00	23714. 36	-0. 03
66. 0	23718. 84	-0. 02	23713. 65	0. 08
67. 0	23718. 14	0. 04	23712. 73	0. 00
68. 0	23717. 34	0. 00	23711. 85	-0. 03
69. 0	23716. 57	0. 01	23711. 00	-0. 02
70. 0	23715. 76	0. 00	23710. 12	-0. 03
71. 0	23714. 96	0. 00	23709. 24	-0. 03
72. 0	23714. 12	-0. 03	23708. 36	-0. 02
73. 0	23713. 33	0. 01	23707. 47	0. 00
74. 0	23712. 45	-0. 03	23706. 54	-0. 01
75. 0	23711. 63	0. 00	23705. 57	-0. 05
76. 0	23710. 78	0. 01	23704. 66	-0. 02
77. 0	23709. 87	-0. 03	23703. 76	0. 03
78. 0	23709. 02	0. 00	23702. 73	-0. 04
79. 0	23708. 13	0. 01	23701. 79	0. 00
80. 0	23707. 19	-0. 02	23700. 82	0. 01
81. 0	23706. 29	-0. 01	23699. 81	0. 02
82. 0	23705. 35	-0. 01	23698. 82	0. 02
83. 0	23704. 42	0. 00	23697. 77	-0. 01
84. 0	23703. 47	0. 00	23696. 76	0. 01
85. 0	23702. 48	-0. 03	23695. 70	0. 00
86. 0	23701. 49	-0. 04	23694. 64	-0. 01
87. 0	23700. 58	0. 04	23693. 59	0. 01
88. 0	23699. 58	0. 04	23692. 48	-0. 02
89. 0	23698. 55	0. 02	23691. 43	0. 01
90. 0	23697. 52	0. 01	23690. 31	0. 00
91. 0	23696. 46	-0. 02	23689. 16	-0. 04
92. 0	23695. 43	-0. 01	23688. 08	0. 00
93. 0	23694. 37	-0. 01	23686. 93	-0. 01
94. 0	23693. 31	0. 00	23685. 79	-0. 01
95. 0	23692. 23	0. 00	23684. 65	0. 01
96. 0	23691. 13	-0. 02	23683. 47	0. 00
97. 0	23690. 05	0. 01	23682. 29	0. 00
98. 0	23688. 91	-0. 01	23681. 09	-0. 01

TABLE 5. 9 Contd.

J	R(J)	O-C	P(J)	O-C
99. 0	23687. 81	0. 00	23679. 87	-0. 02
100. 0	23686. 66	-0. 01	23678. 65	-0. 03
101. 0	23685. 54	0. 01	23677. 44	-0. 02
102. 0	23684. 38	0. 01	23676. 24	0. 02
103. 0	23683. 18	-0. 02	23674. 97	0. 00
104. 0	23682. 02	0. 00	23673. 71	0. 00
105. 0	23680. 82	-0. 01	23672. 48	0. 04
106. 0	23679. 64	0. 01	23671. 19	0. 03
107. 0	23678. 39	-0. 03	23669. 91	0. 04
108. 0	23677. 21	0. 02	23668. 57	0. 00
109. 0	23675. 96	0. 00	23667. 24	-0. 01
110. 0	23674. 72	0. 01	23665. 95	0. 02
111. 0	23673. 50	0. 05	23664. 59	0. 00
112. 0	23672. 21	0. 02	23663. 27	0. 03
113. 0	23670. 92	0. 01	23661. 94	0. 06
114. 0	23669. 61	-0. 01	23660. 53	0. 02
115. 0	23668. 30	-0. 01	23659. 15	0. 02
116. 0	23666. 98	-0. 02	23657. 75	0. 01
117. 0	23665. 69	0. 01	23656. 36	0. 02
118. 0	23664. 36	0. 02	23654. 93	0. 00
119. 0	23663. 01	0. 01	23653. 48	-0. 02
120. 0	23661. 66	-0. 03	23652. 09	0. 02
121. 0	23660. 26	-0. 01	23650. 62	0. 00
122. 0	23658. 90	0. 00	23649. 19	0. 03
123. 0	23657. 53	0. 02	23647. 70	0. 01
124. 0	23656. 13	0. 02	23646. 18	-0. 04
125. 0	23654. 71	0. 01	23644. 73	0. 00
126. 0	23653. 28	0. 01	23643. 22	-0. 01
127. 0	23651. 84	0. 00	23641. 70	-0. 01
128. 0	23650. 42	0. 02	23640. 18	-0. 01
129. 0	23648. 92	-0. 03	23638. 64	-0. 02
130. 0	23647. 47	-0. 01	23637. 12	0. 00
131. 0	23645. 97	-0. 04	23635. 53	-0. 03
132. 0	23644. 52	0. 00	23633. 99	-0. 01
133. 0	23643. 07	0. 05	23632. 40	-0. 02
134. 0	23641. 52	0. 00		
135. 0	23639. 96	-0. 04		
136. 0	23638. 47	0. 00		
137. 0	23636. 93	0. 00		
138. 0	23635. 37	-0. 01		
139. 0	23633. 82	0. 00		

TABLE 5. 10

WAVENUMBERS (cm−1) OF THE ROTATIONAL LINES IN THE
(1−14) BAND OF E−B SYSTEM.

$v_0 = 24139.92$

J	R(J)	O−C	P(J)	O−C
5. 0			24139. 56	0. 04
6. 0	24139. 93	0. 01	24139. 42	0. 02
7. 0			24139. 28	0. 01
8. 0			24139. 10	−0. 02
9. 0	24139. 70	−0. 02	24138. 92	−0. 04
10. 0	24139. 70	0. 07	24138. 73	−0. 06
11. 0	24139. 56	0. 04	24138. 57	−0. 03
12. 0	24139. 42	0. 02	24138. 44	0. 04
13. 0	24139. 28	0. 01	24138. 24	0. 05
14. 0	24139. 10	−0. 02	24138. 04	0. 08
15. 0	24138. 92	−0. 04	24137. 80	0. 07
16. 0	24138. 73	−0. 06	24137. 51	0. 04
17. 0	24138. 57	−0. 03	24137. 24	0. 04
18. 0	24138. 44	0. 03	24136. 98	0. 05
19. 0	24138. 24	0. 05	24136. 69	0. 06
20. 0	24138. 04	0. 07	24136. 34	0. 01
21. 0	24137. 80	0. 07	24136. 05	0. 04
22. 0	24137. 51	0. 07	24135. 71	0. 04
23. 0	24137. 24	0. 03	24135. 36	0. 03
24. 0	24136. 98	0. 05	24134. 98	0. 01
25. 0	24136. 69	0. 05	24134. 62	0. 02
26. 0	24136. 34	0. 01	24134. 23	0. 02
27. 0	24136. 05	0. 03	24133. 82	0. 01
28. 0	24135. 71	0. 02	24133. 46	0. 06
29. 0	24135. 36	0. 00	24132. 96	−0. 01
30. 0	24134. 98	0. 01	24132. 55	0. 01
31. 0	24134. 62	0. 02	24132. 05	−0. 03
32. 0	24134. 23	0. 02	24131. 62	0. 00
33. 0	24133. 82	0. 00	24131. 11	−0. 03
34. 0	24133. 46	−0. 05	24130. 66	0. 01
35. 0	24132. 96	−0. 02	24130. 14	−0. 01
36. 0	24132. 55	0. 00	24129. 61	−0. 02
37. 0	24132. 05	−0. 05	24129. 09	−0. 01
38. 0	24131. 62	−0. 01	24128. 52	−0. 03
39. 0	24131. 11	−0. 04	24127. 97	−0. 03
40. 0	24130. 66	−0. 01	24127. 40	−0. 03
41. 0	24130. 14	−0. 02	24126. 79	−0. 05

TABLE 5. 10 Contd.

J	R(J)	O-C	P(J)	O-C
42. 0	24129. 61	-0. 03	24126. 20	-0. 05
43. 0	24129. 09	-0. 02	24125. 59	-0. 05
44. 0	24128. 52	-0. 05	24125. 06	0. 04
45. 0	24127. 97	-0. 05	24124. 34	-0. 04
46. 0	24127. 40	-0. 05	24123. 67	-0. 06
47. 0	24126. 79	-0. 08	24122. 99	-0. 08
48. 0	24126. 20	-0. 08	24122. 41	0. 01
49. 0	24125. 59	-0. 07	24121. 72	0. 01
50. 0	24125. 06	0. 01	24120. 98	-0. 03
51. 0	24124. 34	-0. 07	24120. 32	0. 02
52. 0	24123. 67	-0. 09	24119. 56	-0. 01
53. 0			24118. 80	-0. 02
54. 0	24122. 41	-0. 02	24118. 10	0. 02
55. 0	24121. 72	-0. 02	24117. 32	0. 01
56. 0	24120. 98	-0. 06	24116. 58	0. 05
57. 0	24120. 32	-0. 01	24115. 79	0. 05
58. 0	24119. 56	-0. 05	24114. 99	0. 05
59. 0	24118. 80	-0. 07	24114. 15	0. 03
60. 0	24118. 10	-0. 02	24113. 31	0. 02
61. 0	24117. 32	-0. 04	24112. 47	0. 02
62. 0	24116. 58	0. 00	24111. 61	0. 02
63. 0	24115. 79	0. 00	24110. 73	0. 01
64. 0	24114. 99	0. 00	24109. 86	0. 02
65. 0	24114. 14	-0. 02	24108. 95	0. 01
66. 0	24113. 31	-0. 04	24108. 00	-0. 03
67. 0	24112. 47	-0. 03	24107. 11	-0. 01
68. 0	24111. 61	-0. 04	24106. 15	-0. 03
69. 0	24110. 73	-0. 06	24105. 22	-0. 02
70. 0	24109. 86	-0. 05	24104. 24	-0. 04
71. 0	24108. 95	-0. 06	24103. 27	-0. 04
72. 0			24102. 28	-0. 04
73. 0	24107. 11	-0. 08	24101. 28	-0. 05
74. 0			24100. 27	-0. 05
75. 0			24099. 26	-0. 03
76. 0			24098. 23	-0. 03
77. 0			24097. 18	-0. 03
78. 0	24102. 41	-0. 01	24096. 13	-0. 02
79. 0	24101. 45	-0. 02	24095. 04	-0. 04
80. 0	24100. 44	-0. 01	24093. 99	-0. 01
81. 0	24099. 41	0. 00	24092. 88	-0. 02

TABLE 5. 10 Contd.

J	R(J)	O-C	P(J)	O-C
82. 0	24098. 39	-0. 01	24091. 78	-0. 01
83. 0	24097. 35	0. 02	24090. 63	-0. 04
84. 0	24096. 26	-0. 01	24089. 53	0. 00
85. 0	24095. 23	0. 02	24088. 36	-0. 01
86. 0	24094. 14	0. 01	24087. 21	-0. 04
87. 0	24093. 04	0. 01	24086. 03	-0. 02
88. 0	24091. 93	0. 00	24084. 84	-0. 03
89. 0	24090. 83	-0. 01	24083. 67	-0. 03
90. 0	24089. 68	0. 00	24082. 45	-0. 01
91. 0	24088. 56	0. 02	24081. 25	0. 01
92. 0	24087. 40	0. 02	24080. 01	0. 00
93. 0	24086. 24	0. 02	24078. 75	-0. 01
94. 0	24085. 05	0. 01	24077. 51	0. 01
95. 0	24083. 88	0. 03	24076. 23	0. 00
96. 0	24082. 65	0. 01	24074. 95	0. 00
97. 0	24081. 43	0. 00	24073. 65	0. 00
98. 0	24080. 25	0. 05	24072. 34	0. 00
99. 0	24079. 00	0. 04	24071. 03	0. 00
100. 0	24077. 75	0. 05	24069. 75	0. 05
101. 0	24076. 47	0. 03	24068. 37	0. 02
102. 0	24075. 20	0. 04	24067. 05	0. 05
103. 0	24073. 90	0. 03	24065. 66	0. 03
104. 0	24072. 56	-0. 01	24064. 31	0. 06
105. 0	24071. 30	0. 05	24062. 89	0. 04
106. 0	24069. 97	0. 04	24061. 46	0. 01
107. 0	24068. 62	0. 02	24060. 07	0. 04
108. 0	24067. 27	0. 02	24058. 63	0. 02
109. 0	24065. 92	0. 03	24057. 16	0. 00
110. 0	24064. 54	0. 03	24055. 73	0. 02
111. 0	24063. 17	0. 04	24054. 24	-0. 01
112. 0	24061. 76	0. 03	24052. 81	0. 04
113. 0	24060. 34	0. 02	24051. 35	0. 06
114. 0	24058. 91	0. 01	24049. 84	0. 05
115. 0	24057. 50	0. 03	24048. 31	0. 03
116. 0	24056. 06	0. 03	24046. 76	0. 01
117. 0	24054. 60	0. 03	24045. 24	0. 02
118. 0	24053. 12	0. 02	24043. 68	0. 01
119. 0	24051. 66	0. 04	24042. 12	0. 01
120. 0	24050. 18	0. 05	24040. 50	-0. 04
121. 0	24048. 66	0. 03	24038, 93	-0. 03

TABLE 5.10 Contd.

J	R(J)	O-C	P(J)	O-C

122.0	24047.11	0.00	24037.33	-0.04
123.0	24045.60	0.01	24035.74	-0.02
124.0	24044.08	0.03	24034.15	0.00
125.0	24042.49	-0.01	24032.51	-0.01
126.0	24040.94	0.00	24030.86	-0.02
127.0	24039.35	-0.02	24029.22	-0.01
128.0	24037.80	0.01	24027.55	-0.02
129.0	24036.20	0.00		
130.0	24034.53	-0.06		
131.0	24032.91	-0.06		
132.0	24031.27	-0.07		
133.0	24029.61	-0.09		
134.0	24027.98	-0.07		

TABLE 5. 10 Contd.

J	R(J)	O-C	P(J)	O-C

---

122. 0	24047. 11	0. 00	24037. 33	-0. 04
123. 0	24045. 60	0. 01	24035. 74	-0. 02
124. 0	24044. 08	0. 03	24034. 15	0. 00
125. 0	24042. 49	-0. 01	24032. 51	-0. 01
126. 0	24040. 94	0. 00	24030. 86	-0. 02
127. 0	24039. 35	-0. 02	24029. 22	-0. 01
128. 0	24037. 80	0. 01	24027. 55	-0. 02
129. 0	24036. 20	0. 00		
130. 0	24034. 53	-0. 06		
131. 0	24032. 91	-0. 06		
132. 0	24031. 27	-0. 07		
133. 0	24029. 61	-0. 09		
134. 0	24027. 98	-0. 07		

TABLE 5. 11

WAVENUMBERS (cm-1) OF THE ROTATIONAL LINES IN THE (1-24) BAND OF E-B SYSTEM.

$v_0 = 23211.14$

J	R(J)	O-C	P(J)	O-C
18. 0			23214. 94	0. 03
21. 0			23214. 25	0. 00
22. 0			23214. 00	-0. 02
23. 0			23213. 79	0. 01
24. 0			23213. 50	-0. 02
25. 0			23213. 28	-0. 02
26. 0			23213. 00	0. 01
27. 0	23214. 94	0. 03	23212. 70	-0. 01
29. 0			23212. 11	-0. 01
30. 0	23214. 25	0. 00	23211. 80	-0. 02
31. 0	23214. 00	-0. 01	23211. 50	0. 00
32. 0	23213. 79	0. 02	23211. 16	-0. 02
33. 0	23213. 50	-0. 02	23210. 83	-0. 02
34. 0	23213. 28	0. 02	23210. 48	-0. 03
35. 0	23213. 00	0. 01	23210. 16	0. 00
36. 0	23212. 70	-0. 01		
37. 0			23209. 43	0. 00
38. 0	23212. 11	-0. 01		
39. 0	23211. 80	-0. 01	23208. 66	-0. 01
40. 0	23211. 50	0. 00	23208. 30	0. 03
41. 0	23211. 16	-0. 01	23207. 89	0. 02
42. 0	23210. 83	-0. 01	23207. 47	0. 00
43. 0	23210. 48	-0. 02		
44. 0	23210. 16	0. 01	23206. 59	-0. 02
45. 0			23206. 18	0. 01
46. 0	23209. 43	0. 00	23205. 71	-0. 01
47. 0			23205. 28	0. 01
48. 0	23208. 66	0. 00	23204. 80	0. 00
49. 0	23208. 30	0. 03	23204. 33	0. 00
50. 0	23207. 89	0. 02		
51. 0	23207. 47	0. 01	23203. 34	-0. 01
52. 0			23202. 85	0. 00
53. 0	23206. 59	-0. 01		
54. 0	23206. 18	0. 01	23201. 83	0. 01
55. 0	23205. 71	0. 01	23201. 31	0. 01
56. 0	23205. 28	0. 02	23200. 74	-0. 02
57. 0	23204. 80	0. 00	23200. 22	0. 00

TABLE 5. 11 Contd.

J	R(J)	O-C	P(J)	O-C
58. 0	23204. 33	0. 01		
59. 0			23199. 07	-0. 03
60. 0	23203. 34	-0. 01	23198. 55	0. 02
61. 0	23202. 85	0. 00	23197. 95	0. 00
62. 0			23197. 36	-0. 01
63. 0	23201. 83	0. 01	23196. 74	-0. 02
64. 0	23201. 31	0. 01		
65. 0	23200. 74	-0. 02	23195. 55	0. 00
66. 0	23200. 22	0. 00	23194. 92	0. 00
67. 0			23194. 30	0. 01
68. 0	23199. 07	-0. 03	23193. 66	0. 01
69. 0	23198. 55	0. 02	23193. 00	0. 00
70. 0	23197. 95	0. 00	23192. 35	0. 01
71. 0	23197. 36	-0. 01	23191. 68	0. 01
72. 0	23196. 74	-0. 02	23191. 02	0. 02
74. 0	23195. 55	0. 00		
75. 0	23194. 92	0. 00		
76. 0	23194. 30	0. 01		
77. 0	23193. 66	0. 01		
78. 0	23193. 00	0. 00		

TABLE 5.12

WAVENUMBERS (cm-1) OF THE ROTATIONAL LINES IN THE (2-21) BAND OF E-B SYSTEM.

$v_0 = 23573.49$

J	R(J)	O-C	P(J)	O-C
8.0			23572.80	0.00
11.0	23573.26	-0.01	23572.39	0.03
12.0	23573.26	0.07		
13.0			23572.06	0.04
15.0	23572.81	-0.05	23571.58	-0.05
16.0	23572.81	0.08	23571.45	0.00
17.0			23571.12	-0.09
18.0	23572.40	-0.05	23570.97	-0.01
19.0			23570.77	0.03
20.0	23572.06	-0.05	23570.43	-0.06
21.0	23571.97	0.04	23570.27	0.04
22.0			23569.94	-0.02
23.0	23571.58	-0.11	23569.79	0.10
24.0	23571.44	0.00	23569.34	-0.04
25.0	23571.12	0.02	23569.07	-0.01
26.0	23570.97	0.10	23568.80	0.03
27.0	23570.66	0.04	23568.44	0.01
28.0	23570.43	0.06	23568.07	-0.04
29.0	23570.06	-0.04	23567.69	-0.08
30.0	23569.79	-0.04		
31.0	23569.47	-0.07	23567.13	0.08
32.0			23566.72	0.05
33.0	23568.94	0.00	23566.26	-0.03
34.0	23568.66	0.04	23565.90	0.01
35.0			23565.49	0.01
36.0	23567.88	-0.08	23565.03	-0.03
37.0	23567.69	0.08	23564.64	0.00
38.0	23567.25	0.00	23564.15	-0.05
39.0	23566.83	-0.05		
40.0	23566.48	-0.02	23563.39	0.10
41.0	23566.13	0.02	23562.80	-0.02
42.0	23565.69	-0.02	23562.40	0.06
43.0	23565.37	0.07	23561.92	0.07
44.0			23561.26	-0.09
45.0	23564.49	0.05	23560.74	-0.10
46.0	23564.02	0.02	23560.30	-0.02
47.0	23563.42	-0.13	23559.72	-0.07

TABLE 5.12 Contd.

J	R(J)	O-C	P(J)	O-C
48.0	23563.06	-0.02	23559.27	0.03
49.0	23562.66	0.05	23558.66	-0.03
50.0	23562.18	0.05	23558.04	-0.09
51.0	23561.64	0.01	23557.45	-0.11
52.0	23561.07	-0.06	23557.11	0.14
53.0			23556.40	0.02
54.0	23560.05	-0.04	23555.85	0.07
55.0	23559.57	0.01	23555.11	-0.05
56.0	23559.10	0.09	23554.44	-0.10
57.0	23558.51	0.06	23553.86	-0.04
58.0	23557.82	-0.07	23553.27	0.01
59.0	23557.28	-0.03	23552.67	0.07
60.0	23556.65	-0.08	23552.09	0.015
61.0	23556.23	0.10		
62.0	23555.43	-0.09	23550.59	0.01
63.0	23554.89	-0.02	23549.93	0.05
64.0	23554.27	-0.01	23549.26	0.08
65.0	23553.68	0.04	23548.43	-0.03
66.0	23553.02	0.03	23547.64	-0.09
67.0	23552.28	-0.06	23547.00	0.00
68.0	23551.63	-0.04		
69.0			23545.42	-0.07
70.0	23550.34	0.04	23544.76	0.03
71.0	23549.68	0.08	23544.01	0.06
72.0			23543.26	0.10
73.0			23542.38	0.01
74.0			23541.75	0.01
75.0			23540.78	0.04
76.0	23546.02	0.06	23539.94	0.02
77.0	23545.19	-0.01	23539.10	0.02
78.0			23538.19	-0.04
79.0			23537.33	-0.04
80.0	23542.87	0.00	23536.60	0.09
82.0	23541.31	0.05	23534.80	0.06
83.0			23533.78	-0.07
84.0	23539.68	0.07		
85.0	23538.71	-0.06	23532.11	0.09
86.0	23537.92	-0.01	23531.05	0.05
87.0	23536.99	-0.08	23530.08	-0.08

TABLE 5. 12 Contd.

J	R(J)	O-C	P(J)	O-C
88. 0	23536. 10	-0. 10	23529. 24	0. 03
89. 0	23535. 30	-0. 02	23528. 33	0. 07
90. 0	23534. 35	-0. 08	23527. 22	-0. 07
91. 0	23533. 50	-0. 04		
92. 0	23532. 65	0. 02	23525. 26	-0. 07
93. 0	23531. 67	-0. 04	23524. 31	-0. 02
94. 0	23530. 86	0. 07		
95. 0	23529. 80	-0. 05	23522. 38	0. 07
96. 0			23521. 35	0. 06
97. 0	23527. 97	0. 02	23520. 30	0. 05
98. 0	23527. 00	0. 02	23519. 11	-0. 10
99. 0	23526. 05	0. 05	23518. 07	-0. 09
100. 0	23525. 10	0. 08	23517. 02	-0. 07
101. 0	23523. 97	-0. 05	23516. 11	0. 09
102. 0	23523. 02	0. 00	23515. 00	0. 06
103. 0	23521. 99	-0. 02		
104. 0	23521. 01	0. 03	23512. 76	0. 02
105. 0	23519. 90	-0. 05	23511. 57	-0. 06
106. 0			23510. 44	-0. 07
107. 0	23517. 89	0. 04	23509. 38	0. 10
108. 0	23516. 79	0. 00	23508. 21	-0. 03
109. 0	23515. 81	0. 09	23507. 03	-0. 06
110. 0	23514. 74	0. 10		
111. 0	23513. 52	-0. 03	23504. 69	-0. 07
112. 0	23512. 40	-0. 05		
113. 0	23511. 42	0. 08	23502. 35	-0. 05
114. 0	23510. 30	0. 08	23501. 28	0. 08
115. 0	23509. 04	-0. 05		
116. 0	23507. 94	-0. 01	23498. 80	0. 02
117. 0	23506. 87	0. 06	23497. 52	-0. 04
118. 0	23505. 59	-0. 06	23496. 32	0. 00
119. 0	23504. 45	-0. 03	23495. 07	-0. 01
120. 0	23503. 40	0. 09	23493. 87	0. 04
121. 0	23502. 13	0. 01		
122. 0	23500. 98	0. 05	23491. 31	0. 02
123. 0			23489. 99	-0. 02
124. 0	23498. 45	-0. 07		
125. 0			23487. 37	-0. 05
126. 0	23495. 97	-0. 09	23486. 19	0. 07

TABLE 5. 12 Contd.

J	R(J)	O-C	P(J)	O-C
128. 0	23493. 59	0. 01	23483. 47	0. 00
129. 0	23492. 25	-0. 07	23482. 12	-0. 02
130. 0	23491. 09	0. 04	23480. 73	-0. 06
131. 0	23489. 74	-0. 03		
132. 0	23488. 46	-0. 03	23478. 01	-0. 07
133. 0	23487. 22	0. 02	23476. 73	0. 02
135. 0	23484. 67	0. 09	23473. 96	0. 02
136. 0	23483. 22	-0. 04		
137. 0			23471. 07	-0. 06
138. 0	23480. 52	-0. 07	23469. 68	-0. 04
139. 0	23479. 26	0. 02	23468. 36	0. 07
140. 0	23477. 83	-0. 06	23466. 80	-0. 06
141. 0	23476. 50	-0. 02	23465. 51	0. 09
142. 0			23463. 89	-0. 08
143. 0	23473. 81	0. 05	23462. 58	0. 07
144. 0	23472. 36	-0. 01	23461. 11	0. 07
145. 0	23471. 07	0. 10	23459. 58	0. 02
146. 0	23469. 50	-0. 06	23458. 04	-0. 03
147. 0	23468. 15	0. 00		
148. 0	23466. 68	-0. 04		
149. 0	23465. 30	0. 02		
150. 0	23463. 89	0. 05		

TABLE 5.13

WAVENUMBERS (cm-1) OF THE ROTATIONAL LINES IN THE
(3-13) BAND OF E-B SYSTEM.

$v_0 = 24443.75$

J	R(J)	O-C	P(J)	O-C
18.0			24440.59	-0.07
21.0	24441.32	-0.08	24439.62	-0.09
23.0	24440.77	-0.09		
24.0	24440.59	0.02	24438.58	-0.05
25.0	24440.16	-0.09		
26.0	24439.92	-0.02	24437.85	0.00
27.0	24439.62	0.02	24437.44	0.01
28.0	24439.20	-0.01	24437.00	0.00
29.0	24438.86	-0.03	24436.53	-0.03
30.0	24438.58	0.06		
31.0	24438.12	0.00	24435.65	-0.02
32.0	24437.75	0.03	24435.15	0.00
33.0	24437.31	0.01	24434.64	-0.01
34.0	24436.84	-0.03	24434.10	-0.04
35.0	24436.44	0.01	24433.59	-0.02
36.0	24436.00	0.04	24433.14	-0.06
37.0	24435.50	0.01	24432.58	-0.05
38.0	24435.00	0.00	24431.99	0.03
39.0	24434.45	-0.05	24431.33	-0.04
40.0	24434.01	0.02	24430.82	0.03
41.0			24430.23	0.05
42.0	24432.88	-0.03	24429.54	-0.01
43.0	24432.34	-0.01	24428.95	0.03
44.0	24431.82	0.03	24428.28	0.01
45.0	24431.20	0.00	24427.59	-0.01
46.0	24430.62	0.01	24426.94	0.01
47.0	24430.00	0.01	24426.26	0.02
48.0	24429.37	0.00	24425.57	0.03
49.0	24428.76	0.03		
50.0	24428.04	-0.03	24424.08	0.00
51.0	24427.44	0.03	24423.32	-0.02
52.0	24426.78	0.05	24422.58	0.00
53.0	24426.04	0.01	24421.87	0.06
54.0	24425.34	0.01	24421.05	0.03
55.0	24424.65	0.04	24420.14	-0.08
56.0	24423.88	0.01	24419.41	0.00
57.0	24423.12	0.00	24418.57	-0.01

TABLE 5.13 Contd.

J	R(J)	O-C	P(J)	O-C
58.0	24422.41	0.05	24417.74	0.00
59.0	24421.56	-0.02	24416.94	0.06
60.0	24420.83	0.02	24416.03	0.02
61.0	24419.99	0.00	24415.14	0.01
62.0	24419.20	0.03	24414.18	-0.05
63.0	24418.32	-0.01	24413.33	0.01
64.0	24417.49	0.00	24412.41	0.01
65.0	24416.64	0.01	24411.50	0.04
66.0	24415.75	-0.01	24410.53	0.02
67.0	24414.87	-0.01	24409.54	0.00
68.0	24413.98	0.00	24408.62	0.05
69.0	24413.05	-0.01	24407.58	0.00
70.0	24412.16	0.02	24406.58	0.01
71.0	24411.21	0.01	24405.63	0.08
72.0	24410.24	0.00	24404.45	-0.07
73.0	24409.24	-0.03	24403.47	0.00
74.0	24408.28	-0.01	24402.41	0.00
75.0	24407.30	0.00	24401.33	-0.01
76.0	24406.32	0.03	24400.22	-0.03
77.0	24405.32	0.05	24399.17	0.02
78.0	24404.25	0.01	24398.03	-0.01
79.0	24403.26	0.07	24396.93	0.02
80.0	24402.15	0.02	24395.84	0.07
81.0	24401.07	0.02	24394.59	-0.02
82.0	24399.99	0.03	24393.44	-0.01
83.0	24398.87	0.01	24392.26	-0.01
84.0	24397.76	0.02	24391.06	-0.01
85.0	24396.62	0.01	24389.86	0.00
86.0	24395.43	-0.04	24388.61	-0.03
87.0	24394.23	-0.08	24387.39	-0.01
88.0	24393.16	0.02	24386.16	0.00
89.0	24391.93	-0.03	24384.86	-0.03
90.0	24390.75	-0.01	24383.61	-0.01
91.0	24389.56	0.01	24382.31	-0.02
92.0	24388.34	0.01	24380.98	-0.05
93.0	24387.09	0.00	24379.71	0.00
94.0	24385.79	-0.05	24378.37	-0.01
95.0			24377.03	-0.01
96.0	24383.27	-0.03	24375.67	-0.01
97.0	24381.95	-0.06		

TABLE 5. 13 Contd.

J	R(J)	O-C	P(J)	O-C
98. 0	24380. 66	-0. 04	24372. 95	0. 01
99. 0	24379. 34	-0. 04	24371. 50	-0. 04
100. 0	24378. 04	-0. 01	24371. 10	-0. 03
101. 0	24376. 73	0. 02	24368. 72	0. 01
102. 0	24375. 36	0. 00	24367. 31	0. 04
103. 0	24373. 93	-0. 05	24365. 83	0. 00
104. 0	24372. 58	-0. 02	24364. 33	-0. 03
105. 0	24371. 21	0. 01	24362. 90	0. 01
106. 0			24361. 42	0. 02
107. 0	24368. 35	-0. 02	24359. 93	0. 03
108. 0	24366. 92	-0. 01	24358. 40	0. 02
109. 0	24365. 49	0. 01	24356. 82	-0. 03
110. 0	24364. 01	-0. 01	24355. 30	-0. 01
111. 0	24362. 54	0. 00	24353. 77	0. 01
112. 0	24361. 04	-0. 01	24352. 20	0. 01
113. 0	24359. 59	0. 04	24350. 62	0. 01
114. 0	24358. 05	0. 01	24349. 02	0. 00
115. 0	24356. 54	0. 03	24347. 43	0. 02
116. 0	24354. 97	0. 00	24345. 79	0. 00
117. 0	24353. 44	0. 03	24344. 15	-0. 01
118. 0	24351. 84	0. 00	24342. 52	0. 01
119. 0	24350. 26	0. 00	24340. 83	-0. 02
120. 0	24348. 74	0. 07	24339. 19	0. 01
121. 0	24347. 10	0. 04	24337. 49	0. 00
122. 0	24345. 44	-0. 02	24335. 87	-0. 09
123. 0	24343. 79	-0. 02	24334. 09	0. 00
124. 0	24342. 16	0. 00	24332. 29	-0. 07
125. 0	24340. 49	-0. 01	24330. 68	0. 05
126. 0	24338. 85	0. 02	24328. 87	0. 00
127. 0	24337. 18	0. 03	24327. 11	-0. 03
128. 0	24335. 42	-0. 03	24325. 32	-0. 01
129. 0	24333. 72	-0. 02	24323. 57	0. 02
130. 0	24332. 01	0. 00	24321. 73	0. 08
131. 0	24330. 28	0. 00	24319. 95	0. 02
132. 0	24328. 55	0. 02	24318. 10	0. 00
133. 0	24326. 76	-0. 01	24316. 27	0. 01
134. 0			24314. 40	-0. 01
135. 0			24312. 53	-0. 01

TABLE 5. 14

WAVENUMBERS (cm-1) OF THE ROTATIONAL LINES IN THE
(3-15) BAND OF E-B SYSTEM.

$\nu_0 = 24241.32$

J	R(J)	O-C	P(J)	O-C
20. 0			24237. 72	-0. 05
22. 0			24237. 08	-0. 04
24. 0			24236. 39	-0. 04
26. 0	24237. 72	-0. 05	24235. 62	-0. 06
27. 0	24237. 40	-0. 06	24235. 25	-0. 04
28. 0	24237. 08	-0. 05		
29. 0			24234. 46	0. 00
30. 0	24236. 39	-0. 04	24234. 03	0. 00
31. 0			24233. 55	-0. 03
32. 0	24235. 62	-0. 06	24233. 08	-0. 04
33. 0	24235. 25	-0. 04	24232. 61	-0. 04
34. 0			24232. 18	0. 01
35. 0	24234. 46	0. 00	24231. 67	0. 00
36. 0	24234. 03	0. 00	24231. 14	-0. 01
37. 0	24233. 55	-0. 03	24230. 65	0. 02
38. 0	24233. 08	-0. 04	24230. 09	0. 00
39. 0	24232. 61	-0. 04		
40. 0	24232. 18	0. 01	24228. 99	0. 01
41. 0	24231. 67	0. 00	24228. 41	0. 01
42. 0	24231. 14	-0. 01	24227. 83	0. 02
43. 0	24230. 65	0. 02	24227. 24	0. 03
44. 0	24230. 09	0. 00	24226. 62	0. 03
45. 0			24225. 96	0. 00
46. 0	24228. 99	0. 01	24225. 34	0. 02
47. 0	24228. 41	0. 01	24224. 71	0. 05
48. 0	24227. 83	0. 02	24224. 03	0. 04
49. 0	24227. 24	0. 03	24223. 34	0. 03
50. 0	24226. 62	0. 03	24222. 65	0. 03
51. 0	24225. 96	-0. 01	24221. 94	0. 03
52. 0	24225. 34	0. 02	24221. 21	0. 02
53. 0	24224. 71	0. 05	24220. 48	0. 03
54. 0	24224. 03	0. 03	24219. 72	0. 02
55. 0	24223. 34	0. 03	24218. 95	0. 01
56. 0	24222. 65	0. 03	24218. 18	0. 01
57. 0	24221. 94	0. 03	24217. 43	0. 05
58. 0	24221. 21	0. 02	24216. 60	0. 02
59. 0	24220. 48	0. 03	24215. 78	0. 01

127

TABLE 5.14 Contd.

J	R(J)	O-C	P(J)	O-C
60.0	24219.72	0.01	24214.99	0.04
61.0	24218.95	0.00	24214.15	0.04
62.0	24218.18	0.01		
63.0	24217.43	0.04	24212.38	-0.01
64.0	24216.60	0.01	24211.50	-0.01
65.0	24215.78	0.01		
66.0	24214.99	0.04	24209.72	0.00
67.0			24208.82	0.02
68.0			24207.88	0.01
69.0	24212.38	-0.01	24206.95	0.02
70.0	24211.50	0.01	24205.99	0.02
71.0			24205.02	0.02
72.0	24209.72	0.00	24204.01	0.00
73.0	24208.82	0.02	24203.02	0.00
74.0	24207.88	0.01	24202.02	0.01
75.0	24206.95	0.02	24200.99	0.00
76.0	24205.99	0.02	24199.93	-0.02
77.0	24205.02	0.02	24198.92	0.01
78.0	24204.01	0.00	24197.83	-0.02
79.0	24203.02	0.00	24196.75	-0.02
80.0	24202.02	0.01	24195.69	0.00
81.0	24200.99	0.00	24194.56	-0.02
82.0	24199.93	-0.02	24193.47	0.00
83.0	24198.92	0.01	24192.32	-0.03
84.0	24197.83	-0.02		
85.0	24196.75	-0.02	24190.04	-0.02
86.0	24195.69	0.00	24188.90	0.00
87.0	24194.54	-0.04	24187.70	-0.02
88.0	24193.47	0.00	24186.51	-0.02
89.0	24192.32	-0.02	24185.31	-0.01
90.0			24184.11	0.00
91.0	24190.04	-0.01	24182.87	-0.01
92.0	24188.90	0.00	24181.64	0.00
93.0	24187.70	-0.01	24180.36	-0.02
94.0	24186.51	-0.01	24179.06	-0.06
95.0	24185.31	-0.01	24177.84	0.00
96.0	24184.11	0.00	24176.52	-0.02
97.0	24182.87	-0.01	24175.21	-0.02
98.0	24181.64	0.00	24173.88	-0.03
99.0	24180.36	-0.02		

TABLE 5.14 Contd.

J	R(J)	O-C	P(J)	O-C
100.0	24179.06	-0.05	24171.23	0.00
101.0	24177.84	0.01	24169.86	-0.01
102.0	24176.52	-0.01	24168.48	0.01
103.0	24175.21	-0.02	24167.11	-0.01
104.0	24173.88	-0.03	24165.70	-0.02
105.0	24172.58	0.00	24164.30	-0.01
106.0	24171.23	0.00	24162.87	-0.02
107.0	24169.86	-0.01	24161.44	-0.01
108.0	24168.49	0.00	24159.99	-0.02
109.0	24167.11	0.00	24158.53	-0.01
110.0	24165.70	-0.01	24157.07	0.00
111.0	24164.30	0.00	24155.58	0.00
112.0	24162.87	-0.01	24154.08	0.00
113.0	24161.44	0.00	24152.58	0.01
114.0	24159.99	0.00	24151.03	-0.01
115.0	24158.53	0.00	24149.53	0.03
116.0	24157.07	0.01	24147.97	0.02
117.0	24155.58	0.01	24146.42	0.03
118.0	24154.08	0.01	24144.86	0.05
119.0	24152.58	0.03	24143.27	0.05
120.0	24151.03	0.00		
121.0	24149.53	0.04		

REFERENCES

1. A. Elliot, Proc. Roy. Soc. London A174, 273 (1940).

2. J. Waser and K. Wieland, Nature, 160, 643 (1947).

3. P. Venkateswarlu, Phys. Rev. 81, 821 (1951).

4. R.D. Verma, Proc. Ind. Acad. Sci. A48, 197 (1958).

5. R.S. Mulliken, J. Chem. Phys. 55, 288 (1971).

6. K. Wieland, J.B. Tellinghuisen and A. Nobs, J. Mol. Spectrosc. 41, 69 (1972).

7. D.L. Rousseau and P.F. Williams, Phys. Rev. Letts. 33, 1368 (1974).

8. D.L. Rousseau, J. Mol. Spectrosc. 58, 481 (1975).

9. M.D. Danyluk and G.W. King, Chem. Phys. 22, 59 (1977).

10. A.D. Williamson, Chem. Phys. Letts. 60, 451 (1979).

11. G.W. King, I.H. Littlewood and J.R. Robins, Chem. Phys. 56, 145 (1981).

12. S.L. Cunha, J.A. Lisboa, R.E. Francke and H.P. Grieneisen and B.P. Chakraborthy, Optics Comm. 28, 321 (1979).

13. J.C.D. Brand, A.K. Kalukar and A.B. Yamashita, Optics Comm. 39, 235 (1981).

14. J.C.D. Brand, J. Mol. Spectrosc. 95, 350 (1982).

15. J. Chevaleyre, J.P. Perrot, J.M. Chastan, S. Valiguat and M. Broyer, Chem. Phys. 67, 59 (1982).

16. Anita L. Guy, K.S. Viswanathan, Abha Sur and Joel Tellinghuisen, Chem. Phys. Letts. 73, 582 (1980).

17. P. Luc, J. Mol. Spectrosc. 80, 41 (1980).

Introduction

The visible absorption band system of I$_2$, involving
B($^3\pi_{0_u^+}$) and X($^1\Sigma_g^+$) states, has been of considerable interest to
many researchers over a period of several decades [1]. Diffe-
rent excitation methods were used to study different properties
of the transition and to characterize the two electronic states
involved. Recently, Gersternkorn and Luc have reanalysed this
system by using high resolution Fourier Transform Spectroscopy
[2,3]. After the advent of lasers, this transition has proved
to be a good testing ground for many laser related phenomena
and techniques like resonance Raman effect and a variety of
single and multiphoton laser induced fluorescence processes.

In the recent years, this transition has been made to lase at a number of wave lengths over the visible and infrared regions [4,5]. The present work deals with the study of the variation of transition moment with R-centroid by the measurement of relative intensities of the fluorescence induced by 5145 Å line of Ar^+ laser.

The fluorescence intensity $I_{v'v''}$ for a transition $(v', J' \longrightarrow v'', J'')$ is given by [6]

$$I_{v'v''} \propto \nu^4_{v'v''} |< v' | \mu_e(R) | v'' >|^2 \qquad (6.1)$$

where the second term on the right hand side is the absolute square of an integral of the product of the radial wave functions of the upper and lower states and the electric dipole strength function $\mu_e(R)$, which is the integral of the dipole moment operator over the electronic co-ordinates of the initial and final states at internuclear separation R. This term is, generally, represented as a product of an average electronic transition strength and a Franck-Condon factor (FCF) as follows:

$$|<v' | \mu_e(R) | v'' >|^2 = |\mu_e(R)|^2 |<v'' (J'') | v'(J')>|^2 \qquad (6.2)$$

where the second term in the above equation is the FCF, $q_{v'v''}$. In the R-centroid approximation $|\mu_e(R)|^2$ is equal to $|\mu_e(\bar{R})|^2$ where $\bar{R}$ is the R-centroid given by

$$\overline{R} = \frac{\langle v''(J'')|R|v'(J')\rangle}{\langle v''(J'')|v'(J')\rangle} \qquad (6.3)$$

Hence, the Equation (6.1) can be rewritten as

$$I_{v'v''} \propto \nu^4_{v'v''} |\mu_e(\overline{R})|^2 q_{v'v''} \qquad (6.4)$$

From the above equation the relative values of transition strength can be calculated from the measured fluorescence intensities.

The variation of electronic transition moment $|\mu_e(\overline{R})|^2$ with R-centroid for this system was first reported by Brewer and Tellinghuisen [7]. Their calculations were based on lifetime and absorption data. In order to account for the steep decrease in the observed Einstein A coefficient as a function of v', they predicted that the transition strength must be strongly peaked around $\overline{R} = 3.0 - 3.2$ Å and decrease rapidly at large $\overline{R}$. In addition, $|\mu_e(\overline{R})|^2$ must approach zero at very large $\overline{R}$, since the transition moment must approach the value for the extremely weak $^2P_{1/2} \longleftrightarrow {}^2P_{3/2}$ atomic iodine transition in the limit of dissociation. Afterwards, a number of people have studied the variation of the transition moment with R-centroid using different methods. Koffend et al. [4] used gain measurements of optically pumped Iodine laser, Bacis et al. [8] and most recently Balasubramanian et al. [9] have used fluorescence intensity measurements. Koffend et al. reported the transition moments over a wide

range of R-centroids (2.795–4.599 Å) but their data happen
to be very meagre, especially so where the $\mu_e(\bar{R})$ vs R-centroid
curve is expected to show a sharp peak. In addition, more
accurate constants of the B and X states are now available
than those used by them to calculate the FCFs and R-centroids.
The range of R-centroid values covered by Bacis et al. in
their study is much above 3.2 Å. The data reported by
Balasubramanian et al. is extensive but they could not study
the region where the peak is expected, owing to the limited
range of their spectrometer. Hence, the study of the varia-
tion of the transition moment with R-centroid is undertaken
in the present work.

Experimental

Fluorescence in I_2 vapour is excited by the 5145 Å
line of Ar^+ laser. The fluorescence cell is made of pyrex
and is 10 cm in length and 1.5 cm in diameter. It has fused-
in windows on both ends. After attaching the cell to the
vacuum system, it is degassed and then evacuated upto 0.01
mtorr. Then, resublimated I_2 was distilled under vacuum and
collected into a side tube attached to the cell by immersing
it in liquid nitrogen. After collecting the required quan-
tity of I_2, the cell was sealed off from the vacuum system.
During the experiment, iodine pressure in the fluorescence
cell was maintained at 40 mtorr by keeping the side tube
immersed in a melting ice-bath. The fluorescence was

detected in a direction perpendicular to the laser beam, which is focussed close to the wall of the cell near the entrance slit of the spectrometer to avoid self-absorption by the iodine molecules. The detection system for the fluorescence consisted of a 0.75m double monochromater (SPEX 1403) and a thermoelectrically cooled photomultiplier tube (RCA C31034) which was operated in photon counting mode. The signal from the PMT was recorded on a strip chart recorder. The experimental set up is shown in Fig. 6.1 and Fig. 6.2 shows part of the observed fluorescence series.

Results and Discussion

The 5145 $\overset{\circ}{A}$ line of argon ion laser is known [3] to cause transitions from the $v'' = 0$, $J'' = 13$ and $v'' = 0$, $J'' = 15$ levels of the ground state $X(^1\Sigma_g^+)$ to the $v' = 43$, $J' = 12$ and $v' = 43$, $J' = 16$ levels of the $B(^3II_{0^+u})$ state respectively. Subsequent decay from the B state to the ground state produces an intense visible fluorescence. As $\Omega = 0$ for the two states involved in the transition, the fluorescence is governed by the selection rule $\Delta J = \pm 1$. So, the fluorescence series from the two excited upper levels is expected to consist of P and R doublets P(13), R(11) and P(17), R(15). As P(13) and R(15) lines have almost the same wavelength in a particular $(v' = 43, v'')$ transition, the overall appearance of the fluorescence series is that of a triplet series with R(15) and
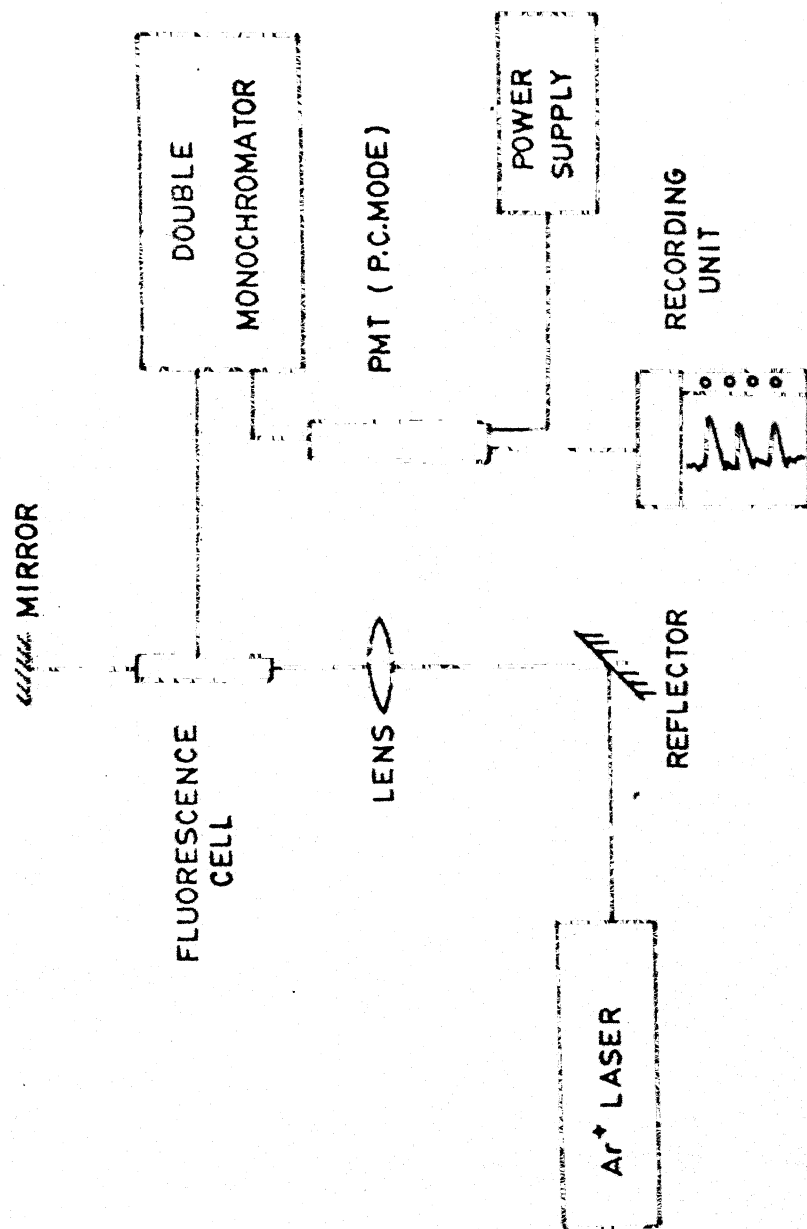
FIG. 6.1 EXPERIMENTAL ARRANGEMENT FOR I₂ FLUORESCENCE
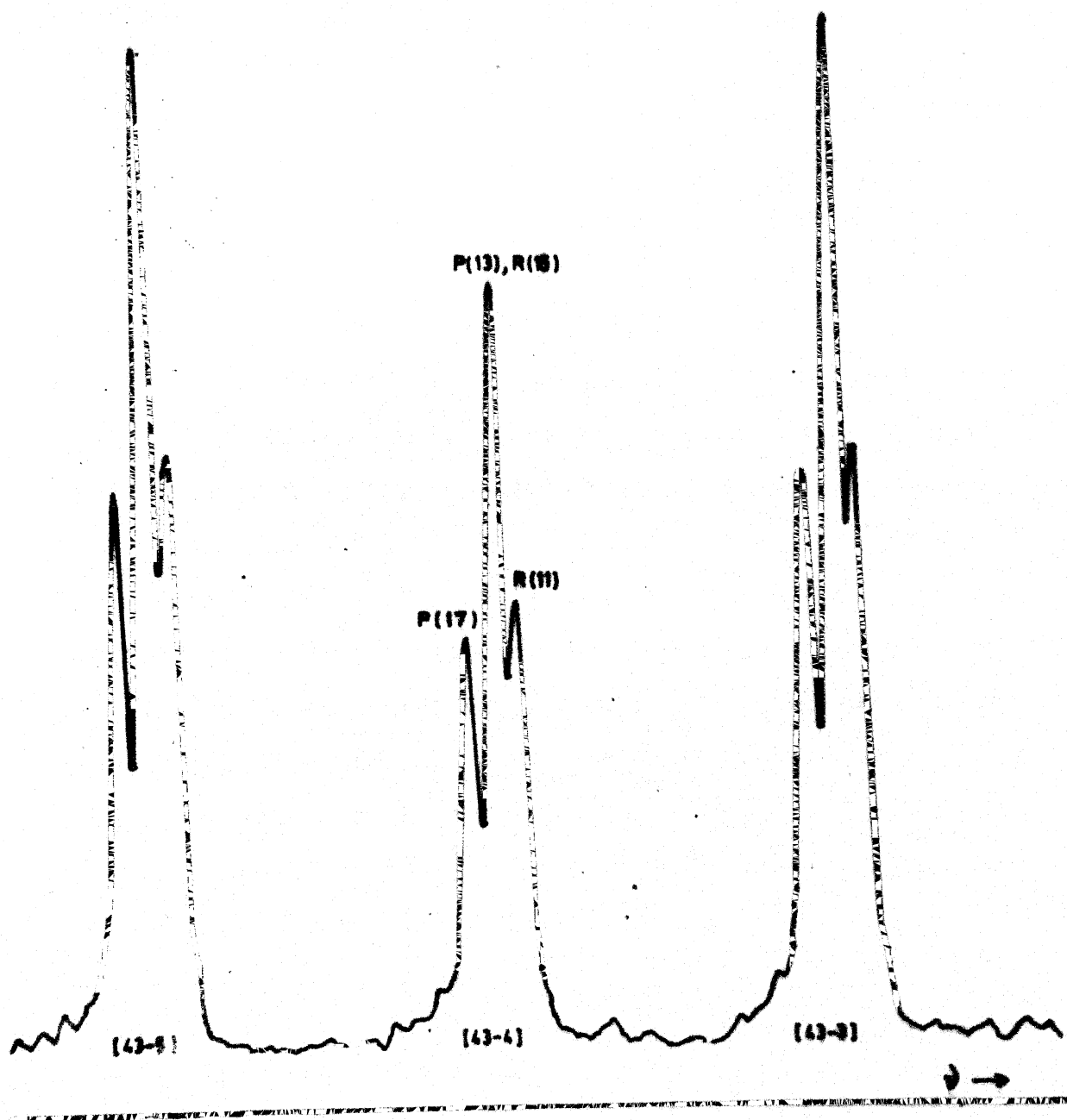
FIG. 6-2 PART OF THE Ar⁺ LASER EXCITED FLUORESCENCE SPECTRUM OF I₂

P(13) lines overlapping. In the present work, the height of the P(17) line is taken to represent the intensity of a band after correcting it to the response of spectrometer-photomultiplier combination. The line frequencies in Equation (6.4) are calculated with the constants of Luc [2] for the B state and the constants of Tellinghuison et al. [10] for the X state. The FCFs and R-centroids are taken from Reference [11].[+] The values of electronic transition strengths calculated from Equation (6.4) are plotted against R-centroids as shown in Fig. 6.3. In Table 6.1, the frequencies, FCFs, R-centroids, intensities and the transition moments for the observed ($v' = 43$, v'') transitions are tabulated. In this work all the transitions from $v'' = 0$ to 36 could be observed. From $v'' = 37$-44, alternate transitions only are observed. This is expected as the missing lines have very low FCFs. The variation of $|\mu_e(\vec{R})|^2$ with R-centroid shows the expected behaviour as can be seen from Fig. 6.3.

[+] Thanks are due to Prof. Tellinghuisen for providing me with the values of FCFs and R-centroids for this system.

138
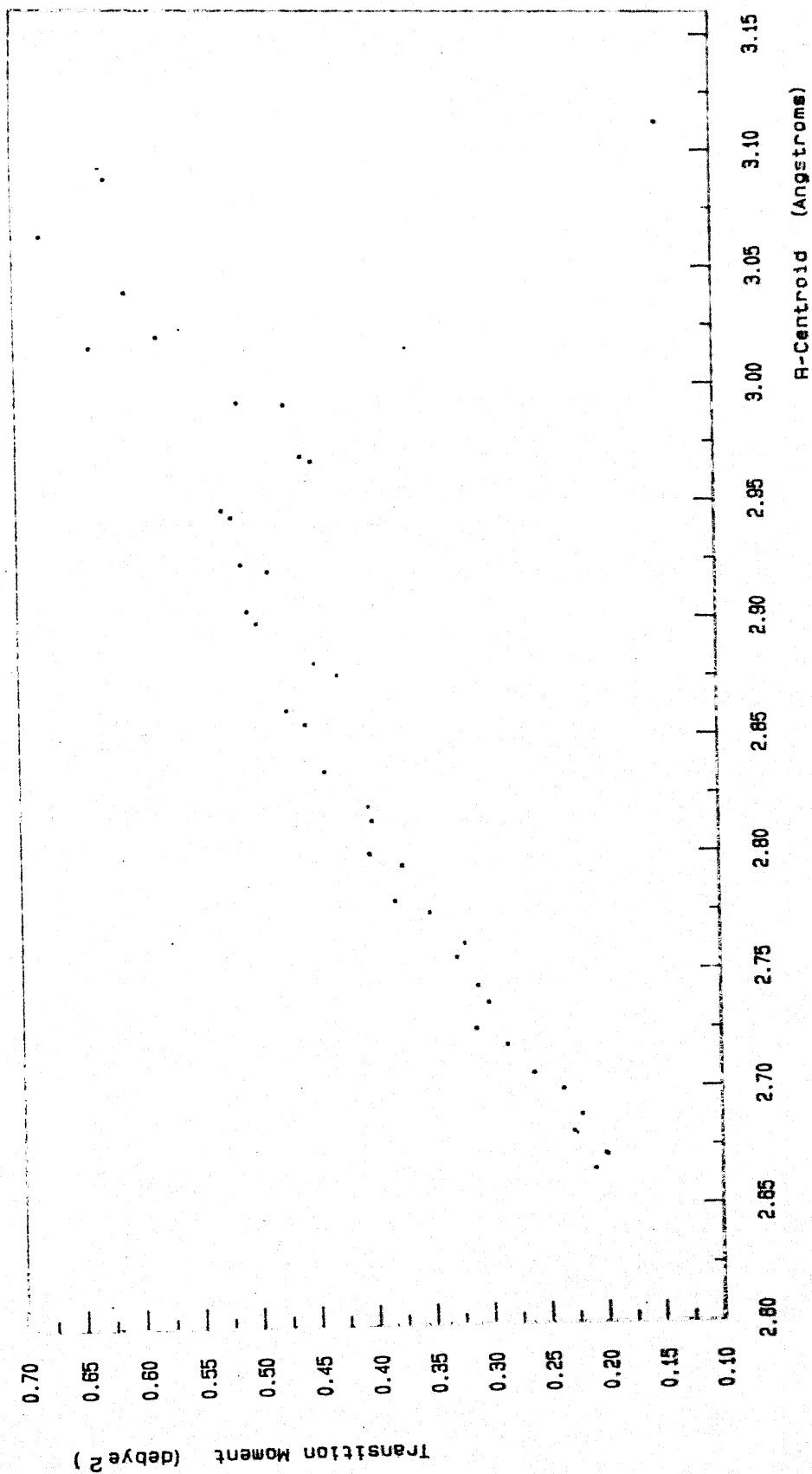
Fig 63   R-Centroid versus Transition Moment

TABLE 6.1

Measurement of Fluorescence Intensity in the B $\longrightarrow$ X System of I_2

v''	ν (cm^{-1})	Intensity (rel.units)	FCF (x10^3)	$\|\mu_e(\overline{R})\|^2$ (debye)^2	R-Centroid (Å)	$\|\mu_e(\overline{R})\|^2$ (debye)^2 Ref.9
1	19214.10	98.04	3.411	0.2108	2.665	0.228
2	19002.06	161.81	6.221	0.1995	2.671	0.218
3	18791.26	123.08	4.337	0.2276	2.681	0.259
4	18581.71	90.05	3.424	0.2206	2.688	0.232
5	18373.40	123.66	4.571	0.2374	2.699	0.286
6	18166.52	63.53	2.227	0.2619	2.706	0.245
7	17960.57	133.76	4.513	0.2848	2.718	0.292
8	17756.08	51.57	1.665	0.3116	2.725	0.262
9	17552.86	123.87	4.341	0.3006	2.736	0.307
10	17350.95	39.74	1.415	0.3099	2.743	0.264
11	17150.34	117.24	4.134	0.3278	2.755	0.362
12	16951.05	35.46	1.337	0.3212	2.761	0.308
13	16753.09	108.15	3.913	0.3509	2.774	0.392
14	16578.27	39.39	1.369	0.3809	2.779	0.324
15	16361.18	98.41	3.669	0.3743	2.794	0.379
16	16167.28	40.65	1.481	0.4016	2.799	0.305
17	15974.68	88.33	3.392	0.3999	2.813	0.406
18	15783.53	41.74	1.667	0.4034	2.819	0.338
19	15593.77	80.00	3.076	0.4398	2.834	0.422
20	15405.46	49.52	1.922	0.4573	2.839	0.357
21	15218.54	66.67	2.728	0.4555	2.854	0.439
22	15033.06	54.00	2.242	0.4716	2.860	0.384
23	14849.03	48.98	2.356	0.4276	2.875	0.493
24	14666.48	54.17	2.611	0.4484	2.880	0.433
25	14485.42	43.01	1.965	0.4971	2.897	0.515
26	14305.86	63.74	3.013	0.5051	2.902	0.458
27	14127.82	30.34	1.564	0.4868	2.919	0.523
28	13951.32	66.29	3.431	0.5099	2.922	0.482

TABLE 6.1 (cont.)

v"	ν (cm^{-1})	Intensity (Rel. units)	FCF (x10^3)	$\|\bar{\mu}_e(\bar{R})\|^2$ (debye)^2	R—Centroid (Å)	$\|\mu_e(\bar{R})\|^2$ (debye)^2 Ref. 9
29	13776.37	21.84	1.170	0.5182	2.942	0.978
30	13603.54	69.41	3.851	0.5263	2.945	0.507
31	13431.23	11.76	0.805	0.4487	2.966	0.580
32	13261.07	60.24	4.251	0.4582	2.968	0.594
33	13092.55	7.41	0.492	0.5124	2.991	0.632
34	12925.69	60.74	4.607	0.4723	2.990	0.812
35	12760.50	3.80	0.247	0.5792	3.019	
36	12597.03	78.48	4.902	0.6358	3.014	
38	12275.30	70.51	5.129	0.6053	3.038	
40	11960.70	73.23	5.293	0.6760	3.062	
42	11653.50	61.76	5.397	0.6204	3.087	
44	11353.83	13.24	5.461	0.1459	3.112	

REFERENCES

1. R.S. Mulliken, J. Chem. Phys. 55, 288 (1971).

2. P. Luc, J. Mol. Spectrosc. 80, 41 (1980).

3. S. Gerstenkorn and P. Luc, J. Mol. Spectrosc. 77, 310 (1979).

4. J.B. Koffend, R. Bacis and Robert W. Field, J. Chem. Phys. 70, 2366 (1979).

5. G.P. Barwood, P. Gill and B.R. Marx, Opt. Comm. 41, 195 (1982).

6. G. Herzberg, Spectra of Diatomic Molecules, Von Nostrand, New York (1950).

7. L. Brewer and J. Tellinghuisen, J. Chem. Phys. 56, 3929 (1972).

8. R. Bacis, S. Churassy, R.W. Field, J.B. Koffend and J. Verges, J. Chem. Phys. 72, 34 (1980).

9. T.K. Balasubramanian, G.L. Bhale, M.N. Dixit, and N.A. Narasimham, J. Mol. Spectrosc. 88, 259 (1981).

10. J. Tellinghuisen, M.R. McKeever and A. Sur, J. Mol. Spectrosc. 82, 225 (1980).

11. J. Tellinghuisen, Private Communication.

SELF-QUENCHING STUDIES OF B —> X SYSTEM

Introduction

The fact that the $B(^3II_{O_u^+})$ state of I_2 is affected
by its proximity to a number of repulsive states, which either
touch or cross the B state potential energy curve, is well-
known and well-studied [1]. B state experiences spontaneous
predissociation to $^1II_{1u}$ state whose potential energy curve
is shown to lie close to the B state potential curve in the
region of all but the lowest vibrational levels and to cross
its left branch at low v values [2]. The B state experiences
induced predissociation also, which is manifested by the
quenching of B —> X fluorescence in the presence of a
strong magnetic field [3,4]. The repulsive state, responsible

for this induced predissociation, is not yet definitely determined though Vigue et al. [5] indicated from their lifetime studies of B state that the same state ($^1II_{1u}$) is responsible for both natural and induced predissociation. Apart from the spontaneous and magnetic induced predissociation, the B state experiences predissociation induced by collisions either with foreign gas molecules or with ground state I_2 molecules. This collisional predissociation also results in the quenching of the B ⟶ X fluorescence. The collisional quenching is expected to be due to the predissociation of B state to some repulsive state, which is probably crossing the B state and to which the selection rules for radiative transitions from B state would be satisfied [1]. All the repulsive states which cause the predissociation of the B state dissociate into two normal $^2P_{3/2}$ iodine atoms. The exact number and nature of these repulsive states and the positions where they touch or cross the B state can be understood only through precise experiments for determining the lifetimes and quenching cross sections of different vibrational levels of B state, because any irregularities in the lifetimes and quenching cross sections are the results of those predissociations. In recent years, lifetimes were measured by using different techniques such as phase-shifts, intensity measurements and direct observation of fluorescence decay [6-8] and from these lifetimes data the quenching cross sections were

deduced through the Stern-Volmer plots [9]. The quenching cross sections can also be determined from a previous knowledge of the lifetime of a particular vibrational or vibrational-rotational transition, by measuring the fluorescence intensity at different pressures of the quenching agent. In the present work, the self-quenching cross sections are calculated for one Stokes (43-1) and one anti-Stokes (51-0) vibrational transitions excited by 5145 Å line of Ar^+ laser through a study of the variation of the fluorescence intensity with the pressure of I_2 molecules.

Theoretical

In the absence of foreign gases or any other external influences like magnetic fields, an excited I_2 molecule after absorbing a photon of energy $h\nu$, can either reradiate this energy as fluorescence or it can redistribute the energy in a collision with an unexcited I_2 molecule. These two processes can be indicated symbolically as

$$I_2^* \longrightarrow I_2 + h\nu \quad \text{(fluorescence)} \tag{7.1}$$

$$I_2^* + I_2 \longrightarrow 2I \ (\text{or } I_2) + I_2 \ \text{(self-quenching)} \tag{7.2}$$
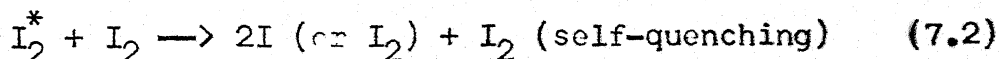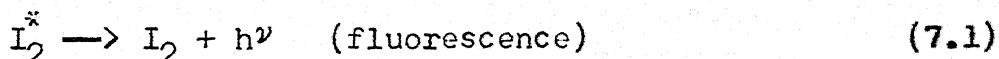
Equation (7.2) indicates that the quenching process may cause the excited I_2 molecule either to be non-radiatively de-excited to the ground state or to dissociate into two unbound atoms. As explained above, the dominant quenching

products in the case of B state of I_2 are most probably free iodine atoms ($^2P_{3/2}$) produced by collision-induced predissociation to the repulsive states. The self-quenching process is proportional to the concentration of the excited I_2 molecules and that of ground state I_2 molecules which can be denoted as $[I_2^*]$ and $[I_2]$ respectively [10]. In a steady state of absorption and decay, the number of excitation transitions per second can be equated to the number of decay transitions per second as follows [11]:

$$\pi \, \sigma_{abs}^2 \, I_0 \, [I_2] = \tau^{-1}[I_2^*] + \pi \, \sigma_{self}^2 \, \overline{v}[I_2][I_2^*] \quad (7.3)$$

where

$\pi \, \sigma_{abs}^2$ = absorption cross section (cm^2) for photons of frequency ν,

I_0 = the irradiance by incident photons ($cm^{-2} \, sec^{-1}$),

τ = the effective lifetime of the excited state (sec.),

$\pi \, \sigma_{self}^2$ = self-quenching cross section of $I_2(cm^2)$,

and $\overline{v}$ = the mean relative collision speed (cm/sec).

The lifetime τ accounts for both the radiative and non-radiative de-excitation of the molecules in the B state, the latter component being due to natural predissociation of the B state. The fluorescence intensity for a particular transition from the excited state is given by

$$I_f = A \, [I_2^*] \quad\quad\quad\quad (7.4)$$

where A is the transition probability per unit time. From
the Equation (7.3) and (7.4) a linear relation between
inverse fluorescence intensity and inverse concentration of
I_2 can be obtained as

$$I_f^{-1} = \pi \, \sigma_{self}^2 \, \bar{v} \, (\pi \, \sigma_{abs}^2 \, A \, I_o)^{-1}$$
$$+ (\pi \, \sigma_{abs}^2 \, A \, I_o \tau)^{-1}[I_2]^{-1} \qquad (7.5)$$

If the concentration of I_2 is expressed in terms of partial
pressures (p_{I_2}) using ideal gas law, Equation (7.5) can be
re-written as

$$I_f^{-1} = \pi \, \sigma_{self}^2 \, \bar{v} \, (\pi \, \sigma_{abs}^2 \, A \, I_o)^{-1} + (\pi \, \sigma_{abs}^2 \, A \, I_o \, \tau)^{-1}$$
$$(p_{I_2}/7.501 \times 10^{-4} \, kT)^{-1} \qquad (7.6)$$

where p_{I_2} is expressed in torrs.

From Equation (7.6) it is evident that a plot of
reciprocal intensity versus the reciprocal of I_2 vapour
pressure (Stern-Volmer plots) should yield a straight line
with,

$$\text{intercept/slope} = (\pi \, \sigma_{self}^2 \, \bar{v} \, \tau)(7.501 \times 10^{-4} kT)^{-1}$$
$$(7.7)$$

where $\bar{v} = \sqrt{(8kT/\pi\mu)}, \quad k = 1.3805 \times 10^{-16} \text{ ergs/}^oK$

μ = the reduced mass of I_2^* and I_2 which are
collision partners (g)

and

T = absolute temperature.

Hence, knowing τ and T the self quenching cross section for I_2 can be calculated from Equation (7.7).

Experimental

The experimental set-up is the same as that used in the previous chapter. The fluorescence spectrum of I_2 under low resolution is recorded at different pressures. The iodine pressure was controlled by maintaining the temperature of the side arm containing solid iodine at a constant temperature by means of a liquid bath contained in a Dewar flask. By filling the thermal bath with water at room temperature, water-ice mixture and ice-salt mixture, temperatures from room temperature to $-17^{\circ}C$ could be obtained. Above $0^{\circ}C$, the temperature was measured with a calibrated thermometer having $0.1^{\circ}C$ scaling and below $0^{\circ}C$ the temperature was measured with copper-constantan thermocouple. The temperature of the liquid bath was constant to $0.1^{\circ}C$ during each run. Iodine pressure was calculated from vapour pressure data given in Ref. [12].

Results

The spectra were recorded under low resolution such that each vibrational transition, which has a triplet structure under high resolution, corresponds to a single line. The first Stokes band (43-1) was recorded several times with the side arm kept at different temperatures in the region

(-17°C to 26.4°C). The values of I_2 vapour pressures and fluorescence intensities in arbitrary units along with inverse intensities and inverse vapour pressures are given in Table 7.1. Intensity vs. vapour pressure plot is shown in Fig. 7.1 and Stern-Volmer plot in Fig. 7.2. Quenching cross section for this band was calculated from the linear least-squares fit of the inverse pressure and inverse intensity. The lifetime for $v' = 43$ level is taken from Ref. [13]. The self-quenching cross section is calculated to be $74.23 (Å)^2$.

During the recording of the fluorescence spectra, only one band could be detected in the anti-Stokes side. This consists of a P-R doublet which is separated by 14.5 cm^{-1} and is spaced at about 19648 and 19633.5 cm^{-1}. A reproduction of this doublet is given in Fig. 7.5. This transition arises from molecules which were initially excited from $v'' = 1$, $J'' = 60$ to $v' = 51$, $J' = 61$ as this transition coincides with 5145 Å line of Ar^+ laser [14]. The observed anti-Stokes doublet lines R(60) and P(62) is a result of the transition from $v' = 51$, $J' = 61$ to $v'' = 0$, $J'' = 60$ and $v'' = 0$, $J'' = 62$ respectively. No other bands in this progression could be detected. The intensity of the doublet is about 1/10 of the first Stokes band and the doublet lines are almost equal in intensity. The self-quenching cross section for this (51-0) band of (B $\longrightarrow$ X) system is calculated in the present work. The lifetime for the $v' = 51$ level

TABLE 7.1

Self-Quenching of Iodine Fluorescence - (43-1) Band

I_2 Vapour Pressur (Torr)	I_2 Fluorescence Intensity (arbitrary units)	$(I_2$ Vapour Pressure$)^{-1}$ $(Torr)^{-1}$	$(I_2$ Fluorescence Intensity$)^{-1}$ (arbitrary units)
0.005	0.88	200.00	1.133
0.018	2.79	54.47	0.365
0.025	3.17	39.89	0.315
0.032	3.80	31.24	0.263
0.042	4.02	23.63	0.249
0.053	5.50	19.05	0.182
0.059	6.04	16.97	0.166
0.070	6.89	14.29	0.145
0.078	7.47	12.76	0.134
0.088	7.02	11.29	0.142
0.096	7.34	10.39	0.136
0.116	8.80	8.64	0.114
0.138	9.62	7.21	0.104
0.171	10.41	5.86	0.096
0.184	11.00	5.43	0.091
0.224	12.28	4.48	0.081
0.243	12.14	4.12	0.082
0.342	13.64	2.93	0.073
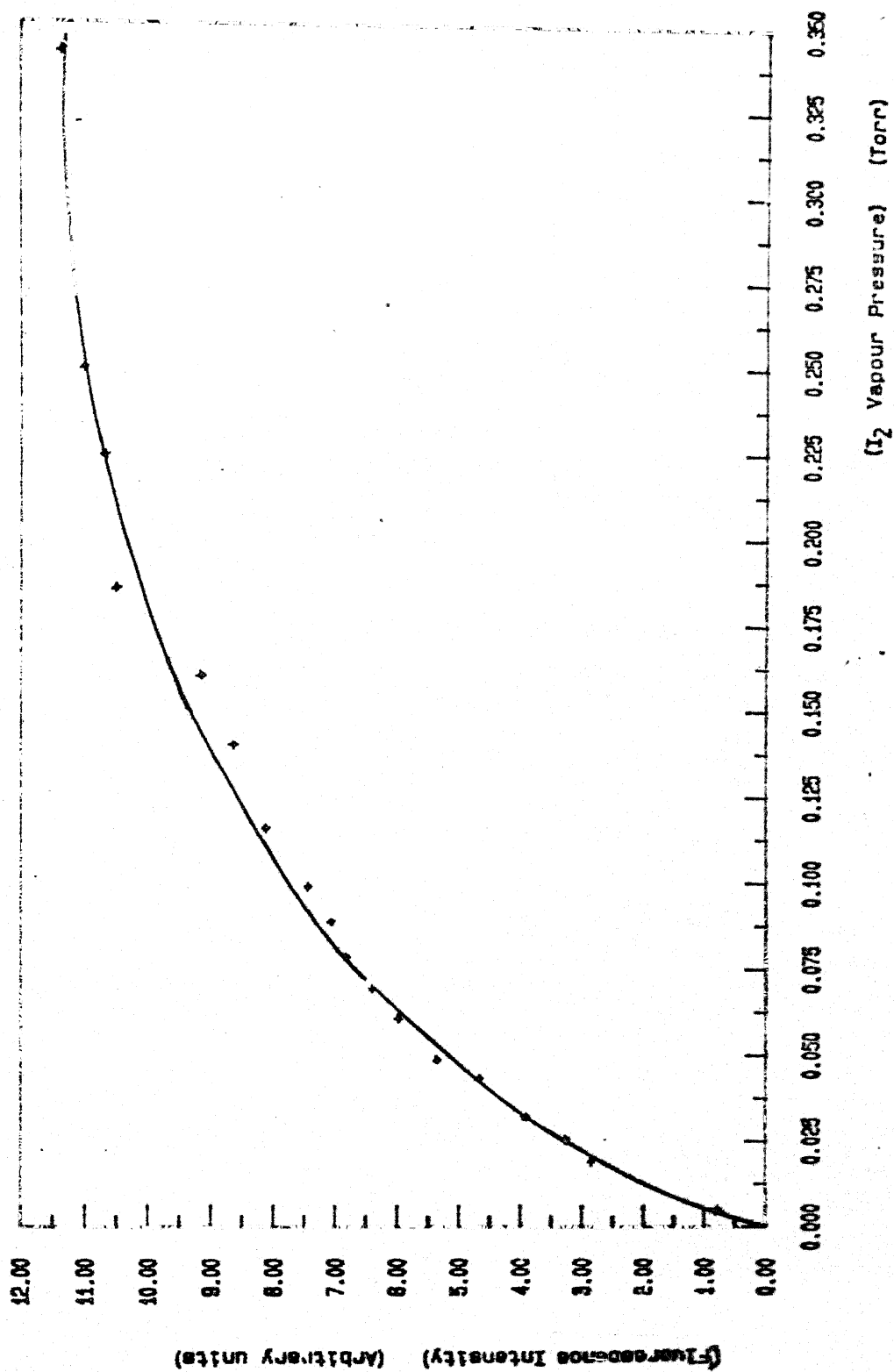
Fig 7.1 I₂ Fluorescence Intensity of the (43-1) Band as a function of I₂ Vapour Pressure.
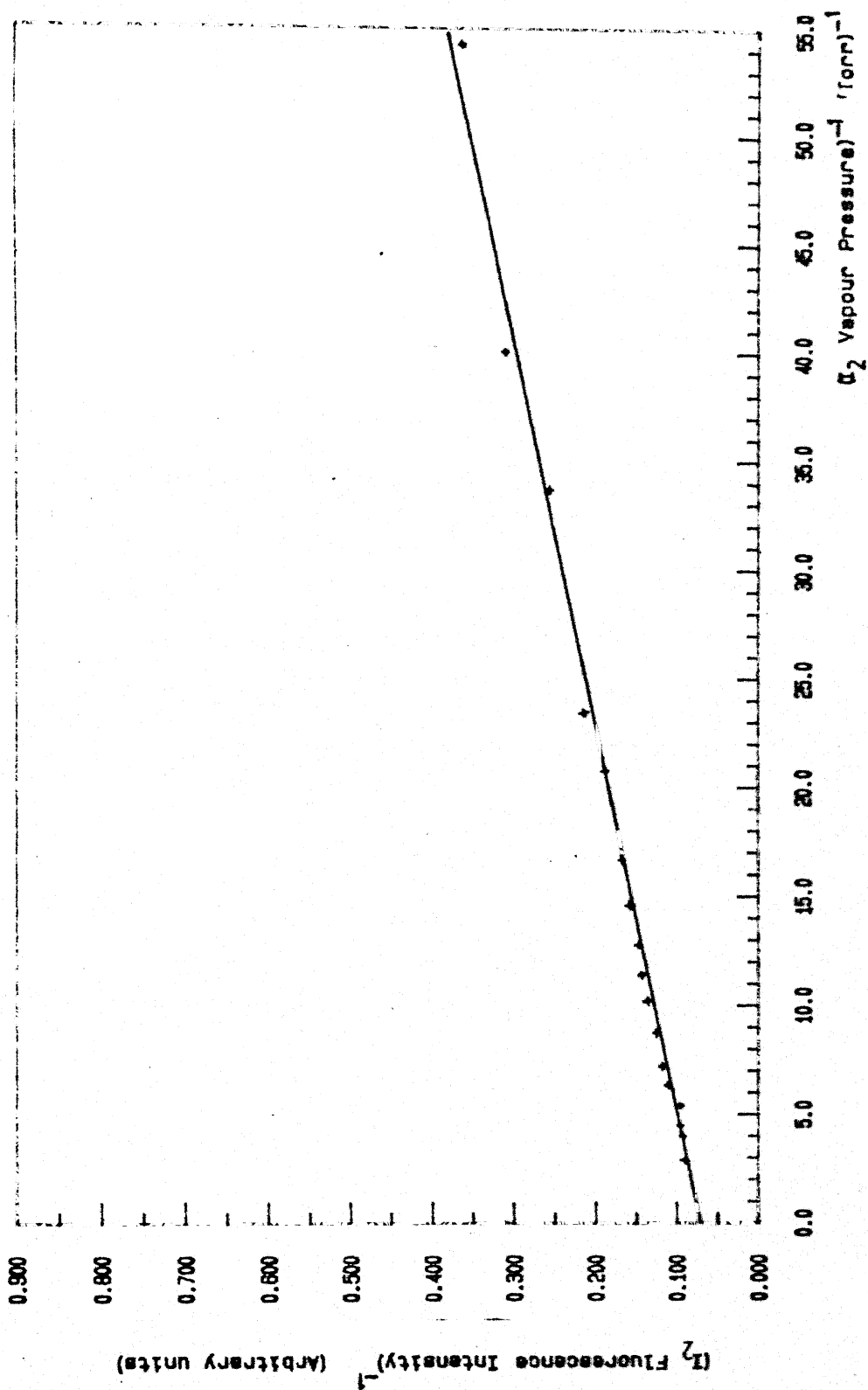
Fig 7.2 Stern-Volmer plot of the reciprocal of I_2 Fluorescence Intensity as a function of the reciprocal of the I_2 Vapour Pressure for the (43-1) Band.

of the B state is taken from Ref. [9]. The values of inten-
sities, vapour pressures, inverse intensities and inverse
pressures are tabulated in Table 7.2. In Fig. 7.3 the values
of intensity are plotted against vapour pressures whereas
Fig. 7.4 gives the Stern-Volmer plot. The transition involved,
the values of $\sigma^2 \tau$, τ and $\pi\sigma^2$ values are tabulated in Table
7.3.

Conclusions

The present calculations of the self-quenching cross
section indicate that the $v' = 43$ level of the B state has
more self-quenching cross section than the $v' = 51$ level.
This result suggests that the repulsive state which is res-
ponsible for the self-quenching is nearer to the $v' = 43$
level of the B state. If the self-quenching cross section
for all the vibrational levels of the B state are calculated
using a tunable laser, which enables one to selectively excite
the individual vibrational levels, the exact position of this
repulsive state with respect to the B state could have been
obtained. Unfortunately, due to the unavailability of the
required laser, such calculations could not be carried out
in the present work.

TABLE 7.2

Self-Quenching of Iodine Fluorescence - (51-0) Band

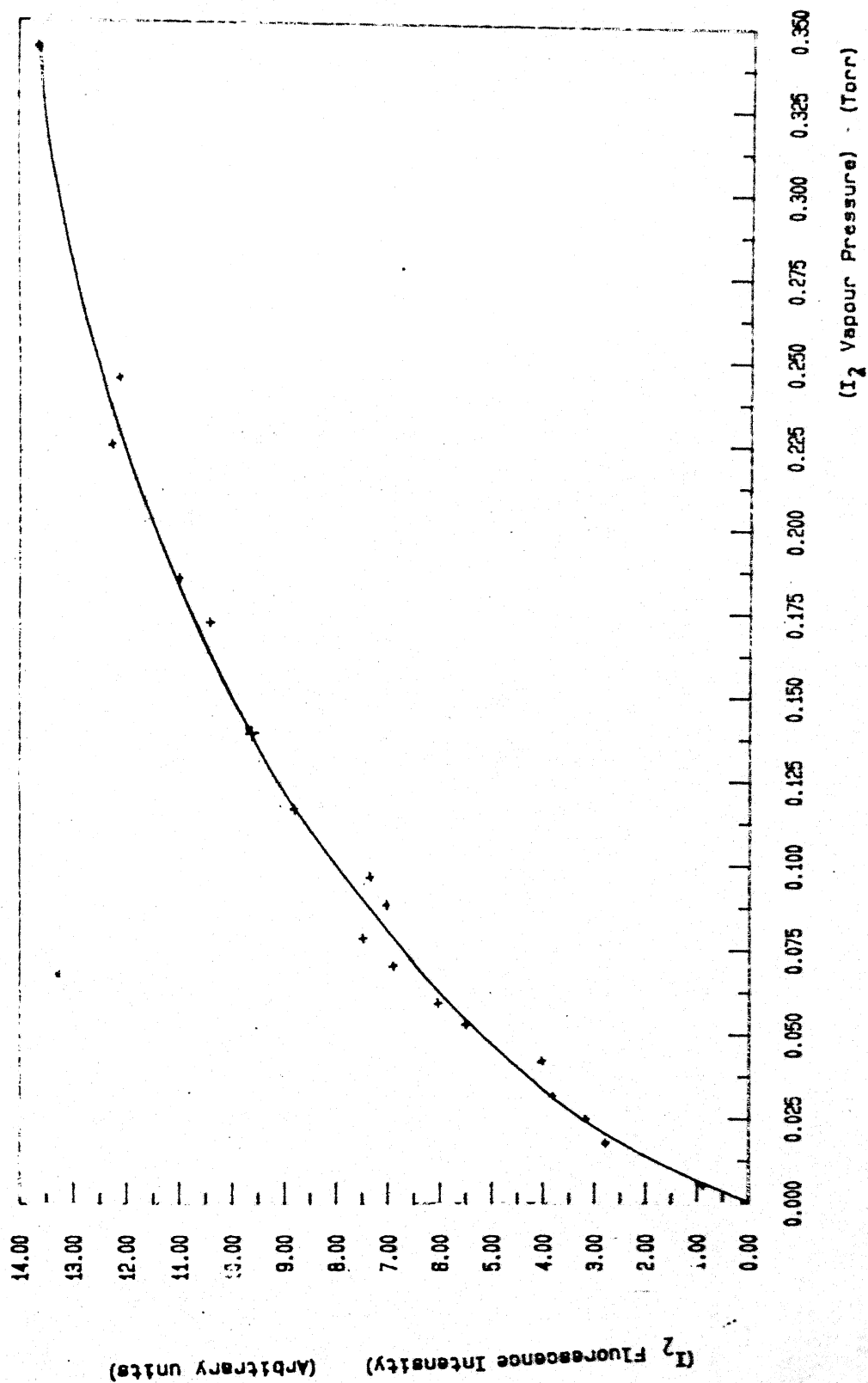| I_2 Vapour Pressure (Torr)	I_2 Fluorescence Intensity (arbitrary units)	$(I_2$ Vapour Pressure$)^{-1}$ $(Torr)^{-1}$	$(I_2$ Fluorescence Intensity$)^{-1}$ (arbitrary units)
0.005	0.81	200.00	1.235
0.018	1.18	54.35	0.848
0.025	1.29	39.87	0.775
0.032	3.92	33.70	0.255
0.043	4.68	23.40	0.214
0.048	5.38	20.73	0.186
0.060	6.00	16.64	0.167
0.069	6.41	14.56	0.156
0.078	6.84	12.76	0.146
0.088	7.08	11.40	0.141
0.098	7.46	10.19	0.134
0.115	8.14	8.73	0.123
0.139	8.66	7.21	0.116
0.159	9.16	6.31	0.109
0.184	10.52	5.43	0.095
0.223	10.70	4.48	0.094
0.248	11.04	4.04	0.091
0.342	11.38	2.93	0.088

Fig 7.9 I_2 Fluorescence Intensity of the (51-0) Band as a function of I_2 Vapour Pressure.
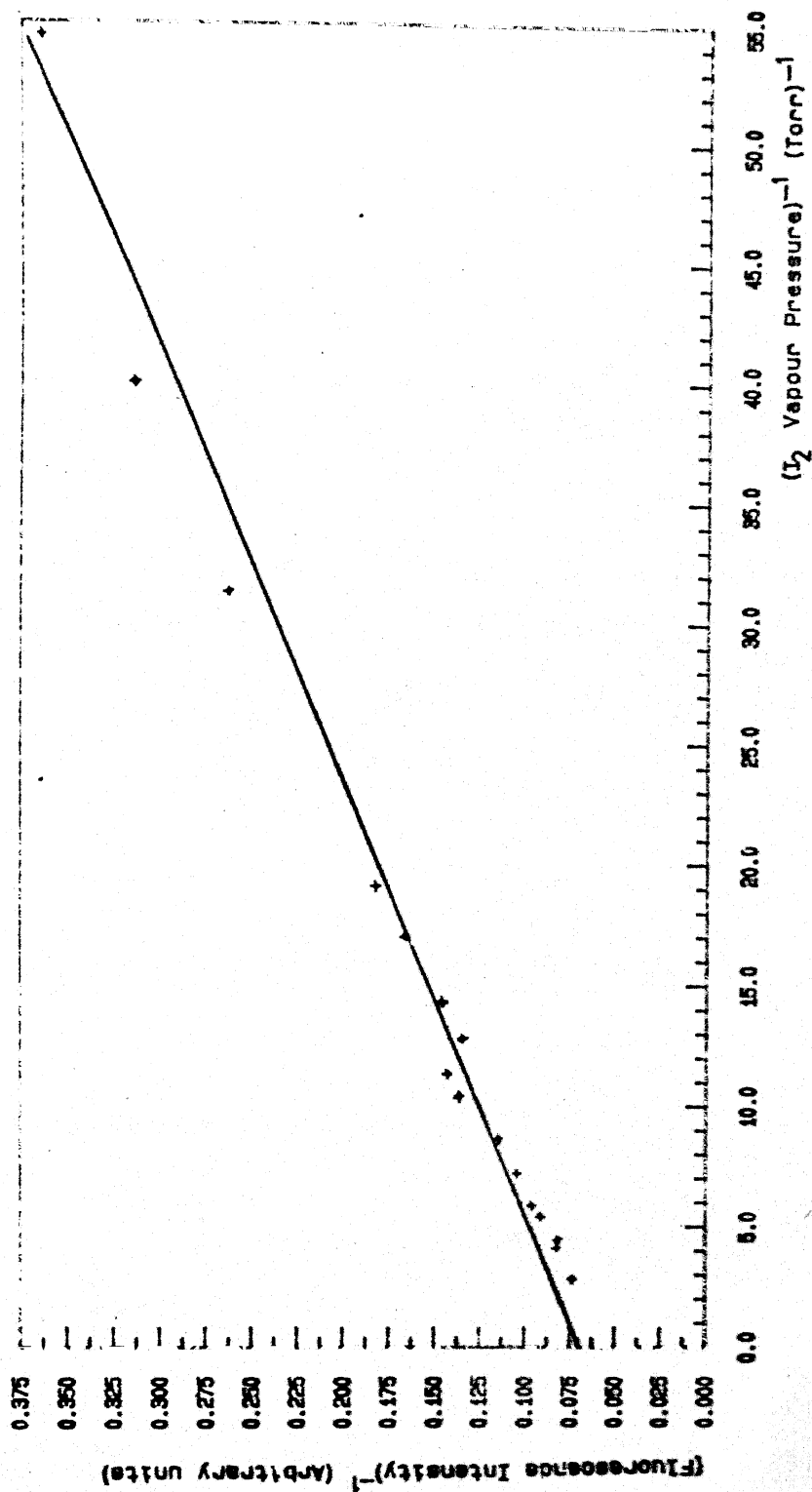
Fig 7.4 Stern-Volmer plot of the reciprocal of I_2 Fluorescence Intensity as a function of the reciprocal of the I_2 Vapour Pressure for the (51-0) Band.
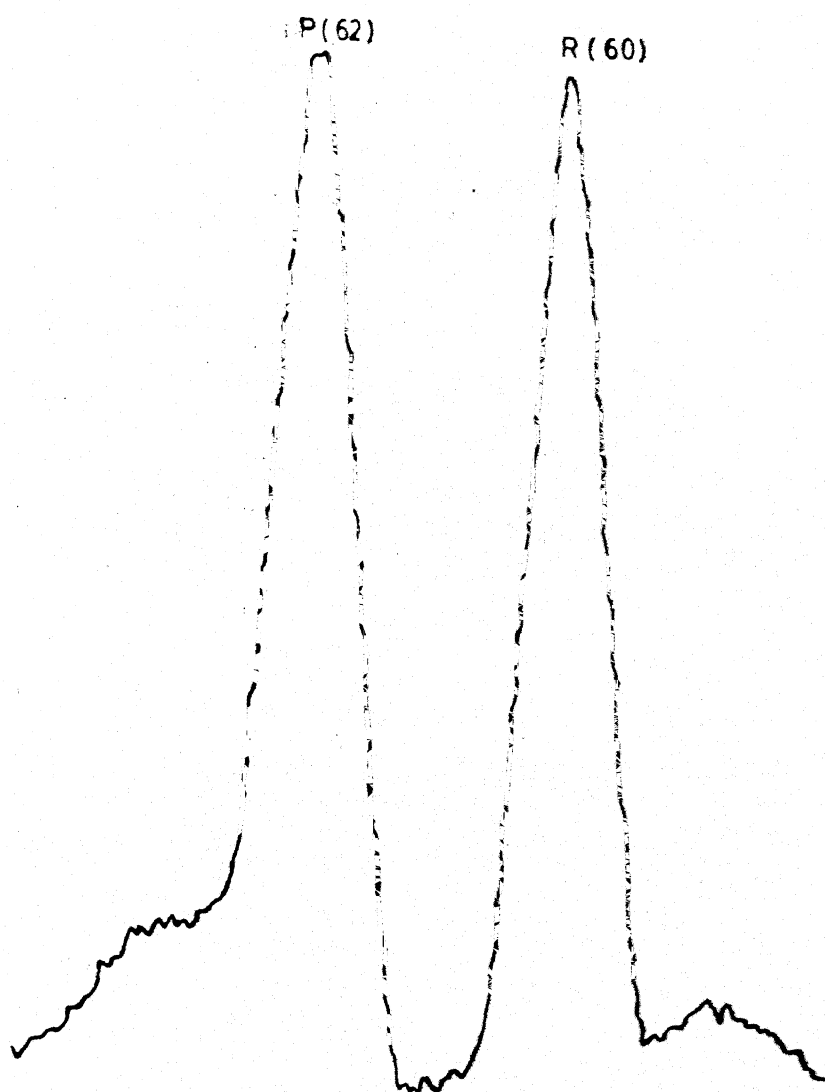
P(62)   R(60)

FIG. 7·5   (51-0) BAND OF Ar LASER EXCITED FLUORESCENCE OF I_2

TABLE 7.3

Self-quenching Cross Sections for $B(^3II_{0^+u})$ State of I_2

Transition	$\sigma^2\tau$ ($10^{-21}cm^2s$)	τ (μsec)	$\pi\sigma^2_{self}$ (Å^2)	$\sigma^2\tau$ (Ref.9)
43 − 1	3.809	2.28	74.23	2.67
51 − 0	4.347	4.57	42.27	4.27

REFERENCES

1. R.S. Mulliken, J. Chem. Phys. 55, 288 (1971).

2. J. Tellinghuisen, J. Chem. Phys. 57, 2397 (1972).

3. L.A. Turner, Z. Physik 65, 464 (1930).

4. J.H. Van Vlack, Phys. Rev. 40, 544 (1932).

5. J. Vigue, M. Broyer and J.C. Lehmann, J. Chem. Phys. 62, 4942 (1975).

6. A. Chutjion, J.K. Link and L. Brewer, J. Chem. Phys. 46, 2666 (1967).

7. A. Chutjion and T.C. James, J. Chem. Phys. 51, 1242 (1969).

8. K.C. Shotton and G.D. Chapman, J. Chem. Phys. 56, 1012 (1972).

9. G.A. Capalle and H.P. Broida, J. Chem. Phys. 58, 4212 (1973).

10. J.I. Steinfeld, J. Chem. Phys. 44, 2740 (1966).

11. Michal H. Ornstein and Vernon E. Derr, J. Opt. Soc. Am. 66, 233 (1976).

12. L. Gillespie and L. Fraser, J. Am. Chem. Soc. 58, 2260 (1936).

13. J.A. Paisner and R. Wallenstein, J. Chem. Phys. 61, 4317 (1974).

14. S. Gersternkorn and P. Luc, J. Mol. Spectrosc. 77, 310 (1979).